*Year :* 2020

# Evaluation of TiO2 nanoparticles exposure in construction workers in contact to photocatalytic cement: a comparative study between Switzerland and Thailand

Batsungnoen Kiattisak

UNIL | Université de Lausanne
Faculté de biologie
et de médecine

**Département Santé, travail et environnement, Centre universitaire de médecine générale et santé publique (Unisanté)**

# Evaluation of $TiO_2$ nanoparticles exposure in construction workers in contact to photocatalytic cement: a comparative study between Switzerland and Thailand

**Thèse de doctorat ès sciences de la vie (PhD)**

présentée à la

Faculté de biologie et de médecine
de l'Université de Lausanne

par

**Kiattisak BATSUNGNOEN**

Master en Sciences d'Hygiène Industrielle et Sécurité
diplômé du Département de Santé au Travail et Sécurité
Faculté de Santé Publique, Université de Mahidol, Thaïlande

**Jury**

Prof. Dr. Pedro Romero, Président
Dr. Nancy Hopf (Private-docent), Directrice de thèse
Asst. Prof. Dr. Michael Riediker, Co-directeur de thèse
Prof. Dr. Enrico Bergamaschi, Expert
Dr. Lynda M. Ewers, Experte

Lausanne
(2020)

UNIL | Université de Lausanne

Faculté de biologie et de médecine

**Ecole Doctorale**

**Doctorat ès sciences de la vie**

# Imprimatur

Vu le rapport présenté par le jury d'examen, composé de

| | | | | |
|---|---|---|---|---|
| **Président·e** | Monsieur | Prof. | Pedro | **Romero** |
| **Directeur·trice de thèse** | Madame | Dre | Nancy B. | **Hopf** |
| **Co-directeur·trice** | Monsieur | Dr | Michael | **Riediker** |
| **Expert·e·s** | Monsieur | Prof. | Enrico | **Bergamaschi** |
| | Madame | Dre | Lynda M. | **Ewers** |

le Conseil de Faculté autorise l'impression de la thèse de

**Monsieur Kiattisak Batsungnoen**

Master industrial hygiene and safety, Mahidol University, Thaïlande

intitulée

**Evaluation of $TiO_2$ nanoparticles exposure in construction workers in contact to photocatalytic cement: a comparative study between Switzerland and Thailand**

Lausanne, le 8 mai 2020

pour le Doyen
de la Faculté de biologie et de médecine

N. Geldner

Prof. Niko GELDNER
Directeur de l'Ecole Doctorale

# ACKNOWLEDGEMENTS

I would like to express my sincere and deepest appreciation to my thesis advisor, Private-docent Dr. Nancy B. Hopf (thesis director), Asst. Prof. Dr. Michael Riediker (thesis co-director) and Dr. Guillaume Suárez (thesis supervisor) for all their kind guidance, valuable advice, supervision and encouragement throughout this study that enables me to carry out this thesis successfully.

I am very grateful to Prof. Dr. Pedro Romero (thesis president), Prof. Dr. Enrico Bergamaschi (thesis expert) and Dr. Lynda M. Ewers (thesis expert) for all valuable advice.

I would like to express my gratitude to the Department of Occupational and Environmental Health, Center for Primary Care and Public Health (Unisanté) (formerly known as the Institute for Work and Health (IST)), Switzerland, the Royal Thai Government, the Ministry of Science and Technology, Thailand and Suranaree University of Technology for study funding and scholarship.

I would like to thank Mr. Nicolas Sambiagio for French translation and all kindness support

I would like to thank Dr. Nicolas Concha Lozano, Ms. Nicole Charriere, Mr. Benoit Allaz, Mr. Nicolas Sambiagio, Mr. Timothée Ndarugendamwo, Mr. Elvar Oskarsson, Mr. Antoine Milon and Mr. Yannick Rodari for all practical laboratory and field support.

I would like to thank my teacher, colleagues, friend, both in Thailand and Switzerland for always support in this study.

Finally, I would like to express my gratitude to my family for their warm support, encouragement, friendship and trust in me.

# ABSTRACT

**Background:** Nanotechnology concerns matter at the nanoscale ranging between 1 and 100 nanometers (nm), and has led to the production of new materials, devices, and structures. An increasing number of nanotechnology-based products are making its way into the construction sector. One such product is photocatalytic cement made by adding nano titanium dioxide (nano $TiO_2$). Nano $TiO_2$ act as a radical-forming catalyst in the presence of oxygen. These radicals potentially have beneficial effects in that they not only react with bacteria, fungi, and other microorganisms but also with air pollutants and deposited volatile organic compounds. The radicals thereby act as biocides rendering surfaces as “self-cleaning”. On the other hand, $TiO_2$ was classified by the International Agency for Research on Cancer (IARC) in 2006 as “possibly carcinogenic to humans” (Group 2B). In addition, nano $TiO_2$ has been shown to increase production of reactive oxygen species (ROS), induce DNA damage, and cell toxicity. Furthermore, nano $TiO_2$ has been reported to be translocated by the blood circulation to organs and accumulate in the kidneys, lymph nodes, heart, liver, and brain.

**Aim of the study:** The aim of the study was to characterize airborne nanoparticle exposures between photocatalytic and regular cement as follows;

1) Compare the nature of photocatalytic and regular cement particles in an aerosolizing system.
2) Simulate typical construction work activities for photocatalytic and regular cement.
3) Evaluate ROS production from airborne particles both photocatalytic and regular cement under laboratory-controlled (UV exposure).

Our results can be directly used in developing risk management strategies for construction workers utilizing photocatalytic cement. In addition, this study will enhance our understanding of airborne nanoparticles’ behaviors in mixtures with other particles.

**Methods:** The airborne nanoparticle size distributions and concentrations ranging from particle size 11 to 1,083 nm were measured with a scanning mobility particle sizer (SMPS). Fine particles i.e., particle size 250 to 32,000 nm, size distributions and concentrations were measured with a portable aerosol spectrometer (PAS). Particle number concentrations for size ranges between 10 and 700 nm were measured with a portable direct-reading instrument with a diffusion size classifier (DISC mini). Aerodynamic mass particle size distributions from 0.52 to 21.30 μm were measured with an 8-stage cascade impactor. Inhalable fraction (50% cut-point: 100 μm) was measured with an IOM cassette fitted with a 25 mm PVC filter. Respirable fraction (50% Cut-point: 4 μm) was measured with a plastic cyclone equipped with a 37 mm PVC filter. Crystalline silica was determined using infrared absorption spectrophotometry. Elemental composition was determined by scanning electron microscope energy dispersive X-ray spectroscopy (SEM-EDX). Nanoparticle morphology was determined by a transmission electron microscope (TEM) and scanning electron microscope (SEM) after TEM grid sampling. Airborne nanoparticles were collected onto the TEM grid using a particle mini sampler (MPS). X-Ray diffraction was used to measure the bagged material phase analysis for both cement types.

**Results:** The aerosolized photocatalytic cement powder contained 5% nanosized particles in number concentration while regular cement had a negligible amount. It is important to note that the $TiO_2$ content in photocatalytic bagged cement powder was only 2 % while reaching 37 % in the aerosolized form. Aerosolized photocatalytic cement had a significantly smaller particle size distribution (p-value $< 0.0005$) and greater particle concentration compared to regular cement (p-value $< 0.0005$). ROS production from photocatalytic cement exposed to UV ($3.34 \cdot 10^{-9}$ nmol/pt) was significantly higher than regular cement both exposed ($0.51 \cdot 10^{-9}$ nmol/pt) and non-exposed ($1.12 \cdot 10^{-9}$ nmol/pt) to UV with 95% confident (p-value $< 0.05$). In addition, ROS production from photocatalytic cement bag emptying activity ($4.60 \cdot 10^{-10}$ nmol/pt) were 3 folds significantly greater than regular cement ($1.58 \cdot 10^{-10}$ nmol/pt) (p-value = 0.04).

Bagged photocatalytic cement had 2.0 wt% $TiO_2$, airborne $TiO_2$reached 16.5 wt% during bag emptying and 9.7 wt% after sweeping. Cutting blocks made from photocatalytic cement alone or part of a concrete block, resulted in a similar amount of airborne nano $TiO_2$ (2.0 wt%) particles as in bagged material. The majority of the particle materials released from both regular and photocatalytic cement was CaO and $SiO_2$. In addition, both photocatalytic and regular cement had a geometric mean diameter (GMD) less than 3.5 µm. On the construction sites, Thai workers were exposed to cement particles mainly during sweeping and Swiss workers during drilling and polishing cement.

**Conclusion/discussion:** Nano $TiO_2$ can be easily mobilized from photocatalytic cement powder and aerosolized during handling.ROS concentrations produced from the photocatalytic cement were mainly due to the presence of nano $TiO_2$ and UV radiation. Both photocatalytic and regular cement had a GMD less than 3.5 µm. These small particles are able to penetrate deep into the human lung. Importantly, nano $TiO_2$ air concentrations cannot readily be extrapolated from their bagged weight fraction. Consequently, photocatalytic cement powder handling will require nanoparticle targeted exposure assessments. Exposure to nano $TiO_2$ adds to the already known particle-related health concerns among construction workers. Finally, for workers using photocatalytic cement, we recommend that they use protection measures similar to recommendations made for nano $TiO_2$ exposures.

# RÉSUMÉ

**Contexte :** Les nanotechnologies s'intéressent à la matière à l'échelle nanométrique comprise entre 1 et 100 nanomètres (nm) et ont conduit à la production de nouveaux matériaux, dispositifs et structures. Un nombre croissant de produits basés sur les nanotechnologies font leur apparition dans le secteur de la construction. Un de ces produits est le ciment photocatalytique contenant des nanoparticules de dioxyde de titane (nano-$TiO_2$). Les nano-$TiO_2$ agissent comme catalyseur de la production de radicaux en présence d'oxygène. Les radicaux ne réagissent pas seulement avec les bactéries, champignons et autres microorganismes, mais aussi avec les polluants atmosphériques, les composés organiques volatils déposés et la suie. Ils agissent ainsi comme des biocides rendant les surfaces « autonettoyantes ». Cependant, le $TiO_2$ a été classé par le Centre International de Recherche sur le Cancer (CIRC) en 2006 comme « potentiellement cancérigène pour l'homme » (groupe 2B). De plus, il a été démontré que les nano-$TiO_2$ augmentent la production d'espèces réactives de l'oxygène (ERO) et induisent des altérations de l'ADN et une toxicité cellulaire. En outre, il a été constaté que les nano-$TiO_2$ peuvent être transférées par la circulation sanguine vers les organes et s'accumuler dans les reins, les ganglions lymphatiques, le cœur, le foie et le cerveau.

**Objectif de l'étude :** L'objectif de l'étude était de caractériser les expositions aux nanoparticules en suspension dans l'air dans les cas du ciment photocatalytique et du ciment ordinaire, de la manière suivante : 1) caractériser le ciment photocatalytique et le ciment ordinaire à l'aide d'un système d'aérosolisation ; 2) simuler des activités typiques de travaux de construction pour le ciment photocatalytique et le ciment ordinaire ; 3) Évaluer la production de ERO à partir de particules de ciment photocatalytique et de ciment ordinaire en suspension dans l'air en condition de laboratoire (exposition aux UV). Nos résultats peuvent être directement utilisés pour développer des stratégies de gestion des risques chez les travailleurs

de la construction qui utilisent du ciment photocatalytique. En outre, elle permettra d'améliorer la compréhension du comportement des nanoparticules en suspension dans l'air dans des mélanges avec d'autres particules.

**Les méthodes :** Les distributions de tailles et les concentrations des nanoparticules en suspension dans l'air de tailles comprises entre 11 et 1'083 nm ont été mesurées à l'aide d'un spectromètre à mobilité électrique (SMPS). Les distributions de taille et les concentrations des particules fines, c'est-à-dire des particules de 250 à 32'000 nm, ont été mesurées avec un spectromètre d'aérosol portable (PAS). Les concentrations en nombre de particules pour des gammes de taille comprises entre 10 et 700 nm ont été mesurées avec un instrument portable à lecture directe des nanoparticules tel qu'un classificateur de taille de diffusion (DiSCmini). Des distributions granulométriques en fonction du diamètre aérodynamique pour des masses allant de 0.52 à 21.3 µm ont été mesurées avec un impacteur en cascade de 8 étages. La fraction inhalable (seuil à 50% : 100 µm) a été mesurée avec une casette IOM équipée d'un filtre en PVC de 25 mm. La fraction respirable (seuil à 50% : 4 µm) a été mesurée avec un cyclone en plastique équipé d'un filtre en PVC de 37 mm. La silice cristalline a été déterminée par spectrophotométrie d'absorption infrarouge. La composition élémentaire a été déterminée par la spectrophotométrie à rayons X à dispersion d'énergie à l'aide d'un microscope électronique à balayage (SEM-EDX). La morphologie des nanoparticules a été déterminée par un microscope électronique en transmission (TEM) et un microscope électronique à balayage (SEM) après un échantillonnage sur la grille du TEM. Les nanoparticules en suspension dans l'air ont été collectées sur la grille TEM à l'aide d'un mini collecteur de particules (MPS). La diffraction de rayons X a été utilisée pour mesurer l'analyse de la phase du matériau dans les sacs pour les deux types de ciment.

**Résultats :** La poudre de ciment photocatalytique en aérosol contenait 5% de particules nanométriques en concentration numérique, alors que le ciment ordinaire n'en contenait qu'une quantité négligeable. Il est important de souligner que la teneur en $TiO_2$ de la poudre de ciment photocatalytique dans le sac n'était que de 2%, alors qu'elle atteignait 37% sous forme d'aérosol. Le ciment photocatalytique en aérosol présentait une distribution granulométrique nettement plus faible (valeur $p < 0.0005$) et une concentration en particules plus élevée que le ciment ordinaire (valeur $p < 0.0005$). La production de ERO à partir de ciment photocatalytique exposé aux UV ($3.34 \cdot 10^{-9}$ nmol/pt) était significativement plus élevée que celle du ciment ordinaire, à la fois exposé ($0.51 \cdot 10^{-9}$ nmol/pt) et non exposé ($1.12 \cdot 10^{-9}$ nmol/pt) aux UV, avec une confiance de 95% (p-value < 0.05). En outre, la production de ERO à partir de l'activité de vidage des sacs de ciment photocatalytique ($4.60 \cdot 10^{-10}$ nmol/pt) était trois fois plus importante que celle du ciment ordinaire ($1.58 \cdot 10^{-10}$) (valeur $p = 0.04$).

Le ciment photocatalytique en sac contenait 2.0% en poids de $TiO_2$, alors que le $TiO_2$ en suspension dans l'air atteignait 16.5% en poids pendant le vidage du sac et 9.7% en poids après le balayage. La découpe de blocs de ciment catalytique, seul ou en partie, a produit une quantité de particules de nano $TiO_2$ (2.0% en poids) en suspension dans l'air similaire à celle d'un matériau en sac. La majorité des particules trouvées dans le ciment ordinaire et le ciment photocatalytique étaient du CaO et du $SiO_2$. En outre, le ciment photocatalytique et le ciment ordinaire avaient tous deux un diamètre moyen géométrique (GMD) inférieur à 3.5 µm. Sur les chantiers, les travailleurs thaïlandais ont été exposés à des particules de ciment principalement lors du balayage et les travailleurs suisses lors du forage et du polissage du ciment.

**Conclusion/discussion :** Les nano-$TiO_2$ peuvent être facilement mobilisés à partir d'une poudre de ciment photocatalytique et mis en aérosol lors de la manipulation du matériau. Les concentrations de ERO produites par le ciment photocatalytique étaient principalement dues à la présence de nano-$TiO_2$ et l'irradiation aux UV. Le ciment photocatalytique et le ciment ordinaire avaient tous deux un GMD inférieur à 3.5 µm Ces petites particules sont capables de pénétrer profondément dans le poumon humain. Il est important de noter que les concentrations de nano-$TiO_2$ dans l'air ne peuvent pas être facilement extrapolées à partir de leur fraction pondérale dans le sac. Par conséquent, la manipulation de la poudre de ciment photocatalytique nécessitera des évaluations d'exposition ciblées sur les nanoparticules. L'exposition au nano $TiO_2$ s'ajoute aux problèmes de santé déjà connus liés aux particules chez les travailleurs de la construction. Finalement, pour les travailleurs utilisant du ciment photocatalytique, nous leur recommandons d'utiliser des mesures de protection similaires aux recommandations faites pour les expositions au nano $TiO_2$.

## บทคัดย่อ

**ที่มาและความสำคัญ:** นาโนเทคโนโลยี คือ เทคโนโลยีที่ศึกษาเกี่ยวกับอนุภาค ที่มีขนาดตั้งแต่ 1 ถึง 100 นาโนเมตร เพื่อพัฒนาวัสดุ อุปกรณ์ ให้มีคุณสมบัติ และโครงสร้างใหม่ เพื่อประโยชน์ในการพัฒนาภาคอุตสาหกรรม ปัจจุบันมีการเพิ่มขึ้นของผลิตภัณฑ์ทางด้านนาโนเทคโนโลยีเป็นจำนวนมาก โดยเฉพาะอย่างยิ่งในงานก่อสร้าง หนึ่งในผลิตภัณฑ์ที่ถูกพัฒนามาจากนาโนเทคโนโลยี คือ “โฟโตคาตาไลติกซีเมนต์ (Photocatalytic cement)” โดยโฟโตคาตาไลติกซีเมนต์นี้ เกิดการการผสมนาโนไทเทเนียมไดออกไซด์ (Nano $TiO_2$) เข้าไป นาโนไทเทเนียมไดออกไซด์มีแสงหรือรังสียูวีเป็นตัวเร่งปฏิกิริยา ทำให้แสดงคุณสมบัติพิเศษ เช่น ทำความสะอาดตัวเอง ฆ่าเชื้อโรค รวมถึงลดมลพิษในสิ่งแวดล้อม อย่างไรก็ตามในปี ค.ศ. 2006 องค์กร International Agency for Research on Cancer (IARC) ได้จัดประเภทของไทเทเนียมไดออกไซด์ ในกลุ่มสารก่อมะเร็งชนิด 2บี คือ มีความเป็นไปได้ที่จะก่อมะเร็งในมนุษย์ มากไปกว่านั้นนาโนไทเทเนียมไดออกไซด์ สามารถกระตุ้นสร้างอนุมูลอิสระ (reactive oxygen species; ROS) ทำลายดีเอ็นเอ และมีความเป็นพิษต่อเซลล์ของสิ่งมีชีวิต จากข้อมูลการวิจัยแสดงให้เห็นถึง นาโนไทเทเนียมไดออกไซด์ สามารถเคลื่อนที่ภายในระบบไหลเวียนโลหิต และไปสะสมยังอวัยวะเป้าหมายอื่น ๆ เช่น ไต ระบบน้ำเหลือง หัวใจ ตับ รวมถึงสมอง

**วัตถุประสงค์ของการศึกษา:** การศึกษาในครั้งนี้มีวัตถุประสงค์เพื่อ จำแนกลักษณะและประเมินการสัมผัสอนุภาคที่แขวนลอยในอากาศ ของปูนซีเมนต์ธรรมดาและโฟโตคาตาไลติกซีเมนต์ โดยมีรายละเอียดของการศึกษา ดังนี้

1) บรรยายลักษณะของปูนซีเมนต์ธรรมดาและ โฟโตคาตาไลติกซีเมนต์ที่แขวนลอยในอากาศ โดยใช้เครื่องกำเนิดอนุภาค (aerosolizing system)
2) จำลองลักษณะการทำงานในงานก่อสร้างของปูนซีเมนต์ธรรมดาและ โฟโตคาตาไลติกซีเมนต์
3) ประเมินค่าความเข้มข้นอนุมูลอิสระ (ROS) ที่เกิดจากปูนซีเมนต์ธรรมดาและ โฟโตคาตาไลติกซีเมนต์ภายใต้การควบคุมสิ่งแวดลอม (การสัมผัสรังสียูวี)

ผลจากการศึกษา สามารถนำมาใช้ประโยชน์ได้โดยตรง ในพัฒนากลยุทธ์สำหรับการบริหารจัดการความเสี่ยงทางสุขภาพ ของผู้ปฏิบัติงานที่ต้องสัมผัสโฟโตคาตาไลติกซีเมนต์ มากไปกว่านั้น ทำให้เกิดความเข้าใจที่เกี่ยวกับ

ลักษณะการแขวนลอยของอนุภาคนาโนที่เกิดจากโฟโตคาตาไลติกซีเมนต์ เมื่อต้องรวมตัวกับอนุภาคที่แขวนลอยในอากาศประเภทอื่น

**วิธีการศึกษา:** วัดการกระจายขนาดและความเข้มข้นของอนุภาคนาโนที่แขวนลอยในอากาศขนาด 11 ถึง 1,083 นาโนเมตร โดยใช้เครื่อง scanning mobility particle sizer (SMPS) วัดอนุภาคขนาดเล็กที่มีขนาดตั้งแต่ 250 ถึง 32,000 นาโนเมตร โดยใช้เครื่อง portable aerosol spectrometer (PAS) วัดความเข้มข้นของอนุภาคขนาดตั้งแต่ 10 ถึง 700 นาโนเมตร ชนิดที่สามารถติดตัวบุคคลโดยใช้เครื่อง diffusion size classifier (DISC mini) วัดการกระจายมวลของอนุภาคขนาดตั้งแต่ 0.52 ถึง 21.30 ไมโครเมตร โดยใช้อุปกรณ์ cascade impactor ชนิด 8 ชั้น วัดความเข้มข้นของฝุ่นทุกขนาดที่แขวนลอยในอากาศ ด้วยตลับเก็บตัวอย่างไอโอเอ็ม (IOM cassette) ร่วมกับกระดาษกรองชนิดพีวีซี ขนาด 25 มิลลิเมตร วัดฝุ่นขนาดเล็กที่สามารถเข้าสู่ถุงลมปอด  ด้วยพาสติกไซโคลน ร่วมกับกระดาษกรองชนิดพีวีซี ขนาด 37 มิลลิเมตร วิเคราะห์เข้มข้นของผลึกซิลิกา (Crystalline silica) โดยใช้เครื่อง infrared absorption spectrophotometry วิเคราะห์องค์ประกอบทางเคมีของธาตุ โดยใช้เครื่อง scanning electron microscope energy dispersive X-ray spectroscopy (SEM-EDX) ศึกษาสัณฐานวิทยาของอนุภาคนาโน โดยใช้เครื่อง transmission electron microscope (TEM) และเครื่อง scanning electron microscope (SEM) ด้วยการเก็บตัวอย่างโดยใช้ particle mini sampler (MPS) บนแผ่นกรองประเภท TEM grid วิเคราะห์โครงสร้างผลึกของผงปูนซีเมนต์โดยใช้เครื่อง X-Ray diffraction

**ผลการศึกษา:** ผลจากการศึกษาพบว่า ในระบบเครื่องกำเนิดอนุภาคแขวนลอยในอากาศ โฟโตคาตาไลติกซีเมนต์ มีอนุภาคนาโนแขวนลอยในอากาศอยู่ 5 เปอร์เซ็นต์ ในขณะที่ปูนซีเมนต์ธรรมดามีอนุภาคนาโนแขวนลอยในระดับที่เล็กน้อย สิ่งที่มีความสำคัญและเป็นที่สนใจของการศึกษานี้ คือ นาโนไทเทเนียมไดออกไซด์ที่ผสมอยู่ในโฟโตคาตาไลติกซีเมนต์ เพิ่มขึ้นจาก 2 เปอร์เซ็นต์ในปูนซีเมนต์ผง เป็น 37 เปอร์เซ็นต์ ของอนุภาคที่แขวนลอยในอากาศ มากไปกว่านั้นอนุภาคของโฟโตคาตาไลติกซีเมนต์มีขนาดเล็ก และมีความเข้มข้นของอนุภาคสูงกว่าปูนซีเมนต์ธรรมดา อย่างมีนัยสำคัญทางสถิติที่ ($p$-value $< 0.0005$) ค่าความเข้มข้นของอนุมูลอิสระ (ROS) ที่เกิดจากโฟโตคาตาไลติกซีเมนต์สัมผัสรังสียูวี มีค่าเท่ากับ $3.34 \cdot 10^{-9}$ นาโนโมลต่ออนุภาคในขณะที่ปูนซีเมนต์ธรรมดาสัมผัสรังสียูวี มีค่าความเข้มข้นของอนุมูลอิสระเท่ากับ $0.51 \cdot 10^{-9}$ นาโนโมลต่ออนุ

ภาค ส่วนความเข้มข้นของอนุมูลอิสระของปูนซีเมนต์ธรรมดาไม่สัมผัสรังสียูวีมีค่าเท่ากับ $1.12 \cdot 10^{-9}$ นาโนโมลต่ออนุภาค ดังนั้นความเข้มข้นของอนุมูลอิสระที่เกิดจากโฟโตคาตาไลติกซีเมนต์สูงกว่าปูนซีเมนต์ธรรมดาอย่างมีนัยสำคัญทางสถิติ ($p\text{-value} < 0.05$) การจำลองลักษณะงานก่อสร้าง โดยการเขย่าถุงปูนให้อนุภาคของปูนซีเมนต์หลุดออกจากถุงจนหมด ในลักษณะงานนี้พบว่า โฟโตคาตาไลติกซีเมนต์มีความเข้มข้นของอนุมูลอิสระเท่ากับ $4.60 \cdot 10^{-10}$ นาโนโมลต่ออนุภาค ซึ่งสูงกว่าปูนซีเมนต์ธรรมดาอย่างมีนัยสำคัญทางสถิติ ($p\text{-value} = 0.04$) ถึง 3 เท่า ที่ความเข้มข้นเท่ากับ $1.58 \cdot 10^{-10}$ นาโนโมลต่ออนุภาค

ผงปูนโฟโตคาตาไลติกซีเมนต์มีนาโนไทเทเนียมไดออกไซด์อยู่ 2 เปอร์เซ็นต์โดยน้ำหนัก ในการจำลองลักษณะงานก่อสร้าง ด้วยการเขย่าถุงปูนให้อนุภาคของปูนซีเมนต์หลุดออกจากถุงจนหมด พบว่า อนุภาคนาโนไทเทเนียมไดออกไซด์แขวนลอยอยู่ในอากาศเพิ่มขึ้นเป็น 16.5 เปอร์เซ็นต์ และ 9.7 เปอร์เซ็นต์ สำหรับการทำความสะอาดโดยการกวาด การจำลองลักษณะงานตัดปูนซีเมนต์ พบว่า อนุภาคนาโนไทเทเนียมไดออกไซด์แขวนลอยอยู่ในอากาศมีค่าเท่ากับผงปูนโฟโตคาตาไลติกซีเมนต์ คือ 2 เปอร์เซ็นต์ องค์ประกอบหลักทางเคมีของปูนซีเมนต์ทั้ง 2 ชนิด คือ แคลเซียมออกไซด์ และ ซิลิกอนไดออกไซด์ ปูนซีเมนต์ทั้ง 2 ชนิด มีขนาดอนุภาคเล็กกว่า 3.5 ไมโครเมตร ในงานก่อสร้างคนงานไทยส่วนใหญ่สัมผัสอนุภาคจากการกวาด ในขณะที่คนงานก่อสร้างในประเทศสวิตเซอร์แลนด์ สัมผัสอนุภาคจากลักษณะงานเจาะและงานขัด

**สรุป / อภิปรายผลการศึกษา:** นาโนไทเทเนียมไดออกไซด์สามารถแขวนลอยในอากาศได้อย่างง่าย จากผงปูนโฟโตคาตาไลติกซีเมนต์ ค่าอนุมูลอิสระที่เกิดจากโฟโตคาตาไลติกซีเมนต์ เกิดจากนาโนไทเทเนียมไดออกไซด์ที่ผสมอยู่ และความเข้มข้นของรังสียูวีที่สัมผัส ปูนซีเมนต์ทั้ง 2 ชนิด มีขนาดอนุภาคเล็กกว่า 3.5 ไมโครเมตร ซึ่งอนุภาคขนาดเล็กนี้สามารถกระจายไปยังปอดส่วนลึก ประเด็นสำคัญคือ เราไม่สามารถคาดการณ์ความเข้มข้นของอนุภาคนาโนที่แขวนลอยในอากาศได้จากปริมาณความเข้มข้นที่ระบุไว้ข้างถุงจากผู้ผลิต ดังนั้นการใช้งานผงปูนโฟโตคาตาไลติกซีเมนต์ต้องมีการประเมินการสัมผัสอนุภาคนาโน เป็นที่ทราบกันดีว่า การสัมผัสอนุภาคนาโนไทเทเนียมไดออกไซด์ ส่งผลกระทบต่อสุขภาพของผู้ปฏิบัติงานก่อสร้าง ดังนั้นผู้ที่ปฏิบัติงานที่เกี่ยวข้องกับโฟโตคาตาไลติกซีเมนต์ ผู้วิจัยแนะนำให้มีมาตรการป้องกันเช่นเดียวกันกับผู้ที่ปฏิบัติงานกับนาโนไทเทเนียมไดออกไซด์

# TABLE OF CONTENT

**LIST OF TABLES**

**LIST OF FIGURES**



**Chapter V Characterization of nanoparticles in aerosolized photocatalytic and regular cement**

**Chapter VI From nano to micrometer size particles – a characterization of airborne cement particles during construction activities**

# LIST OF ABBREVIATIONS

| | |
|---|---|
| Aerosol particle sizer spectrometer, Aerodynamic particle sizer spectrometer | APS |
| American conference of governmental industrial hygienists | ACGIH |
| Automated particle analysis | APA |
| Black carbon monitors, Portable aethalometer | BCM |
| Carbon nanotubes | CNT |
| Chronic Obstructive Pulmonary Disease | COPD |
| Condensation particle counter | CPC |
| Differential Mobility Analyzer | DMA |
| Diffusion charging monitor | DCM |
| Diffusion size classifier | DISC mini |
| Dust monitor | DM |
| DustTrak equipped with a Dorr-Oliver cyclone | DT+DOC |
| Electrical low-pressure impactor | ELPI |
| Electrical mobility spectrometer | EMS |
| Energy-dispersive X-ray analyzer | EDX |
| Engine Exhaust Particle Sizer | EEPS |
| Engineered nanomaterials | ENMs |
| Fast Mobility Particle Sizer | FMPS |
| Gastrointestinal | GI |
| Geometric mean diameter | GMD |
| Geometric standard deviation | GSD |
| High-efficiency particulate air | HEPA |

## LIST OF ABBREVIATIONS

| | |
|---|---|
| International Agency for Research on Cancer | IARC |
| International Commission on Radiological Protection | ICRP |
| Laser photometer, Aerosol photometer | LP |
| Laser-induced breakdown spectroscopy | LIBS |
| local exhaust ventilation | LEV |
| Magnesium oxide | MgO |
| Multiple Path Particle Dosimetry model | MPPD |
| NanoID NPS500 (Naneum) | Nano ID |
| Nanometer | nm |
| Nanoparticles | NPs |
| Occupational exposure limit | OEL |
| Occupational safety and health administration | OSHA |
| Optical particle counter | OPC |
| Optical particle sizer | OPS |
| Particles per cubic centimeter | pt/cm$^3$ |
| Particles per cubic centimeters | pt/cm$^3$ |
| Particulate matter | PM |
| Personal protective equipment | PPE |
| Photoelectric aerosol sensor | PhAS |
| Photometer equipped with a Dorr-Oliver cyclone | PhM+DOC |
| Photometer-optical particle counter | PhM |
| Portable aerosol spectrometer | PAS |

## LIST OF ABBREVIATIONS

| | |
|---|---|
| Portland cement association | PCA |
| Reactive oxygen species | ROS |
| Respiratory protective equipment | RPE |
| Scanning electron microscope | SEM |
| Scanning electron microscope energy dispersive X-ray spectroscopy | SEM-EDX |
| Scanning electron microscopy | SEM |
| Scanning electron microscopy | SEM |
| Scanning electron microscopy energy dispersive X-ray spectroscopy | SEM-EDX |
| Scanning mobility particle sizer | SMPS |
| Scanning mobility particle sizer | SMPS |
| Scanning mobility particle sizer combining a differential mobility analyzer | SMPS+DMA |
| Scanning transmission electron microscopy | STEM |
| The Human Respiratory Tract Model | HRTM |
| Thermal-optical analysis | TOA |
| Time weighted average (8 hours ) | TWA |
| Time-weighted average | TWA |
| Titanium dioxide | $TiO_2$ |
| Transmission electron microscope | TEM |
| Transmission electron microscopy | TEM |
| Transmission electron microscopy | TEM |
| Ultrafine condensation particle counter | UCPC |
| Ultrafine Particles | UFPs |
| Ultraviolet | UV |

# CHAPTER I

# INTRODUCTION

Nanotechnology includes matter at the nanoscale with the range 1- 100 nanometers. Nanotechnology allows the production of new materials, devices, and structures (OSHA, 1999; Surinder Mann, 2006; ISO/TS 27687, 2008; ASTM, 2010; OSHA, 2013). In the construction industry, nanotechnology is used to enhance material strength and surface properties, but also energy conservation, by applying a wide range of nanomaterials such as carbon nanotubes, Quantum dots, and nanoparticles of silicon dioxide, titanium dioxide, iron oxide, copper, silver among others. (Carp et al., 2004; Yank Keles, 2009; Lee et al., 2010; Broekhuizen et al., 2011; Lan et al., 2013; Nano werk, 2015). During the last decade, one of these applications is a new generation of "green" or "photocatalytic cement". This material contains nanoscale titanium dioxide ($TiO_2$) and takes advantage of the fact that nanoscale $TiO_2$ acts as a radical-forming catalyst. Construction products using nanoscale $TiO_2$ thereby act as biocides, making its surface a self-cleaning (Lan et al., 2013; Carp et al., 2004) white color without being painted and removal of air pollutants such as volatile organic compounds (Chen & Poon, 2009).

The International Agency for Research on Cancer (IARC) classified $TiO_2$ into Group 2B "possibly carcinogenic to humans", which means that there is sufficient evidence of carcinogenicity in experimental animals and inadequate evidence of carcinogenicity in humans (IARC, 2015). In addition, nano-scale $TiO_2$ is reported to show genotoxicity, cytotoxicity (NIOSH, 2009; Sayes et al., 2006), DNA damage in erythrocyte and lymphocyte (Falck et al., 2009; Ghosh et al., 2010; WHO, 2010; Sha et al., 2015), reactive oxygen species (ROS), (Sayes et al., 2006; Lee et al., 2010; Long et al., 2006), DNA damage in bronchial epithelial cells (Sha et al., 2015), toxic to lung epithelial cell (Sha et al., 2015), and acute lethality (Lee et al., 2010).

Moreover, nano $TiO_2$ have been shown to accumulate in the lungs, especially in the alveoli, and be translocated into blood circulation where they are transported to different target organs (lymph nodes, kidney, liver, heart, and brain) (Wang et al., 2008; Kreyling et al., 2010; Geiser & Kreyling, 2010).

The health risk associated with handling $TiO_2$ will depend on the physical and chemical properties of the $TiO_2$-cement mixture, working condition, frequency, duration and concentration of exposure, but also particles size and size distribution. Photocatalytic cement use is likely to lead to some extent of exposure to nanosized particles; however, no measurements relating to photocatalytic cement has previously been reported. Inhalation is the most common route of exposure to airborne nanoparticles in the construction workplace (Sha et al., 2015; Tedja et al., 2011).

Indeed, there is a lack of health and safety information regarding photocatalytic cement. Particularly is this true in terms of exposure levels, which health effects are likely to occur, safe handling guidelines as well as recommendations on how to reduce exposure. Although nanomaterials have a large potential for improving construction of cleaner and more ecological buildings, it is important to understand these safety and health issues to ensure that the construction workers are protected during the construction. Thus, this research aims to characterize and compare exposure parameters such as size distribution, concentration, morphology and elemental composition between photocatalytic and regular cement.

Although traditional cement has been on the market for several centuries, no scientific research has been conducted to characterize nanosized particles during work activities. This research will identify possible risks if any, associated with cement and concrete work in the construction industry not previously estimated. Such information may help target exposure reduction strategies among current cement use but as well as future work with photocatalytic cement. Ultimately, we hope that this work will help in reducing workers exposure in construction industry and possible future health effects.

# CHAPTER II

# BACKGROUNG AND RATIONALE

## 2.1 Nanotechnology and nanoparticles

Nanotechnology is the study, associated with spherical matter near atomic-scale which dimensions less than 100 nanometers (1 nanometer = $10^{-9}$ meters). Nanotechnology has been used for developing and improving material properties to produced new structures, and devices (ISO/TS 27687, 2008; OSHA, 1999; Surinder Mann, 2006; OSHA, 2013).

Nanoparticles (NPs) or Ultrafine Particles (UFPs) classified as the particle size between 1 and 100 nm. The nanoparticles are so small that they cannot be seen by the naked eye or even with a normal optical microscope. Therefore, nanoparticles are seen with powerful electron microscopes such as scanning electron microscopy (SEM) or transmission electron microscopy (TEM). Nanoparticles are smaller than human hair dimensions by 10,000 times and smaller than asbestos fibers by 1,000 times, as visualized in Figure 1.

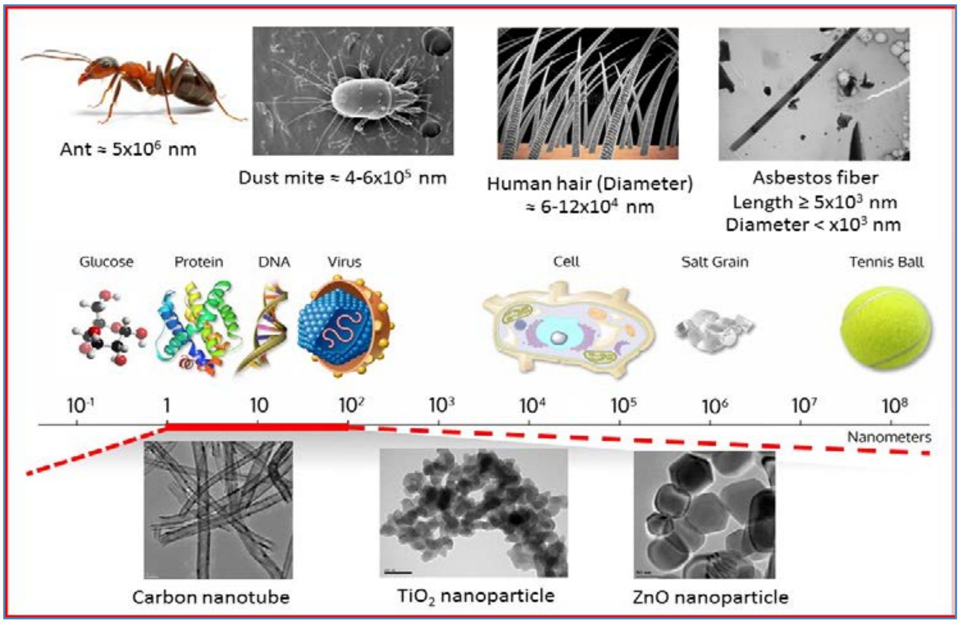


Figure 1: The comparisons of nanoparticles and particulate matter in different sizes.

Nanoparticles can grow from a primary particle by aggregation and agglomeration. During aggregation, particles form strong bonds such as covalent bonds, while in agglomeration, particles assemble with weak physical interaction such as Van der Waals forces. Therefore, agglomerations are easier to break compared to aggregation (Liu, 2013; Ashraf et al., 2018; Zare, 2016; Nichols et al., 2002).

**2.2 Nanoparticles and applications in construction**

Nanotechnology has been implemented in the construction industry for improving material properties, function and energy conservation. Nanotechnology in construction includes nanoparticles such as carbon nanotubes (CNT), silicon dioxide ($SiO_2$) nanoparticles, titanium dioxide ($TiO_2$) nanoparticles, iron oxide (FeO) nanoparticles, copper Cu) nanoparticles, silver (Ag) nanoparticles, and quantum dots (QDs). (Yank Keles, 2009; Nano werk, 2015; Lee et al., 2010; Broekhuizen et al., 2011; Lan et al., 2013; Carp et al., 2004). Nano substances have been implemented in several types of construction products, for example in cement, concrete, ceramic, steel, coating, painting, windows and solar cell (Lee et al., 2010). Engineered nanomaterials (ENMs) in construction provide several advantages in terms of material properties such as lighter and stronger material, heat-insulating, light-reflective, self-cleaning, biocide and removal of air pollutants (Zhi Ge & Zhili Gao, 2008; Lee et al., 2010; Zhu et al., 2004; Paz et al., 1995; G. Li, 2004; Lan et al., 2013).

**2.3 Portland cement or regular cement**

Cement was well-known in the world since the Roman era to make the building strong property when mixed together with water, rock, and sand (Edwin G. Foulke, 2008). The most important ingredients of raw materials were limestone (calcium carbonate; $CaCO_3$) and clay ($SiO_2$) and other additives. Today, the mixture of raw materials feed into a rotating kiln with burning fuels at around 1450 °C (H. P. Notø et al., 2016). The amount of dust generated during grinding of the rock process is considerable. The production of chemical reaction in this process produce Portland cement clinker (Fell & Nordby, 2017). The byproduct is carbon dioxide $CO_2$ emitted during the burning process.

$$\begin{array}{c} \text{Limestone} \\ CaCO_3 \end{array} + \begin{array}{c} \text{Clay} \\ SiO_2 \end{array} \xrightarrow[\text{Burn } 1450\ ^{o}C]{CO_2} \begin{array}{c} \text{Portland Cement Clinker} \\ 3CaO.SiO2 + 2CaO.SiO2 \end{array}$$

Portland cement or often just referred to as regular cement is a cement type often used in the construction sector. Portland cement is the raw material together with sand to make concrete, which is used to construct buildings, as well as for repair and maintenance. The elemental composition of regular cement by weight percent was calcium oxide (CaO) 60-67 wt%, SiO2 17-25 wt%, aluminum trioxide ($Al_2O_3$) 3-8 wt%, ferric oxide ($Fe_2O_3$) 1-6 wt%, sulfur oxide ($SO_3$) 1-5 wt%, and magnesium oxide (MgO) 1-2 wt% respectively (Meo, 2004; Jeff Thomas & Hamlin Jennings, 2008; Fell & Nordby, 2017; Batsungnoen et al., 2019). Nano $TiO_2$ is not present in regular cement.

### 2.4 Photocatalytic cement $TiO_2$ nanoparticles

During the last decade, one nanotechnology application emerged in the construction sector is a "green cement" that relies on the use of engineered nanoparticles. It is called "**photocatalytic cement**". Photocatalytic cement is Portland cement type I (cement-clinker; CE number 266-043-4) with nano $TiO_2$ and additives. Nano $TiO_2$ in photocatalytic cement is advantageous as it is self-cleaning, act as a biocide due to its photocatalysis properties when exposed to UV light

(Lan et al., 2013; Carp et al., 2004; Banerjee et al., 2015; Chen & Poon, 2009; Lee et al., 2010; Zhi Ge & Zhili Gao, 2008). Due to these properties, it stays white in color without the need for painting it. Several buildings have made use of photocatalytic cement such as;

- Misericordia church, Rome, Italy as showed in Figure 2
- Hôtel de police - Bordeaux, France
- Air - France headquarters Roissy, France
- Arts - Chambery, France
- The bell tower - Dalton, Georgia
- West cermak street, Chicago, USA
- Gateway elements - minneapolis, Minnesota, USA

Figure 2: Applications of photocatalytic cement; Misericordia church, Rome, Italy (Michael Chusid, 2017)

## 2.5 Nano $TiO_2$

Titanium dioxide is well known as white pigment material and was discovered from ilmenite (titanium ore) in 1791 in England. Nano $TiO_2$ exists in three different polymorphs as rutile, anatase, and brookite. Rutile and anatase are commonly used in food, paint and cosmetic among others manufacturing (Carp et al., 2004; Lan et al., 2013).

Nano $TiO_2$ has photocatalytic property when it is exposed to ultraviolet (UV) light with wavelengths between 280 and 400 nm. UV-excited electrons (ē) on the nano $TiO_2$ surface has an energy greater than the electron band gap (3.10–4.43 eV). Electrons excited from the valence band to conduction band produce electron (ē) pairs and holes (h+). In addition, ē/ h+ pair reacts with the oxygen ($O_2$) molecule and humidity ($H_2O$) in the air forming series of reactive oxygen species (ROS) and free radicals (Diebold, 2003; Carp et al., 2004; Lan et al., 2013; Hanaor & Sorrell, 2011) as shown in Figure 3.

The self-cleaning property has been shown for nano $TiO_2$. Nano $TiO_2$ exposed to UV presented super hydrophilic and anti-fogging substance it can make a material surface dry very quickly and spread out water instead of a droplet. In addition, nano $TiO_2$ had photocatalytic degradation properties meaning it can destroy organic compounds, hydrocarbon bonds, and particles deposited in material surface (Carp et al., 2004; Lan et al., 2013; Chen & Poon, 2009).

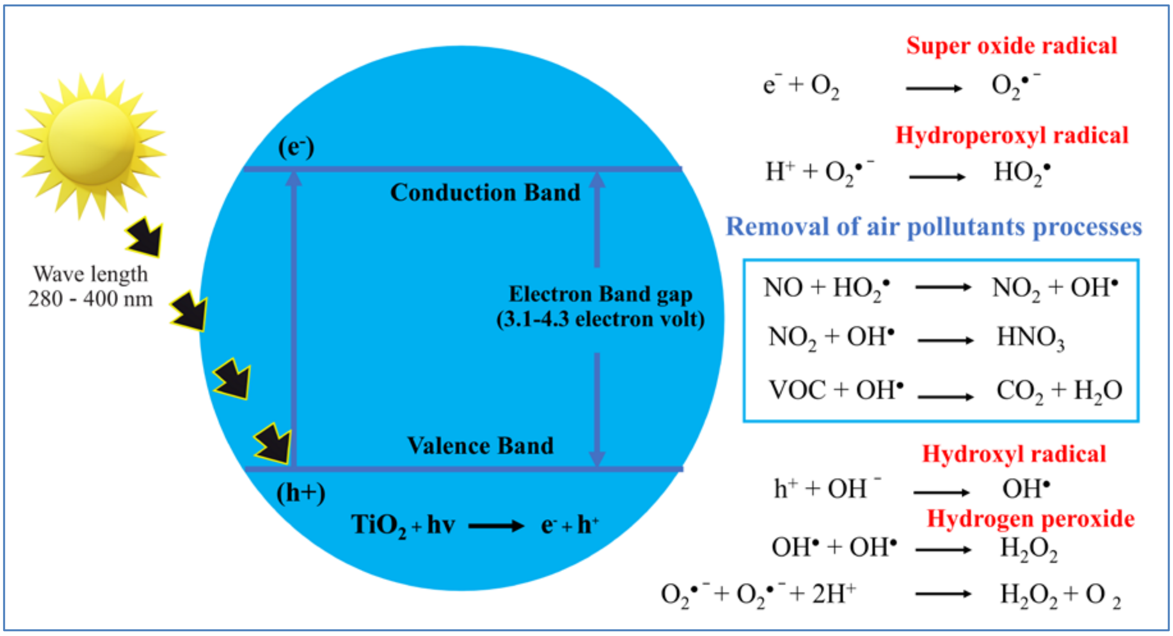


Figure 3: Schematic illustration of nano $TiO_2$ photocatalysis

Numerous scientific articles have described UV induced nano $TiO_2$ photocatalytic properties in destructing microbes such as bacteria, virus, protozoa, and fungi. ROS production from nano$TiO_2$ causes various damages to living cell (Huang et al., 2000). The mechanism started with attacking the cell wall, and then the cytoplasmic membrane before the intracellular components break down. In addition, the hydroxyl radical ($OH^{\bullet}$) and free radicals produced from the nano $TiO_2$ surface inhibited cell respiration and consequently caused cell death (Matsunaga et al., 1985; Lan et al., 2013; Chen & Poon, 2009).

Nano $TiO_2$ exposed to UV light produce electrons (ē) and holes (h+). Electrons from the conduction band react with oxygen ($O_2$) molecules in air and produce superoxide free radicals ($O^{\bullet}{}_2^-$). At the same time, holes (h+) from the valence band react with the hydroxyl ion ($OH^-$) from water ($H_2O$) or humidity and produce hydroxyl radical ($OH^{\bullet}$). Superoxide radical ($O^{\bullet}{}_2^-$) reacts with $H^+$ which is isolated from the water molecule to produce hydroperoxyl radicals ($OH^{\bullet}{}_2$). Common air pollution gases such as nitrogen monoxide (NO), nitrogen dioxide ($NO_2$)

and volatile organic compounds (VOCs) react with reacts with $OH^{\bullet}{}_2$. NO produce $NO_2$ in contact with nano $TiO_2$ surface and then $NO_2$ reacts with $OH^{\bullet}$ to produce ammonia ($HNO_3$). VOCs react with $OH^{\bullet}$ and produce carbon dioxide ($CO_2$) and $H_2O$ (Chen & Poon, 2009; Lim et al., 2000; Dalton et al., 2002, p. 2; Diesen & Jonsson, 2014; Fujishima & Zhang, 2006). The processes are shown in Figure 3.

### 2.6 Cement particle exposures and health effect

In 2013, The Portland cement association (PCA) reported world cement consumption around 158 million metric tons (PCA, 2013). The Federal Statistical Office in Switzerland reported around 319,300 employees or 8% of the Swiss workers working in the construction sector (FSO, 2017). In 2017, the Thai social and quality of life database system estimated around 2.17 million workers employed in the construction sector in Thailand. No information was found regarding the amount of photocatalytic cement consumed in either countries nor the number of workers possibly exposed.

Health effects from exposure to regular cement were describe as early as the 1700 by the Italian physician Bernardino Ramazzini (Fell & Nordby, 2017). Airborne particles inhaled by the workers caused in particular occupational lung diseases. Later, medical reports documented that cement dust caused skin irritation and burns (ILO, 1999). Cement dust exposures are assoicated with many activities performed in construction for example bag emptying, abrasive blasting, concrete drilling, cement mixing, concrete block cutting, brick, sweeping among others.

The International Agency for Research on Cancer (IARC) has classified particulate matter (PM) and crystalline silica $SiO_2$ as group 1 carcinogens for the human lung. In addition, photocatalytic cement contain nano $TiO_2$, which has been classified as group 2B, possibly carcinogenic to humans (IARC, 2017). Inhalation to particulate matter (PM) in general is directly linked to the prevalence of pulmonary and cardiovascular diseases (e.g. COPD, asthma, lung cancer) (Risom et al., 2005; Aust et al., 2002; K Donaldson et al., 2001; Schins et al., 2004; Ghio & Devlin, 2001; Knaapen et al., 2004; Upadhyay et al., 2003; Upadhyay et al., 2003; Park et al., 2018).

Crystalline silica causes chronic obstructive pulmonary disease (COPD), chronic bronchitis, silicosis and exacerbate tuberculosis (Merget et al., 2002; Kaewamatawong et al., 2005; Napierska et al., 2010; Soutar et al., 2000). US OSHA reported around 2 million workers to be exposed to crystalline silica (OSHA, 2002). In addition, amorphous silica causes health effects to the human lung such as reversible inflammation, granulomas, emphysema, and pneumoconiosis (McLaughlin et al., 1997; Merget et al., 2002; Kaewamatawong et al., 2005).

$TiO_2$ was classified by the International Agency for Research on Cancer (IARC) in 2006 as "possibly carcinogenic to humans" (Group 2B) (IARC 2017). In addition, In 2017 European Commission proposed to classify $TiO_2$ as a "category 2 carcinogen" due to its risk of inhalation (NIA, 2017). The classification is to be applicable to liquids as well as powders of mixtures containing 1% or more of titanium dioxide in the form of or incorporated in particles with aerodynamic diameter $\leq 10$ µm.

### 2.7 Nano particles and health effect

Potential adverse health effects associated with exposures to engineered nanoparticles have been reported studies in animals, in vivo, and in vitro human cell lines studies (Simkó & Mattsson, 2010). There is a lack of information relating human exposures and health effects as epidemiological studies are absent. Table 1 gives an overview of health effects associated with different ENMs and their application in the construction industry.

Table1: The toxicity of ENMs was applied in construction industry

| ENMs | Using | Health Effect | References |
|---|---|---|---|
| **Nano $TiO_2$** | • Cement<br>• Paint<br>• Window<br>• Solar cell | • lung damage<br>• DNA damage in embryonic kidney,<br>• DNA damage in erythrocyte and lymphocyte<br>• DNA damage in Bronchial epithelial cells<br>• Genotoxicity and cytotoxicity<br>• Lung cancer (2B)<br>• acute lethality<br>• ROS | (Sha et al., 2015)<br>(Falck et al., 2009)<br>(Ghosh et al., 2010)<br>(NIOSH, 2011a)<br>(WHO, 2010)<br>(IARC, 2015)<br>(Lee et al., 2010) |
| **Carbon nanotube (CNT)** | • Concrete<br>• Ceramics<br>• Solar cell | • cancer (2B)<br>• cell membrane damage<br>• apoptosis<br>• necrosis<br>• inhibit respiratory functions<br>• DNA damage<br>• granulomas<br>• atherosclerotic | (Lee et al., 2010)<br>(IARC, 2015) |
| **Quantum dots** | • Solar cells | • DNA damage<br>• cytotoxicity | (Lee et al., 2010) |

| ENMs | Using | Health Effect | References |
|---|---|---|---|
| **Nano $SiO_2$** | • Concrete<br>• Ceramics<br>• Window | • ROS<br>• apoptosis<br>• tumor necrosis factor<br>• inflammatory and immune responses | (Lee et al., 2010) |
| **Nano Cu** | • Steel | • DNA damage<br>• lipid peroxidation<br>• acute toxicity to liver, kidney, and spleen | (Lee et al., 2010) |

### 2.8 Nanoparticles deposit in respirable tract and translocation

Several existing models describe respiratory tract deposition mechanisms of inhaled particles. The most important deposition factors are particle diameter and size distribution (Geiser & Kreyling, 2010). A commonly used model is The Human Respiratory Tract Model (HRTM), which has been described by the International Commission on Radiological Protection (ICRP). This model predicts that inhaled particles with diameter from 1 nm to 10 µm to deposit in the nasopharyngeal, tracheobronchial, and alveolar regions (ICRP, 1994; Oberdörster et al., 2005; Geiser & Kreyling, 2010). This prediction was based on a mathematical model considering healthy adults, nose breathing only and during rest. Particles greater than 10 µm will **impact** in the upper respiratory region or be carried out by the mucociliar escalator. Particles between 1,000 – 10,000 µm will **diffuse** into the alveoli due to displacement when they collide with air molecules (Sha et al., 2015; Tedja et al., 2011).

Another mathematical model describing nanoparticle deposition in human respiratory system is Multiple-Path Particle Dosimetry model (MPPD) (Anjilvel & Asgharian, 1995; Asgharian et al., 2001; RIVM, 2002; Miller et al., 2016). The MPPD model predict that inhaled nanoparticles size 10 nm (0.01 µm) will in majority deposit in the tracheobronchial region (> 30 %) and to a lesser extent in the pulmonary regions (around 13 %) (Miller et al., 2016)

The respiratory system has clearance systems for deposited particles; coughing and sneezing. These physiological mechanisms are effective in removing coarse particles, while fine particles are removed by several mechanisms: (i) the liquid lining layer and aqueous including mucus that will eventually be swallowed and eliminated through the gastro-intestinal (GI) system; (ii) mucociliar escalator that will move the particles up the respiratory system and into the GI system; and (iii) macrophage phagocytosis the nanoparticles in the macrophages will then be eliminated in the liver and the bile and excreted via feces (Oberdörster et al., 2005; Semmler-Behnke et al., 2007; Geiser & Kreyling, 2010). Nano $TiO_2$ particles have been found to accumulate in the lungs' interstitial tissue, particularly in the alveoli, and then translocated by the blood circulation and lymphatic vessels into different target organs, which include lymph nodes, kidney, liver, heart, and brain (Wang et al., 2008; Kreyling et al., 2010; Geiser & Kreyling, 2010; Gaté et al., 2017).

### 2.9 Analytical techniques for analyzing nanoparticles

At present, there are several techniques for measuring airborne nanoparticles. Selecting the appropriate techniques depend on what you want to know, feasibility, type of samples, and cost. The nanoparticle measurement instruments generally provide size, size distribution, number concentration, mass concentration, surface area, elemental composition and morphology. The instruments used for measuring airborne nanoparticles and their corresponding analytical techniques are shown in Table 2.

Table 2: Nanoparticles instruments and analytical techniques

| Abbreviation | Full name | Technique | Sensitivity |
|---|---|---|---|
| **Particle number concentration** | | | |
| CPC | Condensation particle counter | Condensation particle counter | 10 to 1,000 nm |
| APA | Automated particle analysis | - | 25 nm to100 µm |
| APS | Aerosol particle sizer spectrometer, Aerodynamic particle sizer spectrometer | Spectrometer | 0.5 to 20 µm |
| DCM | Diffusion charging monitor | Diffusion charger plus electrometer | 10 to 1,000 nm |
| DiSCmini | DiSCmini | Diffusion charge particle | 10 and 700 nm |
| DM | Dust monitor | - | 0.25 to 32 mm. |
| DMA | Differential Mobility Analyzer | Charge particle | 2 to 165 nm |
| EEPS | Engine Exhaust Particle Sizer | Unipolar diffusion charger | 5.6 to 560 nm |
| EMS | Electrical mobility spectrometer | Spectrometer | 10 to 420nm |
| FMPS | Fast Mobility Particle Sizer | Charge particle | 5.6 to 560 nm |
| Nano ID | NanoID NPS500 (Naneum) | - | 5 to 500 nm |
| OPC | Optical particle counter | Light scattering | 0.25 to 32 µm |
| OPS | Optical particle sizer | Light scattering | 0.3 to 10 µm |
| PAS | Portable aerosol spectrometer | Light scattering | 0.25 to 32 µm |
| SMPS | Scanning mobility particle sizer | Charge particle | 10 to 1,000 nm |
| SMPS+DMA | Scanning mobility particle sizer combining a differential mobility analyzer | Charge particle | 15 to 710.5 nm |
| UCPC | Ultrafine condensation particle counter | CPC | 14 to 630 nm |

| Abbreviation | Full name | Technique | Sensitivity |
|---|---|---|---|
| **Mass concentration** | | | |
| BCM | Black carbon monitors, Portable aethalometer | Absorption of transmitted light | 0-1 mg BC/m3 |
| ELPI | Electrical low-pressure impactor | Impactor low pressure | 7 nm to 10 µm |
| DT+DOC | DustTrak equipped with a Dorr-Oliver cyclone | Optical particle counter | 0.001 to 100 mg/m3 |
| LP | Laser photometer, Aerosol photometer | Light scattering | 0.001 to 150 mg/m3 |
| PhAS | Photoelectric aerosol sensor | UV radiation | 0 to 4000 ng/m3 |
| PhM | Photometer-optical particle counter | Optical particle counter | 0.001 to 150 mg/m3 |
| PhM+DOC | Photometer equipped with a Dorr-Oliver cyclone | Optical particle counter | 10 nm to 4 µm |
| **Elemental carbon and composition analysis** | | | |
| EDX | Energy-dispersive X-ray analyzer | Energy-dispersive X-ray analyzer | - |
| ICP-MS | Inductively coupled plasma mass spectrometry | Inductively coupled plasma mass spectrometry | - |
| LIBS | Laser-induced breakdown spectroscopy | Laser-induced breakdown spectroscopy | - |
| SEM-EDX | Scanning electron microscopy energy dispersive X-ray spectroscopy | Scanning electron | - |
| TOA | Thermal-optical analysis | Flame ionization detector (FID) | LOD 0.4 µg/m3 |
| **Morphology** | | | |
| SEM | Scanning electron microscopy | Scanning electron | < 1 nm |
| STEM | Scanning transmission electron microscopy | Scanning transmission electron | < 1 nm |
| TEM | Transmission electron microscopy | Transmission electron | < 1 nm |

Two studies from NIOSH called "Nanoparticle Emission Assessment Techniques (NEAT 1.0 and NEAT 2.0)" (Methner et al., 2010; Eastlake et al., 2016) suggested strategy used to measure airborne nanoparticles. The direct reading instruments such as CPC and OPC can detect nanoparticles from release source, working activity and for evaluate the efficiency of engineering control. However, direct reading can not identify type of nanoparticles, therefore personal sampling with a filter has been suggested.

Mass concentration collected on 37 mm diameter open-face cassettes filter equipped with quartz fiber filters (QFF) has been suggested for elemental carbon (EC) following NIOSH Manual of Analytical Methods (NMAM) 5040 using thermal-optical analysis; flame ionization detector (FID) technic (Methner et al., 2010; Eastlake et al., 2016). The TEM study following NMAM 7420, the particles collected onto 37 mm diameter open face cassettes filter equipped with mixed cellulose ester (MCE) filter has also been suggested (Methner et al., 2010) (Eastlake et al., 2016).

Elemental analysis have been suggested to characterize nanoparticles composition. Aerosols collected onto cellulose ester filter and analyzed using electron microscopy with X-ray energy dispersive spectroscopy (SEM-EDX). In addition, another technique for the elemental composition analysis follow NIOSH Method 7300 using inductively coupled plasma atomic emission spectroscopy (ICP-AES) (Methner et al., 2010; Eastlake et al., 2016).

**2.10 Occupational exposure limit (OEL) for $TiO_2$**

The United States Occupational Safety and Health Administration (US OSHA) set a permissible exposure limit (PEL) for Portland cement containing crystalline silica ($SiO_2$) less than 1 % to 15 mg/m$^3$ and PEL of 10 mg/m$^3$ for total dust and 5 mg/m$^3$ for respirable dust (OSHA, 2018; NIOSH, 2011b). The American Conference of Governmental Industrial Hygienists (ACGIH) set a threshold limit value - time-weighted average (TLV - TWA) for Portland cement with no asbestos and the crystalline silica less than 1% to 1 mg/m$^3$ (ACGIH, 2015)

While another country had recommendation for total and respirable dust. Worldwide, only few OELs exist for nano $TiO_2$. In the US, OSHA and National Institute for Occupational Safety and Health (NIOSH) recommended an exposure limit for nano $TiO_2$ for 8 hours as following (NIOSH, 2011a; OSHA, 2013):

- The particle size greater than 100 nm OEL= 2.4 mg/m3
- The particle size below 100 nm OEL= 0.3 mg/m3

The French Agency for Food, Environmental and Occupational Health & Safety (ANSES) recommends a toxicity reference value (TRV) for inhaled $TiO_2$ nanoparticle particle sized 25 nm (P25) of 0.12 µg/m$^3$ (ANSES, 2019).

NIOSH recommend immediately dangerous to life or health (IDLH) exposure to $TiO_2$ particle not exceed 5,000 mg/m$^3$ (NIST, 2015). In addition, many countries have been regulated for $TiO_2$ exposure level based on particle mass fraction as respirable or total dust as shown in Table 3.

Table 3: Occupational exposure limit for $TiO_2$ (WHO, 2010)

| Country | TWA-Concentration ($mg/m^3$) | Remark |
|---|---|---|
| Austria | 6 | |
| China | 8 | Total dust |
| Denmark | 6 | |
| France | 10 | |
| Germany | 1.5 | Respirable dust |
| Hong Kong | 3 | Total dust |
| Norway | 5 | Inhalable dust |
| Poland | 10 | Inhalable dust |
| United Kingdom | 4 | Respirable dust |
| Switzerland (SUVA, 2017) | 3 | Respirable dust |
| Thailand | No standard<br>Inhalable dust = 15 $mg/m^3$, Respirable dust = 5 $mg/m^3$ | |

**2.11 Nanoparticle exposure prevention and control** (NIOSH, 2013; OSHA, 2013; NIOSH, 2012)

Exposures to nanoparticles should be as low as reasonably achievable) (ALARA principle or in Europe the precautionary principle), therefore exposure control measures and exposure reduction strategies are important parts in protecting workers. The hierarchy of control measures for nanoparticles follow the hierarchical occupational hygiene method; elimination, substitution, engineering controls, administrative controls, and use of personal protective equipment (PPE) (NIOSH, 2013).

**Elimination and substitution** are generally the most effective if implemented during a design process. A wet process such as water spray should be considered when working with an airborne nanoparticle. Bello et al. reported wet suppression techniques can reduce carbon nanotubes concentration to background levels during sawing nanocomposite (Bello et al., 2009). Design nanoparticle workplace to separate and isolate from normal work. In addition, design buffer and decontamination zone to ensure that nanomaterials are not released to adjacent workplace (NIOSH, 2013).

**Engineering controls** are effective in reducing nanoparticle exposures at the generation and release point. Enclosed systems for example glove box containment, local exhaust ventilation (LEV) (e.g., capture hood, enclosing hood) and process chamber equipped with high-efficiency particulate air (HEPA) filters are suggested (NIOSH, 2011a; NIOSH, 2012; NIOSH, 2013; OSHA, 2013; Goede et al., 2018). However, in the construction sector, working condition cannot generally be enclosed. Therefore, portable capture hoods and vacuum machines equipped with HEPA filters designed to capture the nanoparticles at the point of generation or release are recommended.

**Administrative controls** are important parts in nanoparticle exposure reduction strategy and focus on human awareness. The administrative control technics suggested in the US are as following (NIOSH, 2011a; NIOSH, 2012; NIOSH, 2013; OSHA, 2013)

- Provide education and training on the safe handling of nanomaterials.
- Provide health safety procedure, instruction and signage.
- Encourage hygiene behavior to workers to i.e. hand-washing before and after eating or leaving the workplace. Avoid eat, drink and smoking in workplaces.
- Provide facilities for changing clothes and showering at the workplace. Avoid taken contamination materials out of working area.

- Avoid direct exposure with nanomaterials.
- Establish procedures to cleanup and spills of nanoparticles to minimize worker exposure (avoid dry sweeping).
- Dispose of all waste material separate from normal waste.

**Personal protective equipment (PPE)** should be used as a last resort when the working conditions cannot be controlled well. The employer should provide the appropriate PPE not only for normal working conditions but also for emergencies. The PPE selection depends on type of nanomaterials, working condition, exposed duration, potential hazards, size distribution and concentration of nanoparticles. In addition, training, fit testing and maintenance are important.

Respiratory protective equipment (RPE) are important for protecting worker from inhaled airborne nanoparticle exposure. OSHA and NIOSH recommend respirator types N100 (not resistant to oil), R100 (resistant to oil) and P100 (oil proof) (OSHA, 2013; OSHA, 2011; NIOSH, 2014; NIOSH, 2012). The European recommendation is to use the highest respiratory protection (P3) and filtering face pieces (FFP3) described in standard (EN 143 and EN 149) (Goede et al., 2018; Rengasamy et al., 2009).

Glove and protective clothing can protect the worker from nanoparticle by skin exposure. In the present, there are no specific standard and guideline for skin protection. Nitrile gloves or other chemically resistant and impermeable nanomaterials gloves have been suggested (NIOSH, 2012). Appropriate protective clothing includes shoes made specifically from low permeability material. Cotton should not be used in work with wet nanomaterials (NIOSH, 2012). Goggles are recommended for eye protection (AIHA, 2015).

# CHAPTER III

# OBJECTIVES

The objective of this study was to characterize airborne particle by determining size distribution, concentration, morphology, elemental composition and ROS between photocatalytic and regular cement.

**Objective 1: Laboratory aerosolization (chapter V)**

The objective of this study was characterized photocatalytic and regular cement using aerosolizing system. The study was compared of size distribution, number concentration, mass size distribution, morphology and elemental composition.

**Objective 2: Simulation working activities and construction site sampling (chapter VI)**

The study aim was to characterize airborne nanoparticle exposures during typical construction work activities for photocatalytic and regular cement in exposure chamber. In addition, in construction were sampling in Switzerland and Thailand. The comparison parameters as following; nanoparticle size distribution, number concentration, mass size distribution, morphology, elemental composition, phase analysis, crystallin silica, respirable and total dust.

**Objective 3: Reactive oxygen species (ROS) measurement (chapter VII)**

The study aims at evaluated ROS production from airborne particles from both photocatalytic and regular cement powders under laboratory-controlled (i.e. UV and relative humidity). In addition, two working activities were compared as cement bag emptying and concrete cutting.

# CHAPTER IV

# STUDY MATERIALS

### 4.3 Study instruments

The airborne nanoparticles were characterized with several nanoparticle measurement instruments such as size distribution, number and mass concentration, morphology, phase analysis and elemental composition analysis. The instruments used on this study showed in Table 4.

Table 4: The instruments used on this study

| Instrument | Technique | Sensitivity | Detection limit |
|---|---|---|---|
| **Direct reading** | | | |
| Scanning mobility particle sizer (SMPS) | Charge particle | 11 to 1,083 nm | $10^8$ pt/cm$^3$ |
| Portable aerosol spectrometer (PAS) | Light scattering | 250 to 32,000 nm | $2x10^6$ pt/cm$^3$ |
| DiSCmini | Diffusion charge particle | 10 and 700 nm | $10^6$ pt/cm$^3$ |
| **Particle mass fraction** | | | |
| Impactor | Gravimetric | 0.52 to 21.3 µm | - |
| Inhalation filter cassette | Gravimetric | 50% Cut-point: 100 µm | - |
| Cyclone | Gravimetric | 50% Cut-point: 4 µm | - |

| Instrument | Technique | Sensitivity | Detection limit |
|---|---|---|---|
| **Morphology study** | | | |
| Transmission electron microscope (TEM) | Transmission electron | < 1 nm | - |
| Scanning electron microscope (SEM) | Scanning electron | < 1 nm | - |
| **Elemental composition analysis** | | | |
| Scanning electron microscope energy dispersive X-ray spectroscopy (SEM-EDX) | Scanning electron | Elemental composition analysis | - |
| X-ray diffraction (XRD) | X-ray diffraction | Identification crystalline phase | - |

**4.3.1 Scanning mobility particle sizer (SMPS):** (SMPS; model SMPS+C model 5400, Grimm Aerosol Technik GmbH & Co. KG, Ainring, Germany) Airborne nanoparticles size distribution and number concentration were measured with SMPS the range size between 11 and 1,083 nm. The operation condition of SMPS as following; sampling flowrate at 0.3 - 0.6 liter per minute (l/min), relative humidity condition from 0 to 95 % and ambient temperature between 0 and 40°C. The concentration limit of SMPS up to $10^8$ pt/cm$^3$. In addition, SMPS provide the geometric mean size of airborne nanoparticle.


Figure 4: Scanning Mobility Particle Sizer (SMPS)

**4.3.2 Portable aerosol spectrometer (PAS):** (PAS; model 1.109, Grimm Aerosol Technik GmbH & Co. KG, Ainring, Germany) Fine particle size distribution between 250 nm to 32 µm and number concentration were measured with PAS. The PAS contained 4 different measurements parameter included particle number concentration, mass concentration, occupational health (inhalable, thoracic and respirable fraction) and environmental (PM1, PM2.5, and PM10). In addition, the concentration limit of fine particle up to 2,000,000 pt/liter.

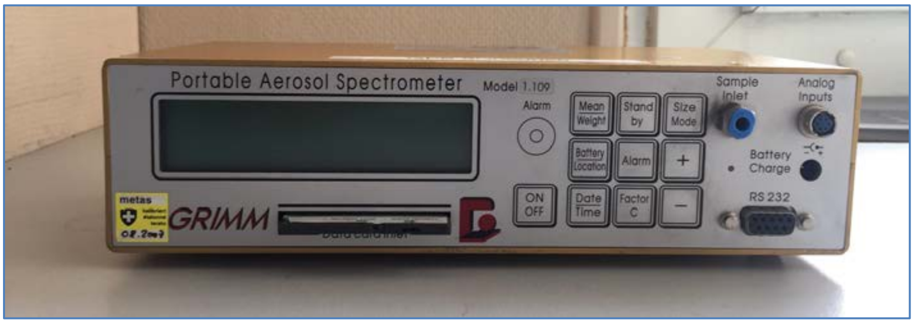


Figure 5: Portable Aerosol Spectrometer (PAS)

**4.3.3 DiSCmini** (DiSCmini; Testo North America, West Chester, PA USA.) is a portable direct reading using for personal nanoparticle monitoring and walk-through surveys on working condition. Nanoparticle size between 10 and 700 nm and particle number concentration around 1,000 to 1,000,000 pt/cm$^3$ were measured with DiSCmini. In addition, DiSCmini provided function to measure lung deposited surface area (LDSA). The probability of particles in the lung both for the alveolar and the tracheobronchial region following by ICRP model. The detection limit of DiSCmini around 1,000,000 pt/cm$^3$.


Figure 6: DiSCmini

**4.3.4 Impactor** (Marple; Thermo Fisher Scientific, Air Quality Instruments, Franklin, MA, USA.) Aerodynamic mass particle size distributions from 0.52 to 21.30 µm were measured with an 8-stage cascade impactor. The operation sampling with personal pump at 2 L/min equipped with 34 mm diameter of Aluminium (on stage 1-8) and PVC filter (on back-up stage)

| Impactor Stage Number | Cut-Point (µm) |
|---|---|
| 1 | 21.3 |
| 2 | 14.8 |
| 3 | 9.8 |
| 4 | 6.0 |
| 5 | 3.5 |
| 6 | 1.55 |
| 7 | 0.93 |
| 8 | 0.52 |
| Back-Up Filter | 0 |

Figure 7: 8-stage cascade impactor

**4.3.5 Inhalable particle sampler (IOM)** (IOM and PVC filter; SKC Inc., Eighty Four, PA, USA)**:** Inhalable fraction (50% cut-point: 100 µm) was measured with IOM equipped with 25 mm PVC filter (PVC filter; SKC Inc., Eighty Four, PA, USA). The operation sampling with personal pump at 2 L/min.

**4.3.6 Cyclone** (Casella US, Buffalo, NY, USA)**:** Respirable fraction (50% cut-point: 4 µm) was measured with plastic cyclone (Higgins-Dewell), sample flow rate 2.2 L/min with 37 mm PVC filter (PVC filter; SKC Inc., Eighty Four, PA, USA). The respirable dust sampling followed NIOSH method 0600. In addition, crystalline silica measured with cyclone follow NIOSH method 7602 using infrared absorption spectrophotometry technique (IR; IRAffinity-1S1, Shimadzu, Kyoto, Japan).

**4.3.7 Elemental composition:** Aerosolized experimental, airborne nanoparticles were collected onto holey Transmission Electron Microscopy (TEM) grids TEM grid; Quantifoil R1/4, Quantifoil Micro Tools GmbH, Germany) using a mini particle sampler (MPS) and a sampling flowrate of 0.3 liters per minute. While construction working activities sampling airborne particles were removed from IOM filter into carbon black sticker. Then, elemental compositions analysis using scanning electron microscope energy dispersive X-ray spectroscopy (SEM-EDX) technique (SEM-EDX; PHENOM XL BSE detector at 15kV).

**4.3.8 Morphology study:** Airborne nanoparticles particles were collected onto TEM grid (TEM grid; Quantifoil R1/4, Quantifoil Micro Tools GmbH, Germany) using particle mini sampler (MPS) with sampling flowrate 0.3 L/min (MPS; Ecomesure, Sacly, France). Nanoparticles morphology were analyzed by a transmission electron microscope (TEM) (TEM; CM-100, JEOL, USA at 80 kV) and scanning electron microscope (SEM) (PHENOM XL BSE detector at 15kV).

**4.3.9 X-ray diffraction:** The polymorphs of cement powder in bags both of photocatalytic and regular cements were analysed by X-ray diffraction. X-Ray diffraction was performed using Panalytical X'pert Pro MPD with a step width 0.0167° from 5° to 70° and time per step of 59.65 s (Malvern Panalytical, Malvern, United Kingdom).

# CHAPTER V

# LABORATORY AEROSOLIZATION

**Published: Journal of Aerosol Science and Technology**

https://doi.org/10.1080/02786826.2019.1578334

## Article topic

### Characterization of nanoparticles in aerosolized photocatalytic and regular cement

**Kiattisak Batsungnoen**[1,2], Nancy B Hopf[1], Guillaume Suárez[1] and Michael Riediker[1, 3]

1. Institute for Work and Health (IST), University of Lausanne and Geneva, Switzerland. Nancy.Hopf@hospvd.ch, Kiattisak.Batsungnoen@chuv.ch, Guillaume.Suarez@chuv.ch
2. Institute of Public Health, Suranaree University of Technology, Thailand
3. Swiss Centre for Occupational and Environmental Health (SCOEH), Winterthur, Switzerland, michael.riediker@alumni.ethz.ch

**Corresponding author:** Nancy B Hopf, PhD

**Keywords:** photocatalytic cement, $TiO_2$ nanoparticle, nano cement, nano construction, nano $TiO_2$

## ABSTRACT

Photocatalytic cement containing nano-$TiO_2$ has been introduced to the construction industry because of its biocidal and self-cleaning properties. Although, $TiO_2$ is classified as possibly carcinogenic to humans, the cancer risk among cement workers is currently unknown. This is partly because an assessment of exposures to airborne photocatalytic cement is missing. We characterized airborne photocatalytic cement in an experimental aerosolization set-up and compared it to regular cement. Aerosolized nanoparticle size distributions and concentrations were measured with a scanning mobility particle sizer (SMPS) and a portable aerosol spectrometer (PAS). Particle morphology was analyzed with a scanning electron microscopy (SEM) and transmission electron microscopy (TEM). Energy Dispersive X-Ray Analysis (SEM-EDX) was used for elemental determination.

The aerosolized photocatalytic cement powder contained 5% nanosized particles in number concentration while regular cement had only a negligible amount. Airborne photocatalytic cement concentration was 14,900 particles per cubic centimeter (pt/cm$^3$) with a geometric mean diameter (GMD) of 249 nm (geometric standard deviation; GSD ±2 nm). Airborne regular cement concentration and GMD (GSD) were 9,700 pt/cm$^3$ and 417 nm (±2 nm), respectively. Photocatalytic cement contained 18.5 times more airborne nano $TiO_2$ (37%) compare to bagged powder (2%).

Aerosolized photocatalytic cement had a significantly smaller particle size distribution and greater particle concentration compared to regular cement. Both types of cement had 99% of the particles with sizes less than 1 µm. Nano $TiO_2$ was directly aerosolized from the cement,

followed with a coagulation/agglomeration process. Future studies should evaluate workers' exposures associated with the use of photocatalytic cement.

## 1. Introduction

Nanotechnology concerns matter at the nanoscale ranging between 1 nanometer (nm) and 100 nm, and has led to the production of new materials, devices, and structures (ISO/TS 27687 2008; OSHA 1999; Mann 2006; OSHA 2013). In the construction industry, a new generation of "green" or "photocatalytic cement" has evolved over the past decade. These cements contain nanoscale titanium dioxide (nano $TiO_2$), which act as a radical-forming catalyst in the presence of oxygen. Radicals do not only react with bacteria, fungi, and other microorganisms, but also with air pollutants, deposited volatile organic compounds and soot. They thereby act as biocides rendering surfaces as "self-cleaning" (Lan, Lu, and Ren 2013; Carp, Huisman, and Reller 2004; Chen and Poon 2009). The world-wide cement consumption was 158 million metric tons in 2013 (PCA, 2013). An estimated 319,300 employees or 8% of the Swiss workforce work in the Swiss construction industry (FSO, 2017). The amount of photocatalytic cement consumed is not known nor is the number of workers using this new type of cement.

$TiO_2$ was classified by the International Agency for Research on Cancer (IARC) in 2006 as "possibly carcinogenic to humans" (Group 2B). The inadequate evidence of carcinogenicity in humans (WHO 2010; IARC 2017), came partially from the lack of exposure assessment in the epidemiological studies (Baan, 2007). No data were available for the IARC Monograph working group regarding the characterization or quantification of exposure to ultrafine (<100 nm) $TiO_2$ particles.

Nano $TiO_2$ exposures depend on the particles' physical and chemical properties, working conditions, frequency of use, task duration, and air concentration. The latter will depend on the particles size. The amount of inhaled nano-$TiO_2$ will depend on the particle size distribution. Particles >10 µm will impact in the upper respiratory region or be carried out by the mucociliar escalator; while particles between 1,000 – 10,000 µm will diffuse into the alveoli (Sha et al. 2015; Tedja et al. 2011). Nano-$TiO_2$ particles have been shown to accumulate in the lungs' interstitial tissue, especially in the alveoli, and translocate into the blood circulation where they are transported to different target organs (lymph nodes, kidney, liver, heart, and brain) (Wang et al. 2008; Kreyling, Hirn, and Schleh 2010; Geiser and Kreyling 2010; Gaté et al. 2017).

About two percent by weight nano-$TiO_2$ is added to regular cement to make photocatalytic cement. We calculated the percentage from the SEM-EDX analysis, as this information is not publicly available. These nano-$TiO_2$ particles are not chemically bound to the cement. Nanoparticles are in general easily airborne but can also agglomerate/aggregate to larger particles depending on their intrinsic physical and chemical properties. This is needed to develop protective measures for workers using photocatalytic cement.

Our aim was to characterize airborne photocatalytic and regular cement by determining size distribution, concentration, morphology and elemental composition using an aerosolizing system previously described by Ding and Riediker (2015, 2016). Special attention was given to particles in the nano-range both in the obtained cement powders as well as for the airborne fraction.

## 2. Materials and Methods

We compared two types of cement: regular Portland cement type I (cement-clinker; CE number 266-043-4) produced in Switzerland, and photocatalytic cement obtained from Italcementi group. We verified that both cements had similar stochiometric compositions apart from $TiO_2$ content measured with SEM-EDX. The cement powders were aerosolized using an aerosolizing system described earlier (Ding & Riediker, 2015) following the experimental procedures described in Ding & Riediker, (2016). Briefly, dry air was blown upwards through a glass funnel containing cement powder (2 g). This aerosolized the powder in the bottom of the funnel where the airflow was turbulent (Figure 1). The aerosolized particles were then diluted with air, adjusted for temperature and humidity, and led into the measurement chamber. The experiments were repeated three times. The size distribution was measured as soon as the aerosolizing system reached stable particle concentration readings.

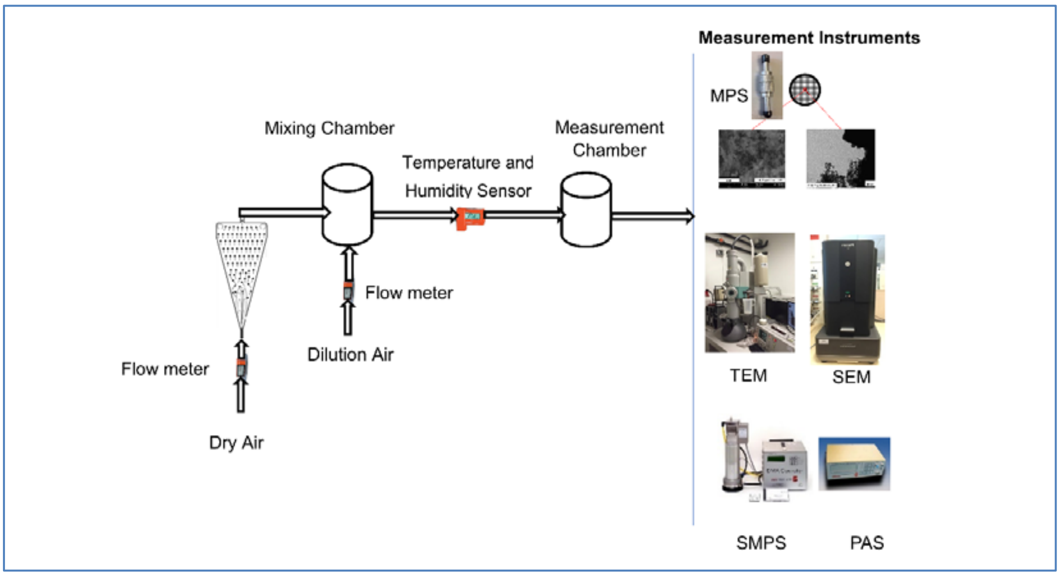


Figure 1: Schematic of the experimental set-up. Cement powder was deposited in the glass funnel and the dry air suspends the particles in the air and moves the fine particle fraction to the mixing and measurement chambers. The analytical instruments used are listed on the right.

Nanoparticle size distributions and concentrations were measured with a scanning mobility particle sizer (SMPS; SMPS+C model 5400, Grimm Aerosol Technik GmbH & Co. KG, Ainring, Germany), configured to measure particle sizes ranging from 11 to 1,083 nm. The SMPS charges the particles that the mobility analyzer classifies by polarity according to their electrical mobility; and lastly, the particle counter determines the number concentration of the mobility-classified particles. A portable aerosol spectrometer (PAS; model 1.109, Grimm Aerosol Technik GmbH & Co. KG, Ainring, Germany) was used to measure concentrations of fine particles from 250 to 32,000 nm. The PAS measures the intensity of light scattered from aerosol particles through a focused light, and the amount of incident scattered light is a function of particle size. The PAS measures particle number concentrations in 31 bins from 250 nm to 32,000 nm and calculates mass concentrations in three particle size fractions ($PM_1$, $PM_{2.5}$, and $PM_{10}$). For particle morphology determination, the aerosol particles were collected onto transmission electron microscopy (TEM) grids (Quantifoil R1/4, Quantifoil Micro Tools GmbH, Germany) using a mini particle sampler (MPS, flowrate 0.3 L/min) (Ecomesure, Sacly, France). TEM-grid sampling was stopped when the cumulative collected number concentration measured by SMPS was around $10^6$ particles. The TEM grids were analyzed by a scanning electron microscope (SEM) (PHENOM XL BSE detector at 15kV) and a transmission electron microscope (TEM) (TEM CM-100 (JEOL, USA) at 80 kV) for morphology; and by energy dispersive X-ray spectroscopy (SEM-EDX) for elemental composition. In addition, a sample of the cement powders as they existed in the cement bag ("bagged powder") was obtained and analyzed chemically as well as morphologically.

Statistical analyses were performed using STATA15. Size difference and concentration difference were compared using two sampled t-test.

## 3. Results

### 3.1 Nanoparticle size number distribution and number concentration

The SMPS showed the photocatalytic cement mean concentration to be 14,900 pt/cm$^3$ and 9,700 pt/cm$^3$ for regular cement. Photocatalytic cement had a geometric mean diameter (GMD) of 249 nm and a geometric standard deviation (GSD) of 2 nm, while regular cement had a GMD of 417 nm (GSD 2 nm). The particle size distribution and concentration for aerosolized photocatalytic and regular cement are shown in Figure 2. Between 11 and 545 nm (11 and 1,083 nm SMPS range) (x-axis), the photocatalytic cement had a greater nanoparticle number concentration (y-axis) than regular cement. Maximum particle number concentration was 12,700 pt/cm$^3$ for photocatalytic cement particles in the range 214.4-241.0 while regular cement had two maximum concentrations: 7,250 and 7,150 pt/cm$^3$ at 271.8 nm and 692.1 nm, respectively.

Particle number size distributions were measured with two different instruments: SMPS (11-1,083 nm) and PAS (250-32,000 nm). For simplicity and because the SMPS is more accurate in the nanoparticle region, we used the SMPS results in the overlapping nanoparticle size region (250-1,083 nm) when we combined the results from the two instruments. We used the SMPS results up to 1,083 nm and PAS results from this size to 32,000 nm. Figure 2 shows the particle size distributions of photocatalytic and regular cement measured by SMPS and PAS. Table 1 shows particle number and mass concentration for photocatalytic and regular cement. The photocatalytic cement size distribution had a mean number concentration of 16,710 pt/cm$^3$ with a GMD of 412 nm and a GSD of 2 nm (Table 1). The regular cement mean was 11,700 pt/cm$^3$ with a GMD of 599 nm and a GSD of 2 nm (Table 1). The nanoparticle size for the photocatalytic cement was significantly smaller than for regular cement (two-sample t-test, p-value < 0.0005). Furthermore, the particle number concentration for photocatalytic cement was significantly greater than for regular cement particles (p-value < 0.0005).

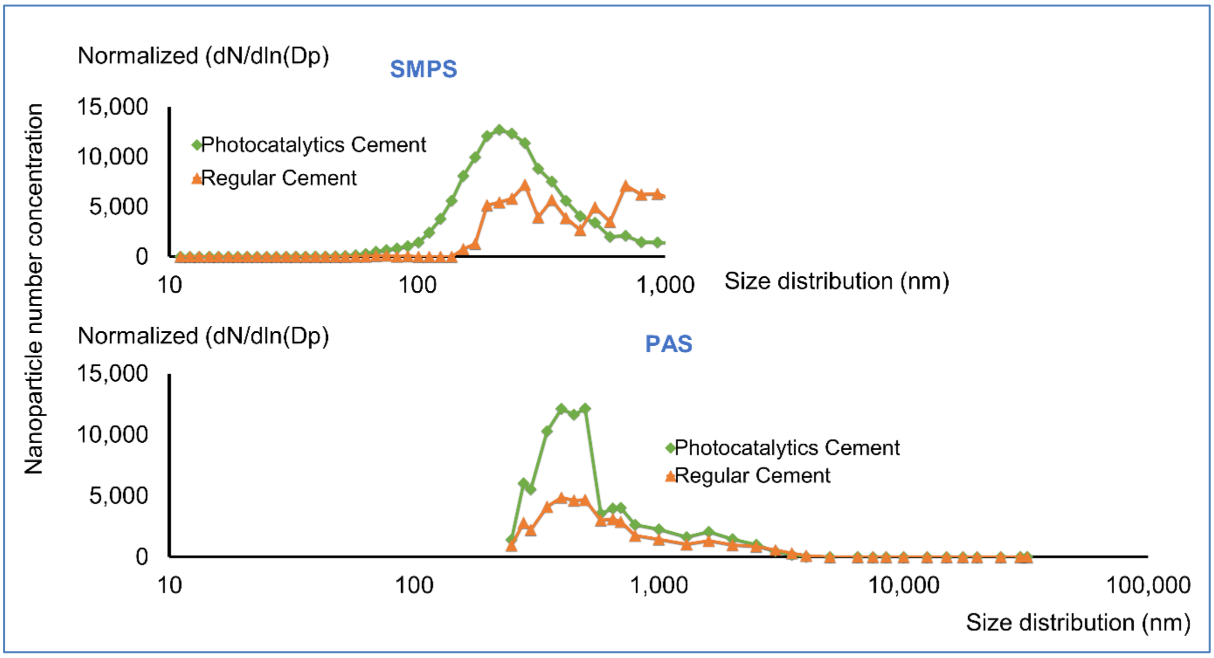


Figure 2: Particle number size distribution for photocatalytic and regular cement the size distribution information obtained by SMPS and PAS. SMPS measure the nanoparticles size range from 11 to 1,083 nm, while PAS measure fine particle from 250 to 32,000 nm.

Photocatalytic cement had about 4.7 % of the aerosolized particles in the nanoscale, while regular cement only had 1/10$^{th}$ of this (0.4 %). Both cement types had over 90 percent of the particle count in the size range less than 1 µm. The mass concentration measured by PAS showed more airborne mass for photocatalytic cement (5,130 µg/m$^3$, SD = 0.3), compared to regular cement (1,916 µg/m$^3$, SD = 0.1) as shown in table1.

Table1: Particle number and mass concentration measured for photocatalytic and regular cement from triplicate experiments.

| Cement type | Total Conc. | Number concentration (pt/cm$^3$) | | | | |
|---|---|---|---|---|---|---|
| | | GSD. | 10- 100 nm | 100- 1,000 nm | 1-10 µm | >10 µm |
| Photocatalytic cement | 16,710 (100%) | 420 | 783 (4.7%) | 14,500 (86.8%) | 1,430 (8.5%) | 0 (0%) |
| Regular cement | 11,700 (100%) | 307 | 43 (0.4%) | 10,600 (90.6%) | 1,050 (9.0%) | 0 (0%) |
| | | Mass concentration (µg/m$^3$) | | | | |
| Photocatalytic cement | 5,103 (100%) | 0.3 | - | 1,210 (23.7%) | 3,879 (76.0%) | 14 (0.3%) |
| Regular cement | 1,916 (100%) | 0.1 | - | 473 (24.7%) | 1,442 (75.3%) | 1 (0.0%) |

Figure 3 shows the mass-size distribution for both cement types. Photocatalytic cement had a maximum value at 2.0 µm and regular cement at 2.5 µm.

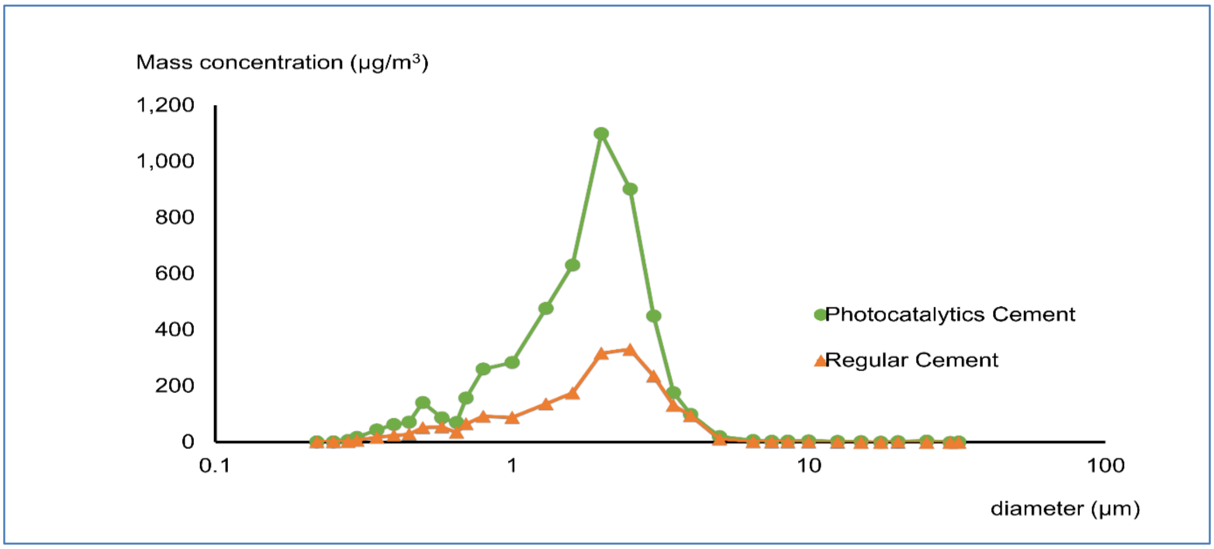


Figure 3: Mass-size distribution of photocatalytic cement and regular cement measured with PAS.

### 3.2 Elemental composition analysis

Elemental composition of the bagged powder and their airborne particles collected onto filters after aerosolization were determined by SEM-EDX analysis. As expected, calcium oxide (CaO) was the most abundant material by mass followed by silicon dioxide ($SiO_2$), as shown in Figure 4. Aerosolized particles from regular cement showed a similar elemental distribution as the material powder. There were however, clear differences in relative mass percentage between the cement types. The relative mass from CaO in photocatalytic cement powder was 62.4%, while this only made up 31.2% in the aerosolized form. The relative contribution of $TiO_2$ showed the opposite pattern with 2.0% in the raw material and 37.4% in the aerosolized particles.

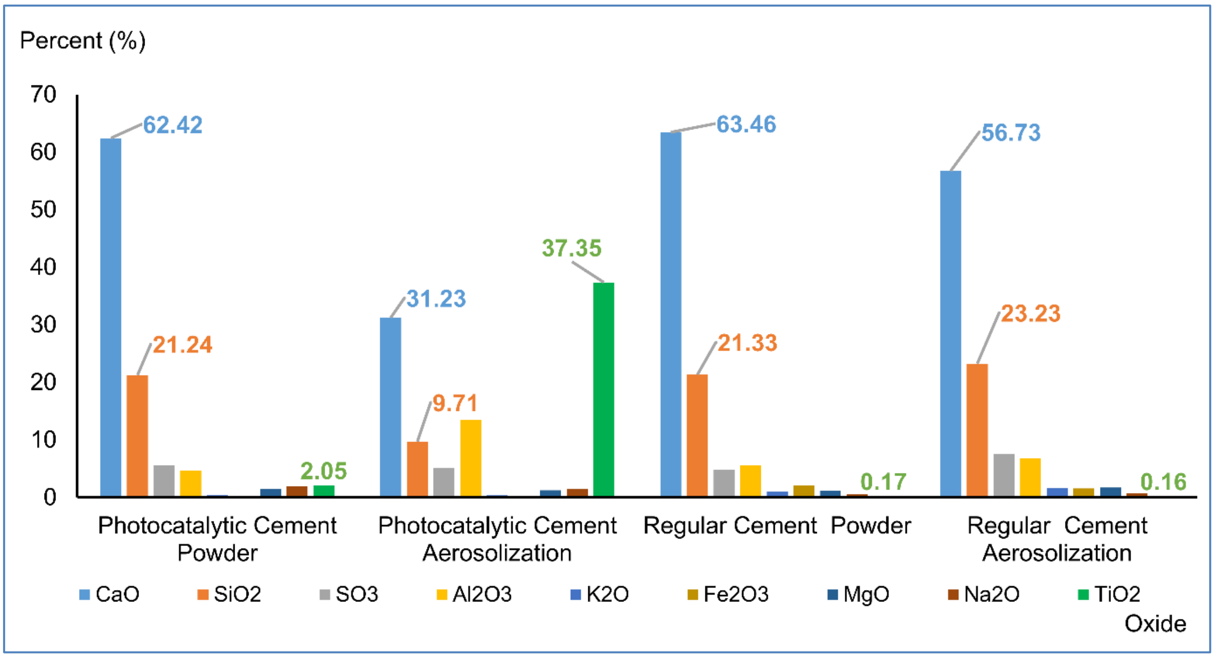


Figure 4: Elemental composition analysis (SEM-EDX) given in percent for each substance contained in regular and photocatalytic cements, both in powder and aerosol forms.

### 3.3 Morphology study

Analysis by SEM and TEM found similar morphology for photocatalytic and regular cement bagged powder (Figures 5A and 5B). Particles collected onto filters after aerosolization, however, differed considerably depending on cement type: photocatalytic cement showed a much greater number of small particles than regular cement. The TEM images also suggest that photocatalytic cement consisted of two distinct particle types that differed in morphology and in size (c.a. 50 nm and > 200 nm, respectively (Figure 5C and 5D) magnification with focus on particles of around 50 nm size). The regular cement contained only coarse particles (Figure 5D). The presence of nano-ranged spherical particles that was only found in the photocatalytic cement might possibly be attributed to nano $TiO_2$ (Figure 5E).

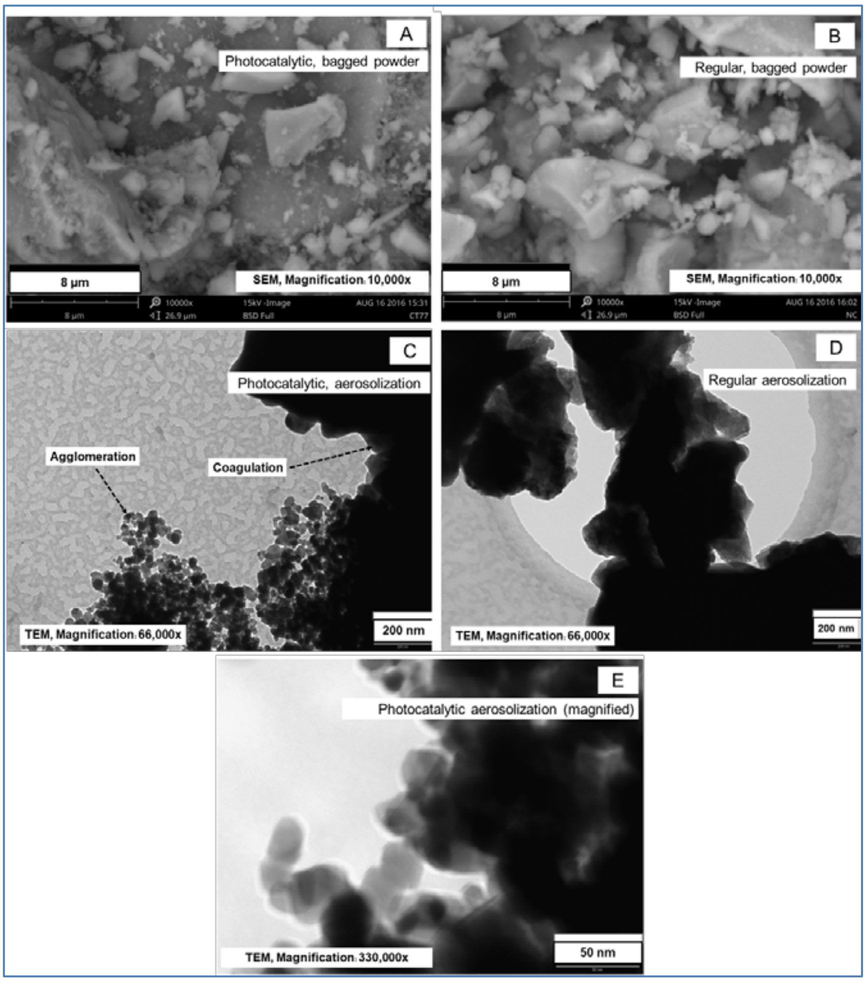


Figure 5: Schematic of SEM and TEM images of photocatalytic and regular cement.

## 4. Discussion

Aerosolized photocatalytic cement had a greater concentration of nanoscale particles compared to aerosolized regular cement. The morphology results confirmed that (1) the photocatalytic cement contained nanoparticles and (2) $TiO_2$ is a constituent of the photocatalytic cement aerosol. Taken together, this suggests that nano $TiO_2$ can be easily mobilized from photocatalytic cement powder when aerosolized. This can be expected if the nano $TiO_2$ particles are not chemically bound to the larger cement particles.

It is important to note that the $TiO_2$ content in photocatalytic bagged cement powder was only 2 % while reaching 37 % in the aerosolized form. In stable conditions, the aerosolized photocatalytic cement contained about 5% of airborne nanoparticle numbers, presumably $TiO_2$. It is likely that a part of the airborne nano$TiO_2$ was present in the form of agglomerates as seen previously by (Ding & Riediker, 2015); however, we did not verify this in our experiments. Since cement particles were only 5% of the nanosized particles, this would not be sufficient to contribute 37% of aerosolized mass. We suggest that these were attachment to larger sized cement particles which was suggested by the morphological examination (Figure 7A).

The size distribution curve obtained for the regular cement showed an unusual discontinuous profile for particles larger than 200 nm. A non-ideal behavior could be due to limitations in the multiple-charge correction (MCC) algorithm applied to the aerosol sample data in the SMPS measurements. For large and anisometric particles the relationship between the aerodynamic and the electrical mobility diameters typically makes the algorithm approximations inaccurate (He & Dhaniyala, 2013). The SMPS data obtained without MCC treatment confirmed this hypothesis showing a smooth size distribution profile for the larger particle range (Figure S1) in regular cement. However, the comparative analysis of both regular and photocatalytic cement in the absence of MCC showed qualitatively similar trend, the mean concentration for the photocatalytic cement being greater than for regular cement. The MCC algorithms for these types of particles should be developed in the future.

Exposure to regular cement is associated with lung function decline at elevated exposures (Karl-Christian Nordby et al., 2016). The majority of the particle material found in both regular and photocatalytic cement was CaO. Inhaled CaO dust can cause inflammation in the upper respiratory tract due to its alkalinity (TOXNET, 2014). The second most abundant particle material was silica ($SiO_2$). Exposure to crystalline silica can lead to health effects such as silicosis, tuberculosis, chronic bronchitis, COPD and lung cancer (IARC 1997; Merget et al. 2002; Kaewamatawong et al. 2005; Napierska et al. 2010). Amorphous silica is associated with reversible inflammation, granuloma formation and emphysema (McLaughlin, Chow, and Levy 1997; Merget et al. 2002; Kaewamatawong et al. 2005). Cement dust as such has been associated with impaired lung function, inflammation, bronchitis, chronic obstructive pulmonary disease, restrictive lung disease, and pneumoconiosis (Eom et al. 2017; Maciejewska and Bielichowska-Cybula 1991; Meo 2004; Penrose 2014). None of these toxicological assessments were made with nano-sized particles. We therefore concluded that exposures to these nano-sized particles could lead to unexplained effects on human health, and consequently, safety and environmental burden should not be neglected (Maynard et al. 2006; Oberdörster, Oberdörster, and Oberdörster 2005). The inhalation pathway is considered the major route of nanoparticle exposure, and the lungs and pleura are the major primary targets for adverse effects (Donaldson and Poland 2012; Oberdörster, Oberdörster, and Oberdörster 2005). It is difficult to say how nano $TiO_2$ might change health hazards already associated with cement exposure, but this should be considered when assessing exposure risks among cement workers.

We have shown that the particle size distribution for photocatalytic cement contain more particle in the smaller size range (<1 um) (Figure 2) and have a greater mass concentration (Figure 4) than regular cement. In order to provide a safe working environment, the industry should develop risk management strategies, (Hämeri et al. 2009; Friedrichs and Schulte 2007). We suggest that the amount of nanoparticles added to the product should be publicly available, and that the risk management strategies should account for the readily airborne nanoparticles.

A number of instruments are available to measure particle distribution as well as physical and chemical properties of airborne nanoparticles. Real time instruments provide information on the metrics under study; however, they are generally unable to differentiate between types of nanoparticles. We used SMPS and PAS in our experiments. These are complimentary as they measure somewhat different particle size ranges; however, they both lack specificity. We used the morphology results to verify that the aerosolized nanoparticles were indeed $TiO_2$ in our experiments.

Understanding the relationship between airborne nano-sized particles and exposure is of great importance for developing efficient control measures. Our experiments are a step in this process; understanding the aerosolized part of bagged powder. We found that aerosolized photocatalytic cement contained 5% nanoparticles compared to the 2% added to the bagged powder. We therefore conclude that we cannot assume the nanoparticles distribution to be the same in aerosolized as in the bagged powder.

The protection measures needed when working with photocatalytic cement should be similar to recommendations made for nano $TiO_2$ exposures. Engineering control is preferred such as closed process chambers installed with high-efficiency particulate air (HEPA) filters (Goede et al., 2018). Indeed, most large construction sites have the cement already mixed with water in Switzerland thereby controlling for dust exposure. Other activities where workers may be especially exposed to nanoscale particles are during bagging and cleaning operations (Fonseca et al. 2015; Plitzko 2009) (associated with dry cement). When work operations cannot be enclosed, it is necessary to implement control measures to mitigate worker exposures. Occupational hygiene strategies should be implemented to reduce exposure to the dry cement (NIOSH 2011;) NIOSH 2012; NIOSH 2013; OSHA 2013). Use of personal respiratory protection (PRP) is of last resort. Current PRP recommendations for working with nanoparticles are for the US: N100, R100, and P100 (OSHA 2011; NIOSH 2014) and Europe (EN 143 EN 149): Class P3 filtering face pieces (FFP3) (Goede et al. 2018; Rengasamy, Eimer, and Shaffer 2009).

In conclusion, we were able to show that in experimental conditions the photocatalytic cement had significantly smaller particle size distribution than the regular cement; and the cement particle concentration was significantly greater for the photocatalytic compared to regular cement. Ninety nine percent of the particles were <1 µm for both cement types. Nano $TiO_2$ can be directly aerosolized from the cement, and a coagulation process is likely followed. Future studied should evaluate exposures associated with the use of photocatalytic cement by construction workers.

## 6. Acknowledgements

The Institute for Work and Health (IST), Switzerland, and the Royal Thai Government, Ministry of Science and Technology, Thailand, funded this study. We greatly appreciate help from Dr. Nicolas Concha Lozano for the morphology analysis and Ms. Nicole Charrier for all practical laboratory assistance. We thank Italcementi group for sending us a free sample. Parts

of the work of Michael Riediker were performed while he was at IOM (Institute of Occupational Medicine) Singapore.

## Supplemental material

### Supplementary Information

*SMPS measurements and multiple charge correction (MCC)*

To evaluate the contribution of the applied MCC algorithm to the discontinuous distribution profile obtained for large regular cement particles, the corresponding SMPS raw data were treated without MCC step. As shown in Figure S1, in the absence of MCC the size distribution becomes smoother and exhibits higher particle concentration, as expected. In the case of photocatalytic cement, the particle concentration is similarly affected since multiply-charged particles do contribute to the overall counted particles. Providing the nature of the regular cement composed of irregularly-shaped particles with high an isometry, the use of alternative MCC algorithm for more accurate SMPS measurements is currently foreseen.

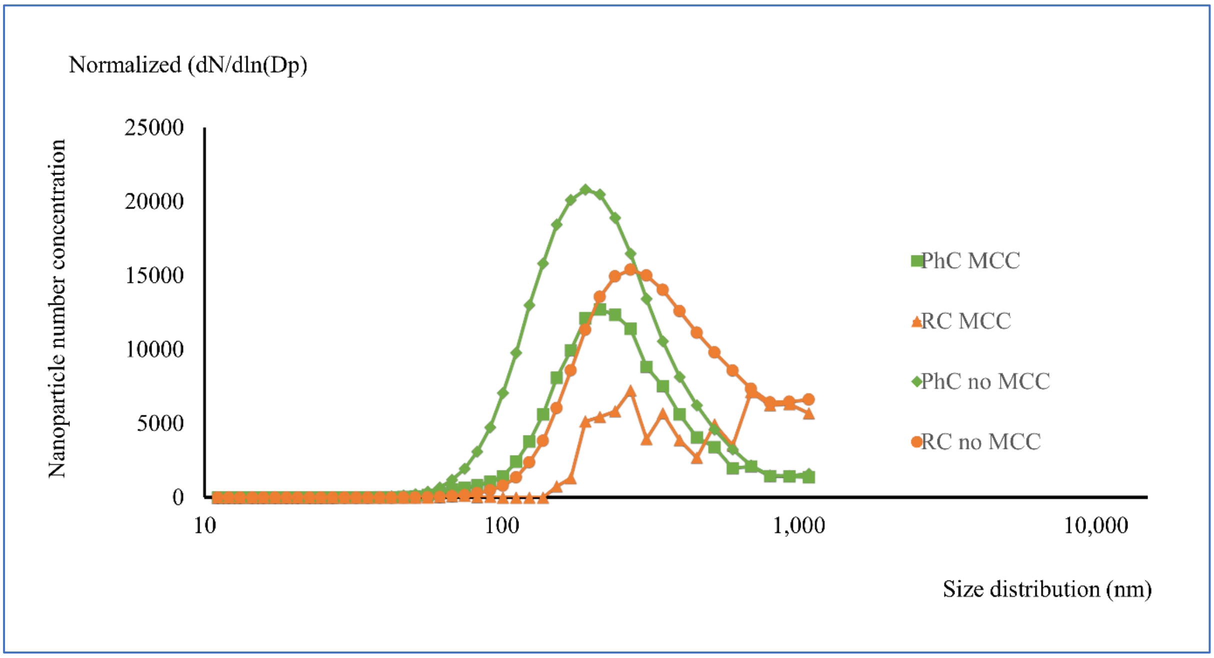


PhC MCC; Photocatalytic cement with multiple charge correction (solid cubic)
RC MCC; Regular cement with multiple charge correction (solid triangle)
PhC no MCC; Photocatalytic cement without multiple charge correction (solid diamond)
RC no MCC; Regular cement without multiple charge correction (solid circle)

Figure SI1: Particles size distributions and concentrations for aerosolized cement particle with and without multiple charge correction treatment.

## 7. References

Baan, R. A. 2007. Carcinogenic Hazards from Inhaled Carbon Black, Titanium Dioxide, and Talc Not Containing Asbestos or Asbestiform Fibers: Recent Evaluations by an IARC Monographs Working Group. Inhalation Toxicology 19 (sup1): 213–28. https://doi.org/10.1080/08958370701497903.

Carp, O., C. L. Huisman, and A. Reller. 2004. Photoinduced Reactivity of Titanium Dioxide. Progress in Solid State Chemistry 32 (1–2): 33–177. https://doi.org/10.1016/j.progsolidstchem.2004.08.001.

Chen, J., and C.-S. Poon. 2009. Photocatalytic Construction and Building Materials: From Fundamentals to Applications. Building and Environment 44 (9): 1899–1906. https://doi.org/10.1016/j.buildenv.2009.01.002.

Ding, Y., and M. Riediker. 2015. A System to Assess the Stability of Airborne Nanoparticle Agglomerates under Aerodynamic Shear. Journal of Aerosol Science 88 (October): 98–108. https://doi.org/10.1016/j.jaerosci.2015.06.001.

Ding, Y., and M. Riediker. 2016. A System to Create Stable Nanoparticle Aerosols from Nanopowders. JoVE (Journal of Visualized Experiments), no. 113 (July): e54414–e54414. https://doi.org/10.3791/54414.

Donaldson, K. and C. A. Poland. 2012. Inhaled Nanoparticles and Lung Cancer - What We Can Learn from Conventional Particle Toxicology. Swiss Medical Weekly 142 (2526). https://doi.org/10.4414/smw.2012.13547.

Eom, S.-Y., E.-B. Cho, M.-K. Oh, S.-S. Kweon, H.-S. Nam, Y.-D. Kim, and H. Kim. 2017. Increased Incidence of Respiratory Tract Cancers in People Living near Portland Cement Plants in Korea. International Archives of Occupational and Environmental Health 90 (8): 859–64. https://doi.org/10.1007/s00420-017-1244-9.

Fonseca, A. S., A.-K. Viitanen, A.J. Koivisto, A. Kangas, M.Huhtiniemi, T. Hussein, E. Vanhala, M. Viana, X. Querol, and K. Hämeri. 2015. Characterization of Exposure to Carbon Nanotubes in an Industrial Setting. The Annals of Occupational Hygiene 59 (5): 586–99. https://doi.org/10.1093/annhyg/meu110.

Friedrichs, S., and J. Schulte. 2007. Environmental, Health and Safety Aspects of Nanotechnology—implications for the R&D in (Small) Companies. Science and Technology of Advanced Materials, APNF International Symposium on Nanotechnology in Environmental Protection and Pollution (ISNEPP2006), 8 (1): 12–18. https://doi.org/10.1016/j.stam.2006.11.020.

FSO. 2017. Full-Time Job Equivalent per Sector, Switzerland. Federal Statistical Office, Swiss Confederation. https://www.bfs.admin.ch/bfs/en/home/statistics/industry-services/businesses-employment/jobs-statistics/jobs.assetdetail.3243521.html.

Gaté, L., C. Disdier, F. Cosnier, F. Gagnaire, J. Devoy, W. Saba, E. Brun, M. Chalansonnet, and A. Mabondzo. 2017. Biopersistence and Translocation to Extrapulmonary Organs of Titanium Dioxide Nanoparticles after Subacute Inhalation Exposure to Aerosol in Adult and Elderly Rats. Toxicology Letters 265 (January): 61–69. https://doi.org/10.1016/j.toxlet.2016.11.009.

Geiser, M., and W. G. Kreyling. 2010. Deposition and Biokinetics of Inhaled Nanoparticles. Particle and Fibre Toxicology 7: 2. https://doi.org/10.1186/1743-8977-7-2.

Goede, H., Y. Christopher-de Vries, E. Kuijpers, and W. Fransman. 2018. A Review of Workplace Risk Management Measures for Nanomaterials to Mitigate Inhalation and Dermal Exposure. Annals of Work Exposures and Health. https://doi.org/10.1093/annweh/wxy032.

Hämeri, K., T. Lähde, T. Hussein, J. Koivisto, and K. Savolainen. 2009. Facing the Key Workplace Challenge: Assessing and Preventing Exposure to Nanoparticles at Source. Inhalation Toxicology 21 (sup1): 17–24. https://doi.org/10.1080/08958370902942525.

He, M. and S. Dhaniyala. 2013. A Multiple Charging Correction Algorithm for Scanning Electrical Mobility Spectrometer Data. Journal of Aerosol Science 61 (July): 13–26. https://doi.org/10.1016/j.jaerosci.2013.03.007.

IARC. 1997. IARC Monographs on the Evaluation of Carcinogenic Risk to Human Silica, Some Silicates, Coal Dust and Para-Aramid Fibrils. Vol. 68. World health organization, International Agency for Research on Cancer. http://monographs.iarc.fr/ENG/Monographs/vol68/.

IARC. 2017. IARC Monographs on the Evaluation of Carcinogenic Risk to Human; List of Classification. Vol. 1–120. World health organization, International Agency for Research on Cancer. http://monographs.iarc.fr/ENG/Classification/latest_classif.php.

ISO/TS 27687. 2008. ISO/TS 27687: Nanotechnologies. International Organization for Standardization. https://www.iso.org/obp/ui/#iso:std:iso:ts:27687:ed-1:v2:en.

Kaewamatawong, T., N. Kawamura, M. Okajima, M. Sawada, T. Morita, and A. Shimada. 2005. Acute Pulmonary Toxicity Caused by Exposure to Colloidal Silica: Particle Size Dependent Pathological Changes in Mice. Toxicologic Pathology 33 (7): 745–51. https://doi.org/10.1080/01926230500416302.

Kreyling, W. G., S. Hirn, and C. Schleh. 2010. Nanoparticles in the Lung. Nature Biotechnology 28 (12): 1275–76. https://doi.org/10.1038/nbt.1735.

Lan, Y., Y. Lu, and Z. Ren. 2013. Mini Review on Photocatalysis of Titanium Dioxide Nanoparticles and Their Solar Applications. Nano Energy 2 (5): 1031–45. https://doi.org/10.1016/j.nanoen.2013.04.002.

Maciejewska, A., and G. Bielichowska-Cybula. 1991. [Biological effect of cement dust]. Medycyna Pracy 42 (4): 281–89.

Mann, S. 2006. Nanotechnology and Construction. Institute of Nanotechnology. http://nanotech.law.asu.edu/Documents/2009/10/Nanotech%20and%20Construction%20Nanoforum%20report_259_9089.pdf.

Maynard, A. D., R. J. Aitken, T. Butz, V. Colvin, K. Donaldson, G. Oberdörster, M. A. Philbert, et al. 2006. Safe Handling of Nanotechnology. Comments and Opinion. Nature. November 15, 2006. https://doi.org/10.1038/444267a.

McLaughlin, J. K., W. H. Chow, and L. S. Levy. 1997. Amorphous Silica: A Review of Health Effects from Inhalation Exposure with Particular Reference to Cancer. Journal of Toxicology and Environmental Health 50 (6): 553–66. https://doi.org/10.1080/15287399709532054.

Meo, S. A. 2004. Health Hazards of Cement Dust. Saudi Medical Journal 25 (9): 1153–59.

Merget, R., T. Bauer, H. U. Küpper, S. Philippou, H. D. Bauer, R. Breitstadt, and T. Bruening. 2002. “Health Hazards due to the Inhalation of Amorphous Silica.” Archives of Toxicology 75 (11–12): 625–34.

Napierska, D., L. C. J Thomassen, D. Lison, J. A. Martens, and P. H. Hoet. 2010. The Nanosilica Hazard: Another Variable Entity. Particle and Fibre Toxicology 7 (December): 39. https://doi.org/10.1186/1743-8977-7-39.

NIOSH. 2011. Occupational Exposure to Titanium Dioxide. U.S. Department of Health and Human Services, Centers for Disease Control and Prevention, National Institute for Occupational Safety and Health.

NIOSH. 2012. General Safe Practices for Working with Engineered Nanomaterials in Research Laboratories. U.S. Department of Health and Human Services, Centers for Disease Control and Prevention, National Institute for Occupational Safety and Health. http://www.cdc.gov/niosh/docs/2012-147/pdfs/2012-147.pdf.

NIOSH. 2013. Current Strategies for Engineering Controls in Nanomaterial Production and Downstream Handling Processes. U.S. Department of Health and Human Services, Centers for Disease Control and Prevention, National Institute for Occupational Safety and Health. http://www.cdc.gov/niosh/docs/2014-102/pdfs/2014-102.pdf.

NIOSH. 2014. NIOSH Guide to the Selection and Use of Particulate Respirators, Certified Under 42 CFR 84. U.S. Department of Health and Human Services, Centers for Disease Control and Prevention, National Institute for Occupational Safety and Health. http://www.cdc.gov/niosh/docs/96-101/.

Nordby, K.-C., H. Notø, W. Eduard, M. Skogstad, A. K. Fell, Y. Thomassen, Ø. Skare, et al. 2016. Thoracic Dust Exposure Is Associated with Lung Function Decline in Cement Production Workers. The European Respiratory Journal 48 (2): 331–39. https://doi.org/10.1183/13993003.02061-2015.

Oberdörster, G., E. Oberdörster, and J. Oberdörster. 2005. Nanotoxicology: An Emerging Discipline Evolving from Studies of Ultrafine Particles. Environmental Health Perspectives 113 (7): 823–39.

OSHA. 1999. Nanotechnology Safety and Health Topic. U.S. Department of Labor, Occupational Safety and Health Administration. https://www.osha.gov/dsg/nanotechnology/nanotechnology.html.

OSHA. 2011. Respiratory Protection. - 1910.134. U.S. Department of Labor, Occupational Safety and Health Administration. https://www.osha.gov/pls/oshaweb/owadisp.show_document?p_table=STANDARDS&p_id=12716.

OSHA. 2013. Working Safely with Nanomaterials. U.S. Department of Labour, Occupational Safety and Health Administration. https://www.osha.gov/Publications/OSHA_FS-3634.pdf.

PCA. 2013. World Cement Consumption. The Portland Cement Association. http://www.cement.org/.

Penrose, B.. 2014. Occupational Exposure to Cement Dust: Changing Opinions of a Respiratory Hazard. Health and History 16 (1): 25–44.

Plitzko, S. 2009. Workplace Exposure to Engineered Nanoparticles. Inhalation Toxicology 21 (sup1): 25–29. https://doi.org/10.1080/08958370902962317.

Rengasamy, S., B. C. Eimer, and R. E. Shaffer. 2009. Comparison of Nanoparticle Filtration Performance of NIOSH-Approved and CE-Marked Particulate Filtering Facepiece Respirators. The Annals of Occupational Hygiene 53 (2): 117–28. https://doi.org/10.1093/annhyg/men086.

Sha, Ba., W. Gao, X. Cui, L. Wang, and F. Xu. 2015. The Potential Health Challenges of TiO2 Nanomaterials. Journal of Applied Toxicology: JAT, July. https://doi.org/10.1002/jat.3193.

Tedja, Roslyn, Christopher Marquis, May Lim, and Rose Amal. 2011. "Biological Impacts of TiO2 on Human Lung Cell Lines A549 and H1299: Particle Size Distribution Effects." Journal of Nanoparticle Research 13 (9): 3801–13. https://doi.org/10.1007/s11051-011-0302-6.

Toxicology data network (TOXNET). 2014. Calcium Oxide. Toxicology Data Network, U.S. National Library of Medicine. https://toxnet.nlm.nih.gov/cgi-bin/sis/search2/r?dbs+hsdb:@term+@DOCNO+1615.

Wang, Jiangxue, Chunying Chen, Ying Liu, Fang Jiao, Wei Li, Fang Lao, Yufeng Li, et al. 2008. "Potential Neurological Lesion after Nasal Instillation of TiO2 Nanoparticles in the Anatase and Rutile Crystal Phases." Toxicology Letters 183 (1–3): 72–80. https://doi.org/10.1016/j.toxlet.2008.10.001.

WHO. 2010. IARC Monographs on the Evaluation of Carcinogenic Risks to Humans: Carbon Black, Titanium Dioxide, and Talc. Vol. 93. World health organization, International Agency for Research on Cancer. http://monographs.iarc.fr/ENG/Monographs/vol93/mono93.pdf.

# CHAPTER VI

# SIMULATION WORKING ACTIVITIES AND CONSTRUCTION SITE SAMPLING

**Published: Journal Hazardous Material**

https://doi.org/10.1016/j.jhazmat.2020.122838

## Article topic

### From nano to micrometer size particles – a characterization of airborne cement particles during construction activities

**Kiattisak Batsungnoen**[1,2], Michael Riediker[3], Guillaume Suárez[1], Nancy B Hopf[1]

1. Center for Primary Care and Public Health (Unisanté), University of Lausanne, Switzerland. (kiattisak.batsungnoen@unisante.ch, nancy.hopf@unisante.ch, guillaume.suarez@unisante.ch)
2. Institute of Public Health, Suranaree University of Technology, Thailand
3. Swiss Centre for Occupational and Environmental Health (SCOEH), Winterthur, Switzerland. (michael.riediker@alumni.ethz.ch)

**Corresponding author:** Nancy B Hopf, PhD

**Keywords:** Photocatalytic cement, Nano cement, Nano $TiO_2$, Photocatalytic cement exposure, Nano $TiO_2$ exposure, Cement particle exposure

**Abstract**

Although, photocatalytic cement contains nanosized $TiO_2$, a possibly carcinogen, no exposure assessments exist for construction workers. We characterized airborne nanoparticle exposures during construction activities simulated in an exposure chamber. We collected some construction site samples for regular cement in Switzerland and Thailand for comparison. Airborne nanoparticles were characterized using scanning mobility particle sizer (SMPS), portable aerosol spectrometer (PAS), diffusion size classifier (DiSCmini), transmission electron microscopy (TEM), scanning electron microscope energy dispersive X-ray spectroscopy (SEM-EDX), and X-ray diffraction. Bagged photocatalytic cement had 2.0 wt% (GSD±0.55) $TiO_2$, while $TiO_2$ in aerosols reached 16.5 wt% (GSD±1.72) during bag emptying and 9.7 wt% (GSD±1.36) after sweeping. The airborne photocatalytic cement particles were far smaller (approximately 50 nm) compared to regular cement. Cutting blocks made from photocatalytic cement or concrete, resulted in similar amounts of airborne nano $TiO_2$ (2.0 wt% GSD±0.57) particles as in bagged material. Both photocatalytic and regular cement had a geometric mean diameter (GMD) < 3.5 µm. Main exposures for Thai workers were during sweeping and Swiss workers during drilling and polishing cement blocks. Targeted nanoparticle exposure assessments are needed as a significantly greater exposure to nano $TiO_2$ were observed than what would have been predicted from the material's nano- $TiO_2$ contents.

## 1. Introduction

An increasing number of nanotechnology-based products are making its way into the construction sector (Zhu et al., 2004). One such product is photocatalytic cement made by adding nano-scaled (less than 100 nm in size) titanium dioxide ($TiO_2$) particles. This gives the cement self-cleaning properties (Lan, Lu, and Ren 2013; Paz et al. 1995). The increasing use of nanomaterials have led to an increased need for hazard and exposure information on these materials in order to anticipate, recognize, evaluate, and control factors in the workplace, which otherwise may cause impaired health among workers.

$TiO_2$ was classified as "possibly carcinogenic to humans" (class 2B) by the International Agency for Research on Cancer (IARC) (IARC, 2017; WHO, 2010). In the U.S., the National Institute for Occupational Safety and Health (NIOSH) provided a more nuanced assessment by classifying only ultrafine (nanoscale) $TiO_2$ as a potential carcinogen, while considering the data to be insufficient for making such a statement for fine (larger) $TiO_2$ (NIOSH, 2011). The hazard associated with exposures to nano-sized $TiO_2$ particles (nano $TiO_2$) has been reported by a series of studies (NIOSH, 2009). Nano $TiO_2$ was found to increase reactive oxygen species (ROS) production (Arenberg and Arai 2020; H. Ma, Brennan, and Diamond 2012; Sayes et al., 2006; Lee et al., 2010; Long et al., 2006), and induce DNA damage (Falck et al., 2009; Ghosh et al., 2010; WHO, 2010; Sha et al., 2015) and cell toxicity (C. Xue, Luo, and Yang 2015; Sha et al., 2015; Lee et al., 2010 Sayes et al., 2006). Furthermore, nano $TiO_2$ can be translocated to different organs and accumulate in the kidneys, lymph nodes, heart, liver, and brain (Wang et al., 2008; Kreyling et al., 2010; Geiser and Kreyling, 2010; Shi et al., 2013; Shinohara et al. 2015).

Nano $TiO_2$ particles are highly photoreactive. They react with organic and inorganic gases (Chen and Poon 2009; Lim et al. 2000; Dalton et al. 2002; Diesen and Jonsson 2014; Fujishima and Zhang 2006) and induce phototoxicity in microorganisms (Lan et al., 2013; Carp et al., 2004; Banerjee et al., 2015; Chen and Poon, 2009; Lee et al., 2010; Zhi Ge and Zhili Gao, 2008). This biocidal effect is one of the reasons why nano $TiO_2$ is an interesting additive because it renders building surfaces “self-cleaning” because it kills any organic growth.

Photocatalytic cement is mainly regular cement with $TiO_2$ nanoparticles and additives. Regular cement has been used since the Roman era to build strong structures by mixing cement with water, rock, and sand (Edwin G. Foulke, 2008). Only 2-3 wt% nano $TiO_2$ were added to cement to produce photocatalytic cement (Ma et al. 2015; Jimenez-Relinque et al., 2015; Batsungnoen et al., 2019). The particle size distributions of aerosolized photocatalytic cement generated during work activities are not known. Given that nano $TiO_2$ is not chemically bound to the cement particles, they might still behave like nanoparticles, and may easily be released (Aitken et al., 2004; Ostiguy et al., 2006; Friedlander and Pui, 2003; Ding et al., 2017).

The risk for work related diseases over a lifetime in a construction trade is 2–6 times greater compared to non-construction work. About 16% of construction workers develop chronic obstructive pulmonary disease (COPD) (Ringen et al., 2014). Cement dust exposures are one of the health concerns. They are generated during many construction activities (van Deurssen et al., 2014) such as abrasive blasting, bag emptying, cement mixing, concrete drilling, concrete block cutting, sawing, and sweeping. Inhalation is the most common route of entry for airborne cement as well as for nanoparticles. Inhaled cement dust can lead to multiple lung diseases such as chronic respiratory symptoms, lung function impairment, bronchitis, COPD, pneumoconiosis, silicosis, and lung cancer (Eom et al., 2017; Maciejewska and Bielichowska-

Cybula, 1991; Meo, 2004; Penrose, 2014; Nordby et al., 2011; Yang et al., 1996; Moghadam et al., 2017).

Cement also contains silicon dioxide ($SiO_2$). Crystalline silica, as quartz and cristobalite, are carcinogenic to humans (IARC, 2012; IARC, 2017; IARC, 1997). Moreover, crystalline silica causes chronic bronchitis, COPD, and silicosis (Kaewamatawong et al., 2005; Napierska et al., 2010; Soutar et al., 2000). Higher concentrations of amorphous silica might cause pneumoconiosis, granuloma formation, reversible inflammation, and emphysema (McLaughlin et al., 1997; Merget et al., 2002; Kaewamatawong et al., 2005). For crystalline silica, NIOSH recommends an exposure limit of 0.05 mg/m$^3$ (OSHA, 2018), and for amorphous silica 6 mg/m$^3$ (NIOSH, 2018).

The construction industry employs millions of workers. Many die or suffer from occupational diseases arising from accumulated exposure to hazardous substances (ILO, 2014). Managing hazardous exposures properly can reduce the burden of disease, but can only be done effectively if exposures have been characterized. Currently, there are no studies characterizing airborne nano $TiO_2$ in cement during work activities.

Our aim was to characterize airborne nano- and micrometer particle exposures during typical construction work activities for photocatalytic and regular cement. Our results can be directly used in developing risk management strategies among construction workers using photocatalytic cement. In addition, it will enhance our understanding of airborne nanoparticles and their size distributions, concentrations, and morphologies in mixtures with other particles.

## 2. Materials and methods

### *Materials*

Portland cement type I (cement-clinker; CE number 266-043-4) was obtained from Jura cement (Wildegg, Switzerland). Photocatalytic cement was acquired as a sample from the manufacturer (TX-Active®, Italcementi group, Nazareth, US). Fine sand used to make concrete was bought from a general home improvement store in Switzerland.

### *Characterization of the two cement types*

Airborne particles were characterized by assessing their size distribution, number and mass concentration, morphology, phase analysis, and elemental composition. The instruments and measurement techniques used are shown in Table 1. Airborne nanoparticle concentrations and size distributions were measured with three different devices: the size distribution in the range from 11 to 1,083 nm was measured with a scanning mobility particle sizer (SMPS; model SMPS+C model 5400, Grimm Aerosol Technik GmbH & Co. KG, Ainring, Germany); the size distributions in the range from 250 to 32,083 nm with a portable aerosol spectrometer (PAS; model 1.109, Grimm Aerosol Technik GmbH & Co. KG, Ainring, Germany); and the fast (1 Hz) particle number count concentration in the range from 10 to 700 nm with a diffusion size classifier (DiSCmini; Testo North America, West Chester, PA USA). Elemental composition was determined by scanning electron microscope energy dispersive X-ray spectroscopy (SEM-EDX) (SEM-EDX; PHENOM XL BSE detector at 15kV). The SEM-EDX analysis returns the atomic and weight concentrations. Composition of objects as small as 10 nm can be assessed with SEM-EDX analysis. We averaged the results of three randomly selected wide scanning surface zones ( 15x15 μm) to calculate the weight percent for each element (wt%). Bagged material was analyzed directly with the SEM-EDX. Nanoparticle morphology was determined by transmission electron microscopy (TEM) (TEM; CM-100, JEOL, USA at 80 kV). X-Ray diffraction was used to measure the bagged material phase analysis for both cement types using step width 0.0167° from 5° to 70° and time per step of 59.65s (Panalytical X'pert Pro MPD, Malvern Panalytical, Malvern, United Kingdom).

Table1: Nanoparticles instruments and analytical techniques

| Instrument | | Technique | Sensitivity |
|---|---|---|---|
| Scanning mobility particle sizer | SMPS | Charge particle | 11 to 1,083 nm |
| Portable aerosol spectrometer | PAS | Light scattering | 250 to 32,000 nm |
| DISC mini | DISC mini | Diffusion charge particle | 10 to 700 nm |
| Impactor | Marple | Gravimetric | 0.52 to 21.3 µm |
| Inhalable sampler | IOM | Gravimetric | 50% Cut-point: 100 µm (Sampling flow rate 2.0 l/min) |
| Plastic cyclone (Higgins-Dewell) | Cyclone | Gravimetric | 50% Cut-point: 4 µm (Sampling flow rate 2.2 l/min) |
| Transmission electron microscope | TEM | Transmission electron | < 1 nm |
| Infrared absorption spectrophotometry | IR | Infrared absorption spectrophotometry | Limit of detection (LOD) 5µg/sample |
| Scanning electron microscope energy dispersive X-ray spectroscopy | SEM-EDX | Scanning electron | ± 1% |
| X-ray diffraction | XRD | X-ray diffraction | ± 0.1% |

### *Characterization of the collected airborne particles*

Aerodynamic mass particle size distributions from 0.52 to 21.30 µm were measured with an 8-stage cascade impactor (Marple; Thermo Fisher Scientific, Air Quality Instruments, Franklin, MA, USA.). Inhalable fraction (50% Cut-point: 100 µm) was measured with an IOM cassette fitted with a 25 mm PVC filter and a personal pump operating at a flowrate of 2 L/min (IOM and PVC filter; SKC Inc., Eighty Four, PA, USA). Respirable fraction (50% Cut-point: 4 µm) was measured with a plastic cyclone (Higgins-Dewell) (Casella US, Buffalo, NY, USA) operating at a flow rate of 2.2 L/min and equipped with a 37 mm PVC filter (PVC filter; SKC Inc., Eighty Four, PA, USA) as described in NIOSH method 0600 (NIOSH, 1998). Crystalline silica was determined using infrared absorption spectrophotometry (IR; IRAffinity-1S1, Shimadzu, Kyoto, Japan) as described in NIOSH method 7602 (NIOSH, 2003). SEM-EDX analyzes were performed after removing the airborne particles from the IOM filter. We extracted the deposited particles on the filter using carbon adhesive disc stickers (12 mm diameter, Plano GmbH, Wetzlar Germany). Airborne nanoparticles were collected onto the TEM grid (TEM grid; Quantifoil R1/4, Quantifoil Micro Tools GmbH, Germany) using a particle mini sampler (MPS) with a sampling flowrate of 0.3 L/min (MPS; Ecomesure, Sacly, France).

### *Airborne particle concentration calculations*

Particle concentrations were calculated according to NIOSH method 0500 for gravimetric filters.

Particle concentration (mg/m$^3$) = $[(W_2 - W_1) - (B_2 - B_1)] \times 10^3 / V$

Where: $W_1$ = Pre-weight of sampling (mg)

$W_2$ = Post-weight of sampling (mg)

$B_1$ = Pre-weight of blank (mg)

$B_1$ = Post-weight s of blank (mg)

V = Air volume sampling (l) or Sampling flowrate (l/min) x time (min)

### *Work activity simulation experiments*

The work activities were simulated in an exposure chamber (2.2m x 2.2m x 2.2m) equipped with a controlled, HEPA-filtered ventilation (class H13 with efficiency 99.5 %, EN 1822) (Guillemin, 1975). Baseline airborne particle concentration in the chamber was sampled after running the ventilation for 2 hours prior to the experiment start. The workers simulating the activity wore a protective chemical suit, respiratory protection (N100, P3, or FFP3), nitrile gloves, goggles, and safety shoes (Figure 1). The ventilation was not operating during the work activity. Ventilation was turned back on and running while the measurements inside the exposure chamber continued for 2 hours after the work activity had finished.

Each of the three simulated activities; bag emptying, concrete cutting, and sweeping were performed in triplicates i.e., three different workers simulated the same task in separate experiments to address potential between-worker differences. **Bag emptying** was performed by cutting open a 25-kg cement bag, and then turning the bag upside-down to pour the cement into a vat on the floor. At the end, the bag was shaken until completely empty as shown in Figure 1A. We made blocks (size 25 x 36 x 6 cm) of concrete (cement and sand mixture) as well as cement blocks without sand. The **concrete block cutting** activity was performed with a circular saw (grinding disc diameter 230 mm and maximum rated speed 6,600 round per minute (RPM) (PWS 20-230 J, BOSCH, Leinfelden-Echterdingen, Germany). We used this saw to cut the blocks for 10 seconds in each experiment as shown in Figure 1B. The **sweeping** activity was performed after pouring one kilogram of cement on the floor, and then sweeping using an ordinary broom. The sweeping activity continued for 1 minute in each experiment as shown in Figure 1C.

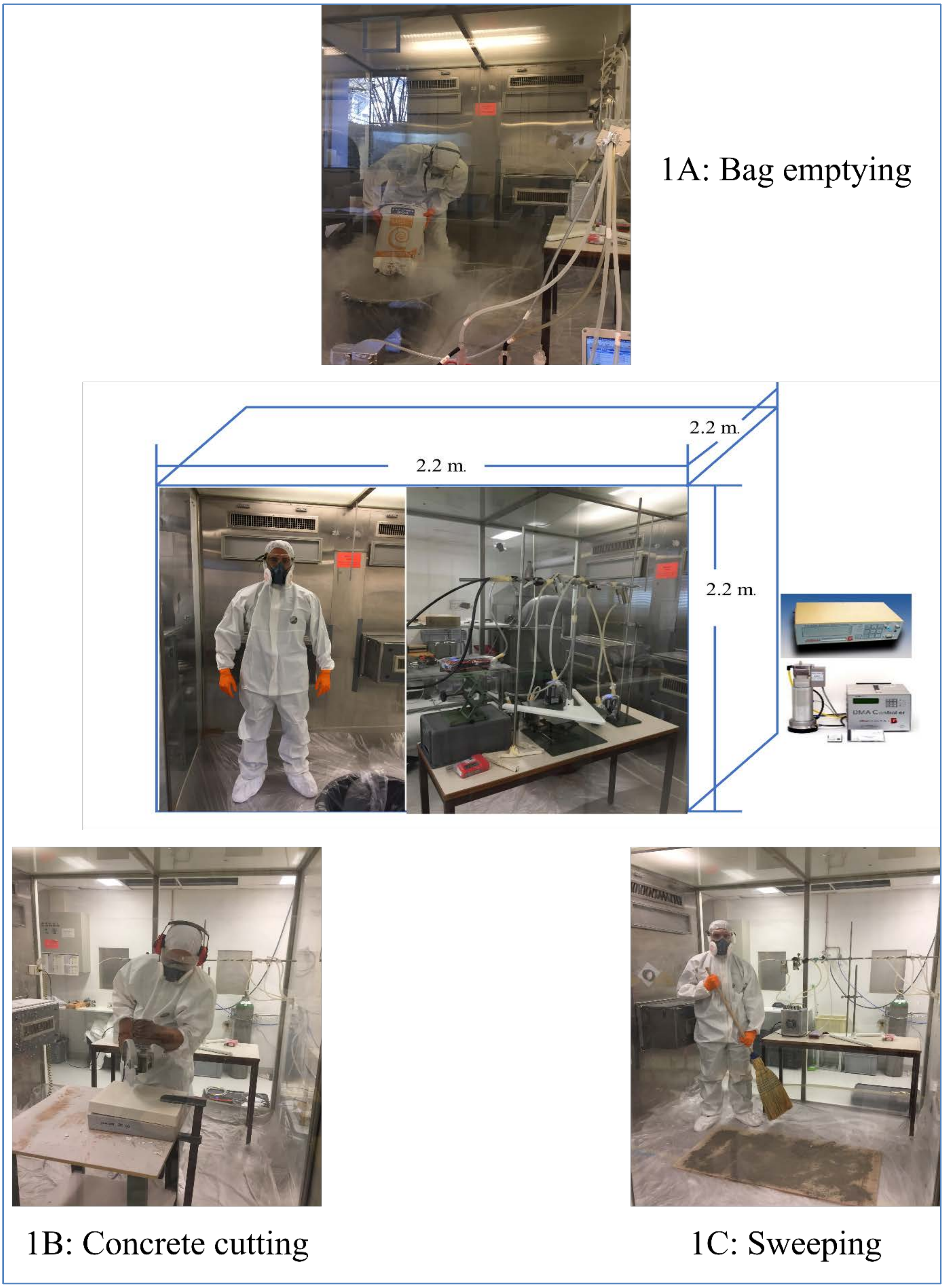


Figure 1: **Experimental setting:** Three working activities such as bag emptying (1A), concrete cutting (1B) and sweeping (1C) in the chamber size: 2.2 x 2.2 x 2.2 meters. Workers wear whole body protection with personal protective equipment (PPE) as following; dust protection cloth, rubber gloves, goggles, safety shoes, and respirator.

### ***Field sampling approach***

*Company description, Switzerland*

In Switzerland, two construction companies and 15 workers were recruited. A convenience sampling approach was used by contacting companies using cement that had previously been sampled for other hazards. One company was housed in a two-story building partially open and no windows. In a large open hall (80 m x 25 m x 10 m), workers constructed large reinforced concrete walls (size ranged from 3 - 5m tall x 1- 3 m long x 0.3 - 0.7 m thick). A cement mixing truck filled an overhead concrete hopper connected to a crane. The crane operator moved the hopper to different workstations using a control panel. The wet concrete was poured into steel molds (Figure 2A). Workers in this area would wire steel rods, build and remove steel molds or wooden frames (Figure 2B). Once the concrete had dried, workers moved the blocks to the polishing station. The polishing workers used hand-held sanding machines on horizontally mounted walls standing on a ladder, or vertical walls laying on a bench (Figure 2C). These pre-manufactured reinforced concrete walls were then loaded onto a truck aimed for the construction site. We sampled workers at the second construction company during work at a building repair site. The workers worked indoors and in pairs. One worker drilled into the concrete wall to remove parts of it using a handheld hammer drill. The second worker held a vacuum cleaner nozzle close to the drill bit to remove dust particles as they were generated (Figure 2D).

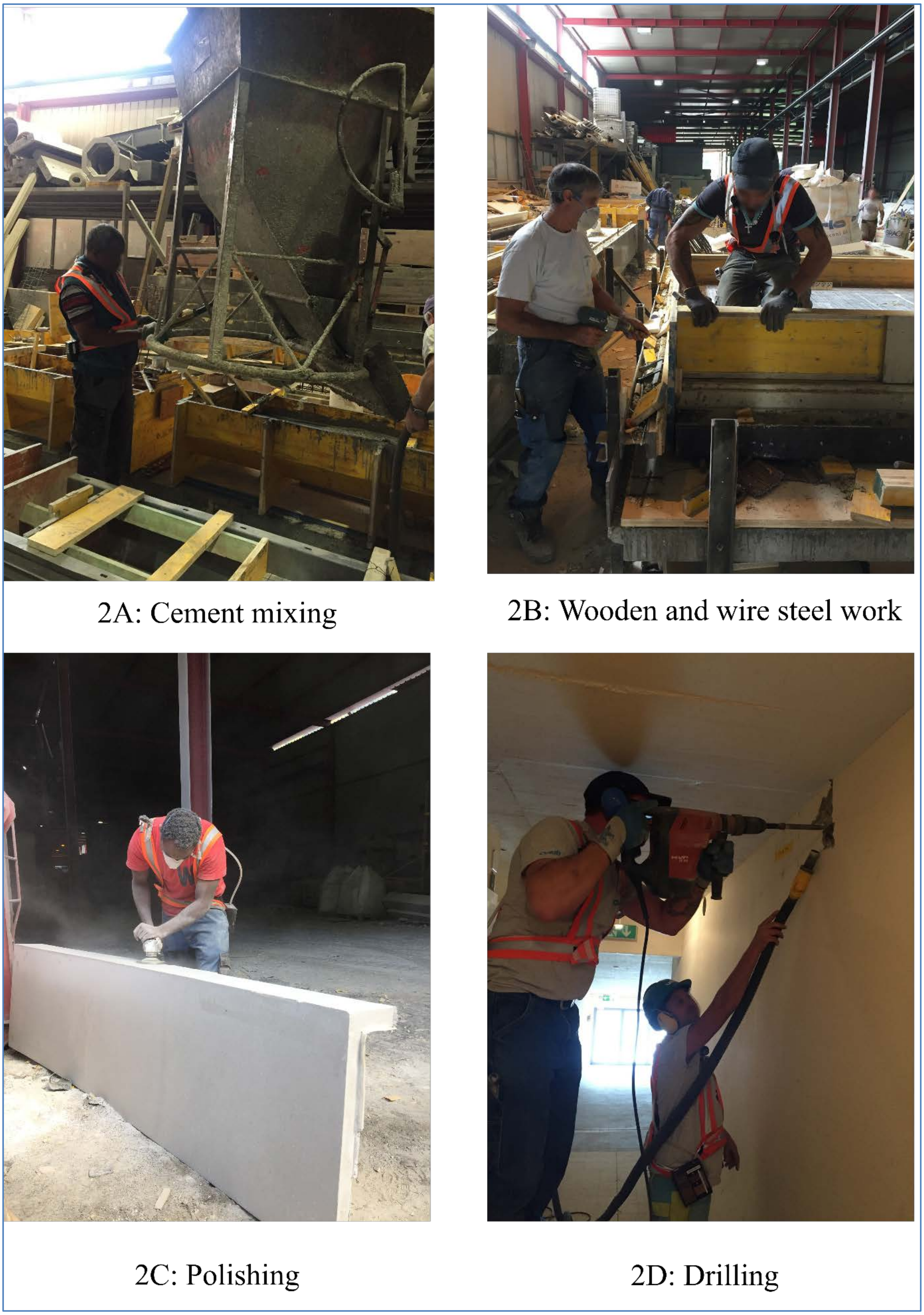

2A: Cement mixing

2B: Wooden and wire steel work

2C: Polishing

2D: Drilling

Figure 2: Construction working activities in Switzerland

*Personal air sampling, Switzerland*

Each worker carried a personal sampling train equipped with an IOM inhalable particle sampler (n=15) and a cyclone (n=15), and a DiSCmini (n=15) while performing a specific work activity. Area air concentrations were sampled with SMPS, PAS, DiSCmini, and an impactor. Sampling times were about 2 hours.

*Company description, Thailand*

In Thailand, 40 workers were recruited from three construction companies. The companies and their workers were recruited while working on the Suranaree University of Technology campus. All companies constructed new buildings such as hospitals, laboratories, and dormitories. Cement mixing was manual (Figure 3A) and semi-automatic (Figure 3B). Workers loaded the vat or cement mixer by cutting open a 25-kg cement bag, pouring, and shaking it until empty. Workers added sand and water to the cement and in manual mixing, used a hoe to mix the wet concrete in the vat. At the end of the task, workers swept the spilled dry cement with a broom (Figure 3C). Sometimes the workers wet-sprayed the cement before sweeping to prevent dust-formation and sometimes they did not. Sweeping and cement mixing were performed inside and outside of the unfinished building. Small hand-held hammer drills were used inside the building to fit electrical wiring (Figure 3D).

*Personal air sampling, Thailand*

Each worker was equipped with three personal sampling trains: an IOM cassette (n=10), a cyclone (n=10) and an impactor (n=3). No stationary nano sampling instruments were readily available in Thailand, and we could not ship them from Switzerland as the SMPS has a radioactive source. Consequently, no direct-reading instruments were used during the Thai sampling campaigns. Sampling times were about 2 hours per worker.

3A: Manual cement mixing

3B: Semi-automatic mixing

3C: Sweeping

3D: Drilling

Figure 3: Construction working activities in Thailand

### *Statistical analysis*

Descriptive statistical analyses such as geometric mean diameter (GMD) and geometric standard deviation (GSD) were calculated using Excel. Descriptive statistical analyses for particle number and mass concentration were mean and SD, and were calculated using the software integrated in the direct reading instruments.

## 3. Result

### *Cement bag emptying*

Particle number concentrations during activity and post-activity were similar for the two cement types. For photocatalytic cement, bag emptying generated 3.7 x $10^3$ particles per cubic centimeter (pt/$cm^3$) giving a GMD of 322 nm and a GSD of 2.90; and 3.6 x $10^3$ pt/$cm^3$, GMD 227 nm and GSD 3.31 for regular cement. Figure 4A shows nanoparticle number concentrations and size distributions for both photocatalytic and regular cement during bag emptying measured with the SMPS. Cement bag emptying generated higher particle number concentrations for regular compared to photocatalytic cement in the size range from 11 to 241 nm. Above 241 nm, the number concentrations for photocatalytic cement were higher. Both cement types had a single peak at 692 nm: the modal values were 3.2 x $10^3$ pt/$cm^3$ for photocatalytic and 1.4 x $10^3$ pt/$cm^3$ for regular cement (Figure 4A).

Particles with sizes from 1,083 nm to 32,000 nm were measured with PAS (Figure 4B). Photocatalytic cement had a higher number concentration than regular cement across the entire size range. Irrespective of cement type, 99% of the cumulative airborne particle number during bag emptying was in the size range below 3.5 µm.

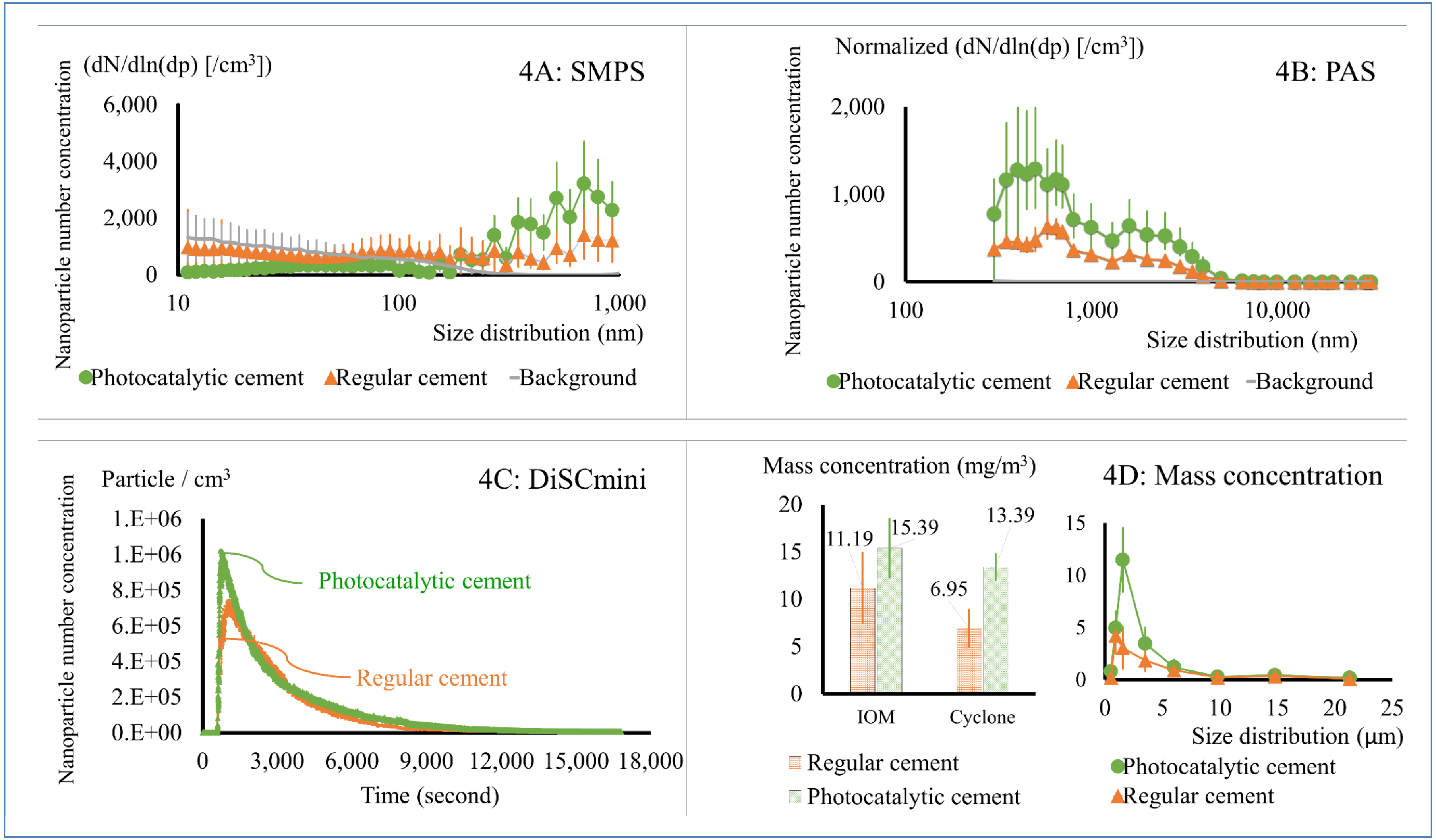


Figure 4: **<u>Bag emptying</u>**: nanoparticle mass and number size distributions and concentrations for photocatalytic cement (solid circles) and regular cement (solid triangle)

Peak concentrations during the bag emptying measured with DiSCmini was approximately 1.0 x $10^6$ pt/$cm^3$ for photocatalytic cement and somewhat lower for regular cement (7.7 x $10^5$ pt/$cm^3$) (Figure 4C). In the DiSCmini's most accurate size range (10-300 nm), the photocatalytic cement GMD was 37 nm, while that of regular cement was 40 nm.

Figure 4D shows the particle mass fractions and concentrations during bag emptying. Inhalable dust mass concentration (measured as inhalable dust) was 15.16 (SD±3.12) mg/$m^3$ and respirable dust (cyclone) was 13.34 (SD±1.36) mg/$m^3$ for photocatalytic cement. Inhalable and respirable dust mass concentrations were ~31% and ~49% lower for regular cement, respectively during bag emptying with 10.74 (SD±3.70) mg/$m^3$ for inhalable dust and 6.75 (SD±1.97) mg/$m^3$ for respirable dust. Mass particles size distribution showed a peak concentration of 10.67 (SD±5.09) mg/$m^3$ at 1.55 µm for photocatalytic cement. Regular cement had half the mass concentration (3.99 mg/$m^3$ SD±1.70) compared to photocatalytic cement and at a smaller size (0.93 µm) as shown in figure 4D.

Airborne photocatalytic cement particles were both nanoparticles and fine particles as observed with the TEM images (Figure 5A and Figure 5B). Regular cement particles are shown in Figure 5C and Figure 5D. The particle boundary layer showed a much greater number of small particles (size around 50 nm) for photocatalytic cement (Figure 5A and Figure 5B) compared to regular cement (Figure 5C and Figure 5D). The presence of nano-sized spherical particles was only found in the photocatalytic cement and might be attributed to nano $TiO_2$ (Figure 5B). Our measuring device did not have the spatial resolution to determine the elemental composition of the nanoscale particulates; however, we analyzed the chemical composition of the aerosol samples collected during cement working activities with SEM-EDX, and confirmed that these were indeed TiO2 nanoparticles. The regular cement contained mostly coarse particles. Note that the SMPS reported a smaller GMD than what we observed in the TEM, which were mostly particles around 1 µm, as shown in figure 5C and figure 5D.

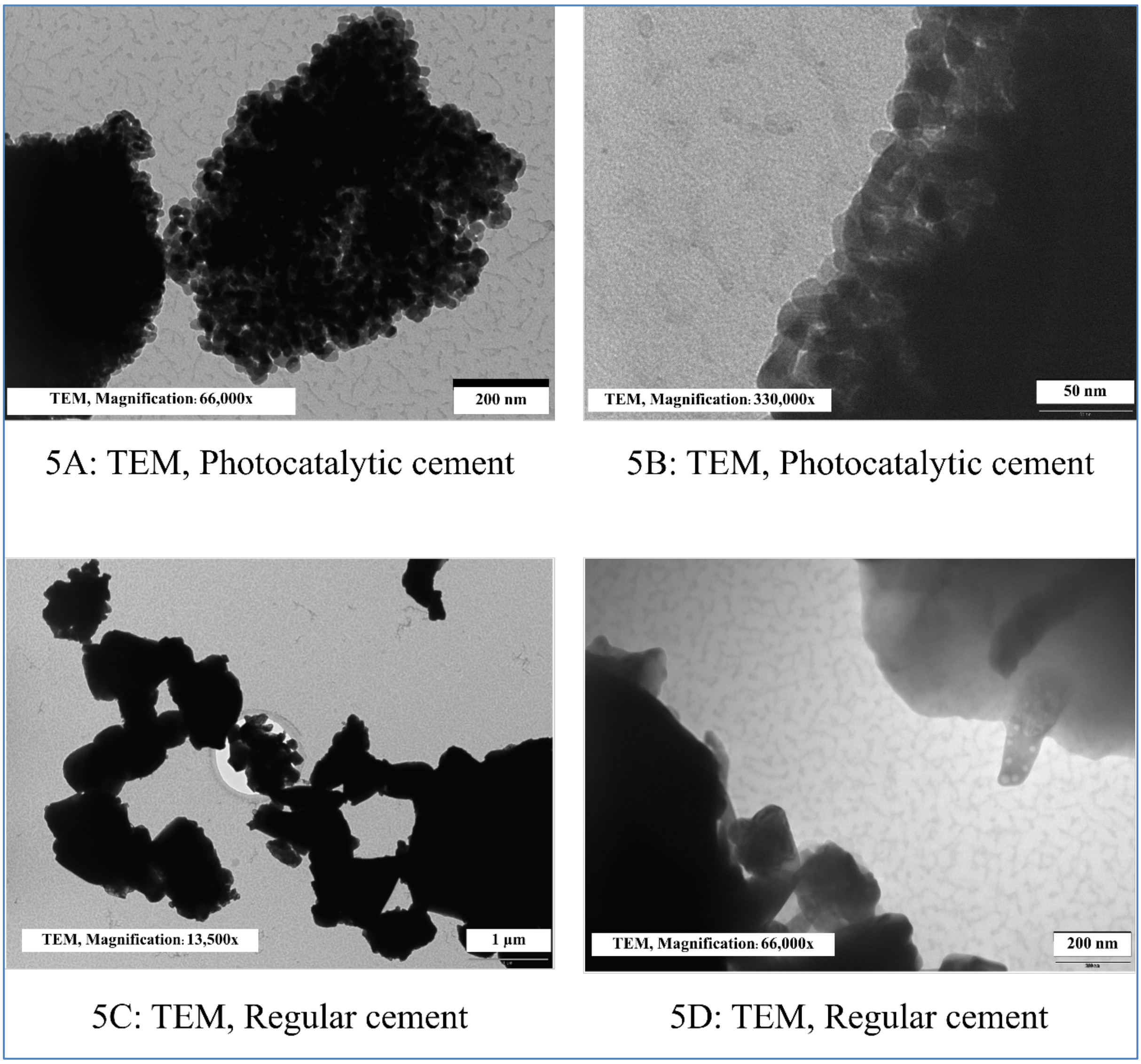


5A: TEM, Photocatalytic cement

5B: TEM, Photocatalytic cement

5C: TEM, Regular cement

5D: TEM, Regular cement

Figure 5: **Bag emptying:** particles morphology between photocatalytic and regular cement

*Concrete block cutting*

Mean particle number concentration during cutting concrete blocks made with photocatalytic cement was 1.0 x $10^4$ pt/$cm^3$, GMD of 287 nm and GSD of 2.22. Cutting blocks made with regular cement gave 1.9 x $10^4$ pt/$cm^3$, GMD 345 nm and GSD 1.96. Figure 6A shows the nanoparticle size distributions and concentrations for both photocatalytic and regular concrete block cutting measured with SMPS. The size distributions were similar; increasing at particle size 137.8 and fluctuating between 277.8 and 930.5 nm. The peak number concentration was about double for regular cement (1.2 x $10^4$ pt/$cm^3$) at 348.9 nm compared to the peak for photocatalytic cement (5.8 x $10^3$ pt/$cm^3$) at 271.8 nm.

The particle size number distributions measured with PAS were similar for both cement types, except for particle sizes between 300 and 500 nm where regular cement had a greater number concentration than photocatalytic cement. Irrespective of cement type, concrete cutting had 99% of cumulative airborne particle number in sizes below 3.5 µm (Figure 6B).

Figure 6C shows particle number concentrations measured with DiSCmini during concrete cutting. The particle counts were extremely high for both cement types. Photocatalytic cement had peak concentration around 9 million pt/$cm^3$ while regular cement had a peak at 6 million pt/$cm^3$. The corresponding GMDs reported by the DiSCmini were 31 nm and 42 nm, respectively.

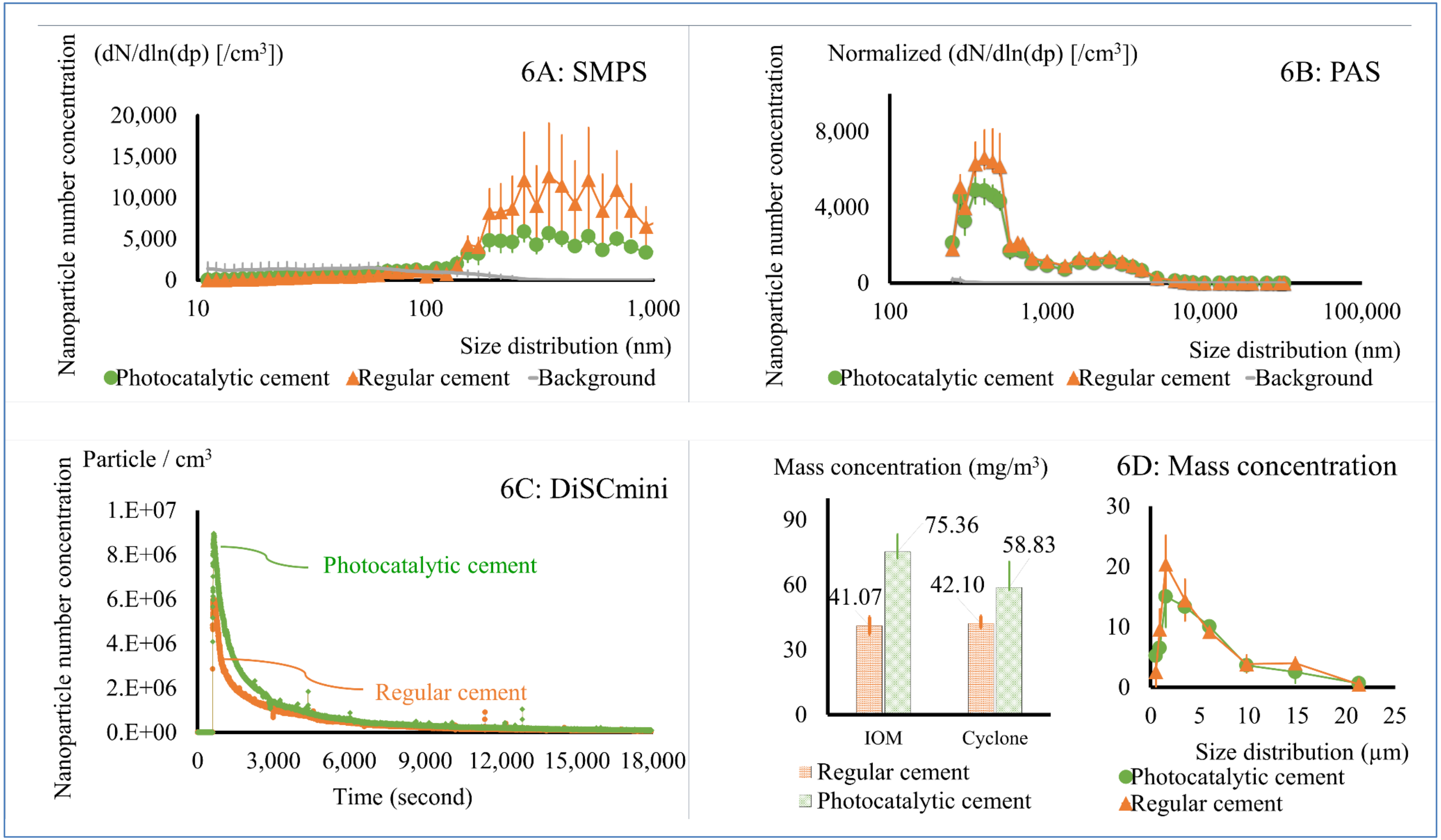


Figure 6: **<u>Concrete block cutting:</u>** nanoparticle mass and number size distributions and concentrations for photocatalytic cement (solid circles) and regular cement (solid triangle)

Inhalable photocatalytic concrete dust mass concentrations during cutting were almost double (75.10 $mg/m^3$, SD±7.92) compared to regular cement (40.95 $mg/m^3$, SD± 4.16) with a ratio of photocatalytic to regular cement of 1.8. Respirable dust concentrations generated during concrete cutting were somewhat similar for photocatalytic cement (57.99 $mg/m^3$, SD± 11.96) and regular cement (42.01 $mg/m^3$, SD± 3.52) with a ratio of photocatalytic to regular cement of 1.4. Cutting photocatalytic and regular cement concrete had the same peak mass concentrations at 1.55 µm mean size and airborne concentrations of 19.90 (SD± 5.06) and 14.54 (SD±4.79) $mg/m^3$, respectively (figure 6D).

Figure 7 displays particle morphology images for airborne photocatalytic (Figure 7A and Figure 7B) and regular (Figure 7C and Figure 7D) cement sampled with a TEM grid during cutting. The morphology for fine particles generated during concrete cutting was similar for the two cement types. The presence of nano $TiO_2$ spherical particles was not observed for photocatalytic cement concrete cutting.

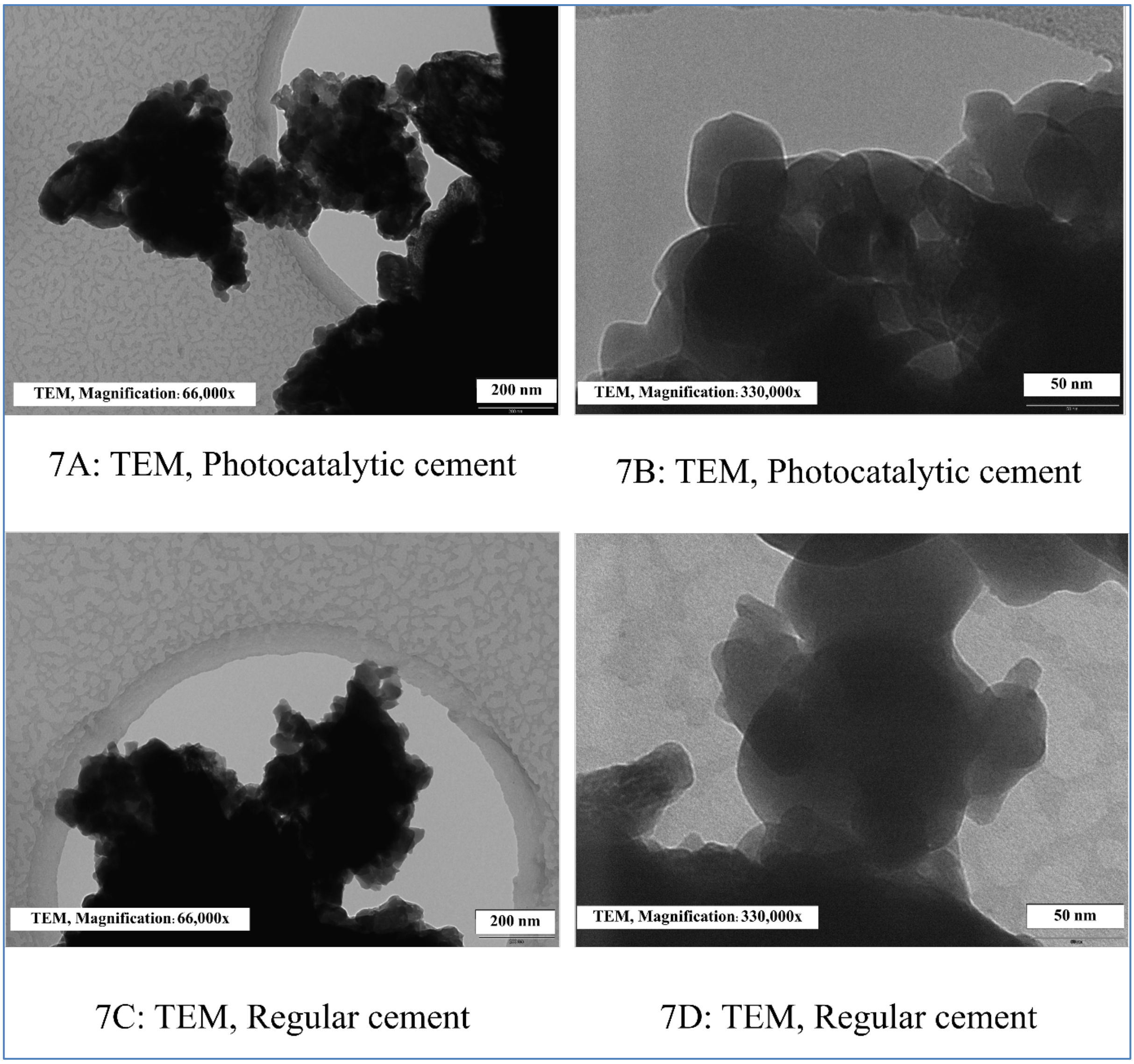


Figure 7: **Concrete cutting**: particles morphology between photocatalytic and regular cement

***Cement sweeping***

Nanoparticle size number distributions and number concentrations measured during sweeping with SMPS showed photocatalytic cement mean particle number concentrations of 1.8 x $10^3$ pt/$cm^3$, GMD of 194 nm and GSD of 3. The same particle number concentrations (2.2 x $10^3$ pt/$cm^3$) was observed for regular cement but for larger particles (GMD 283 nm and GSD 3) (Figure 8A). Sweeping had a particles peak size of 692 nm with number concentrations double for photocatalytic (1.0 x $10^3$ pt/$cm^3$) compared to regular (5.1 x $10^2$ pt/$cm^3$) cement.

Figure 8B shows particle size number distributions and number concentrations for particles between 250 and 32,000 nm. Again, sweeping had a greater particle number concentration for photocatalytic cement compared to regular cement.

Photocatalytic cement had a peak concentration around 9.3 x $10^5$ pt/$cm^3$ while regular cement had a peak at 8.3 x $10^5$ pt/$cm^3$ (Figure 8C) measured with DiSCmini during cement sweeping.

Mass particle size distributions and concentrations for photocatalytic and regular cement during sweeping measured with three different personal air instruments (IOM filter cassette, cyclone and impactor) are shown in Figure 8D. Inhalable dust concentrations were 30% greater (15.19 (SD± 2.35) mg/$m^3$ for photocatalytic compared to regular cement (10.53 (SD± 1.60) mg/$m^3$). Respirable dust concentrations for photocatalytic cement were about double the concentration (9.52 (SD± 2.99) mg/$m^3$) of regular cement (4.98 (SD± 1.98) mg/$m^3$). Photocatalytic and regular cement during sweeping had the same peak at 1.55 µm with 5.26 (SD± 2.33) and 3.86 (SD±1.47) mg/$m^3$, respectively.

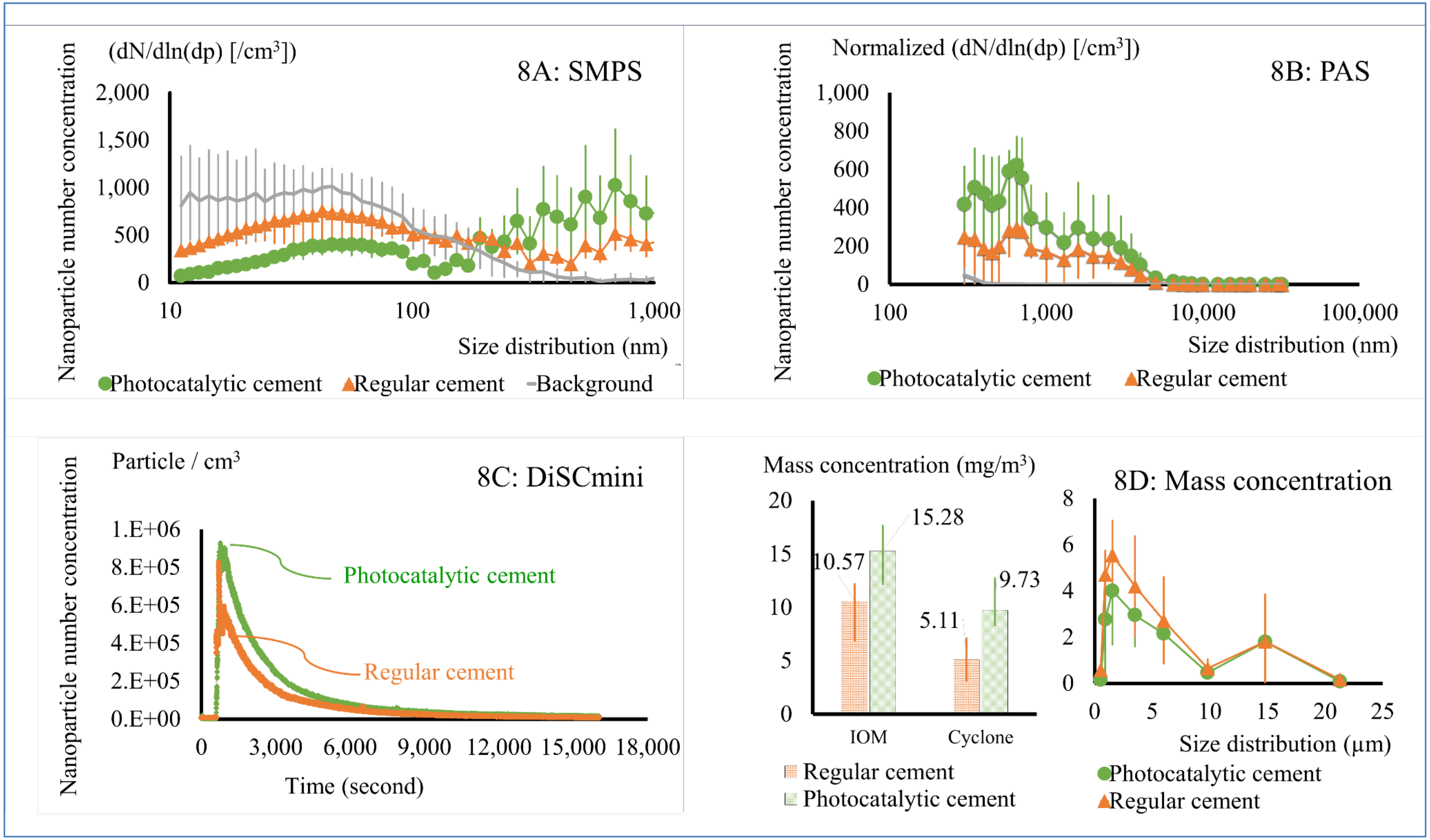


Figure 8: **<u>Sweeping:</u>** nanoparticle mass and number size distributions and concentrations for photocatalytic cement (solid circles) and regular cement (solid triangle)

Airborne photocatalytic cement contained two distinct types of nanoparticles as well as coarse particles (Figure 9A and 9B). The presence of nano-ranged spherical particles was only observed for photocatalytic cement and we attribute this to the presence of nano $TiO_2$ (Figure 9A and 9B). The regular cement contained mostly coarse particles (particles size around 1 μm) as shown in figure 9C and 9D.

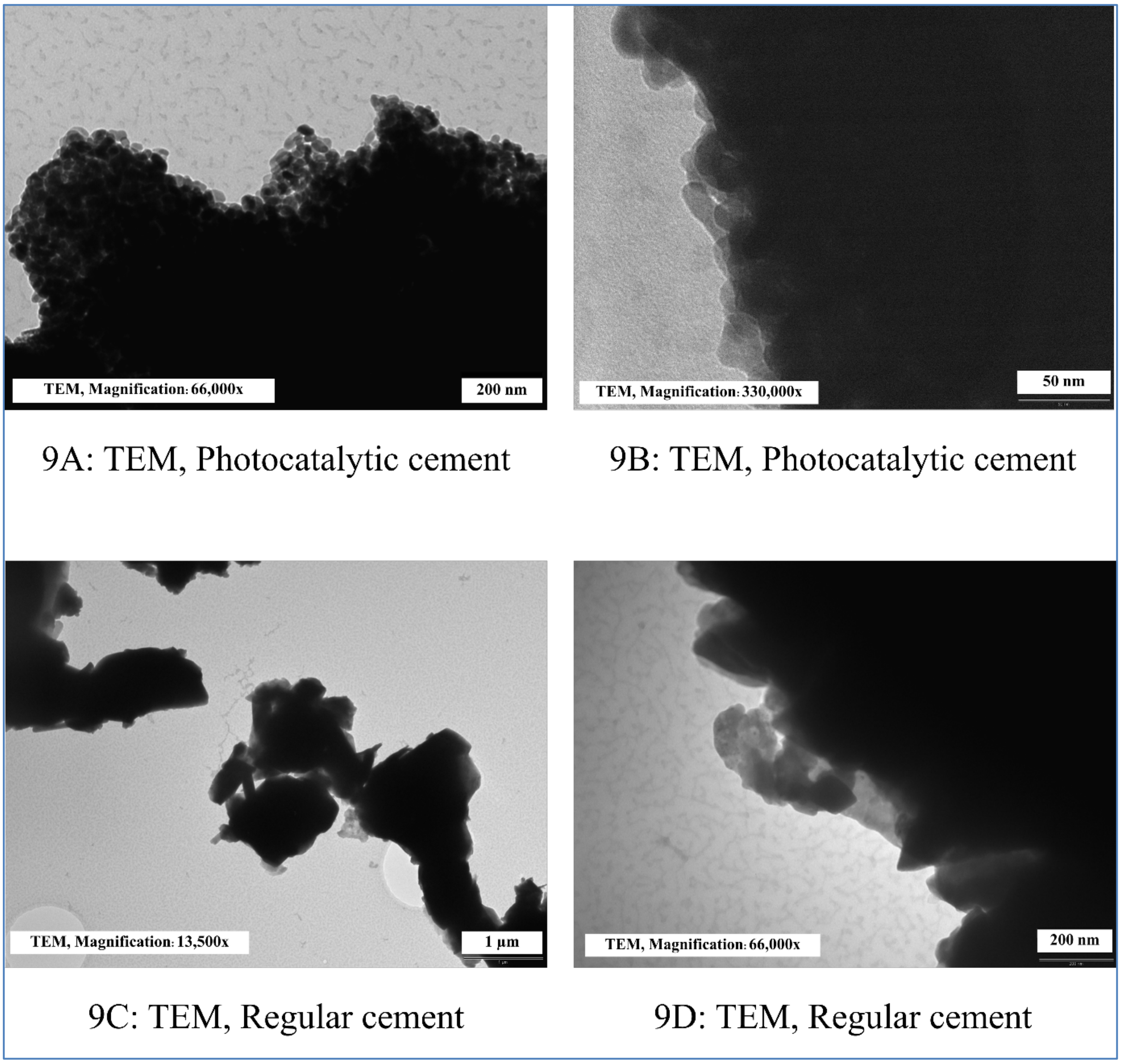


Figure 9: **Sweeping:** particles morphology between photocatalytic and regular cement

### *Elemental composition analysis*

Elemental compositions were analyzed by SEM-EDX and the results for both cement types by working activities are shown in Figure 10. Calcium oxides (assumed to be CaO) and silicon dioxides (assumed to be $SiO_2$) were the elemental substances detected in greatest quantity. Photocatalytic cement (bag sample) contained around 2 wt% nano $TiO_2$. This assumes that the information from the photocatalytic cement manufacturer was true that they added nano$TiO_2$ (percent nano$TiO_2$ was not given). The components were then defined based on what is known about the various oxides expected in cement. As nanoscale particles contained Ti and O in the expected ratio of approximately 1:2, it is sound to assume that these are $TiO_2$ nanoparticles. Furthermore, the TEM image from the bag emptying showed the presence of nanosized particles for photocatalytic cement but not for regular cement, and finally, the SMPS measurements showed nanosized particle fraction for bag emptying at 17%. Regular cement (bag sample) contained no detectable nano $TiO_2$. Photocatalytic cement bag emptying and sweeping had the highest airborne nano $TiO_2$ concentration 16.5 wt% (GSD±1.72) and 9.7 wt% (GSD±1.36), respectively. Photocatalytic cement concrete cutting contained 2.0 wt % nano $TiO_2$, which was the same concentration found in the bag sample. None of the airborne aerosol samples collected during activities with regular cement contained nano $TiO_2$. The mass concentration of nano $TiO_2$ in photocatalytic cement was calculated from element composition and inhalable dust mass concentration (sampled on the filter). Our work activity simulation showed airborne $TiO_2$ mass concentrations for photocatalytic cement bag emptying 2.50 mg/m$^3$, concrete cutting 1.53 mg/m$^3$, and sweeping 1.48 mg/m$^3$, respectively, for particles size >100 nm.

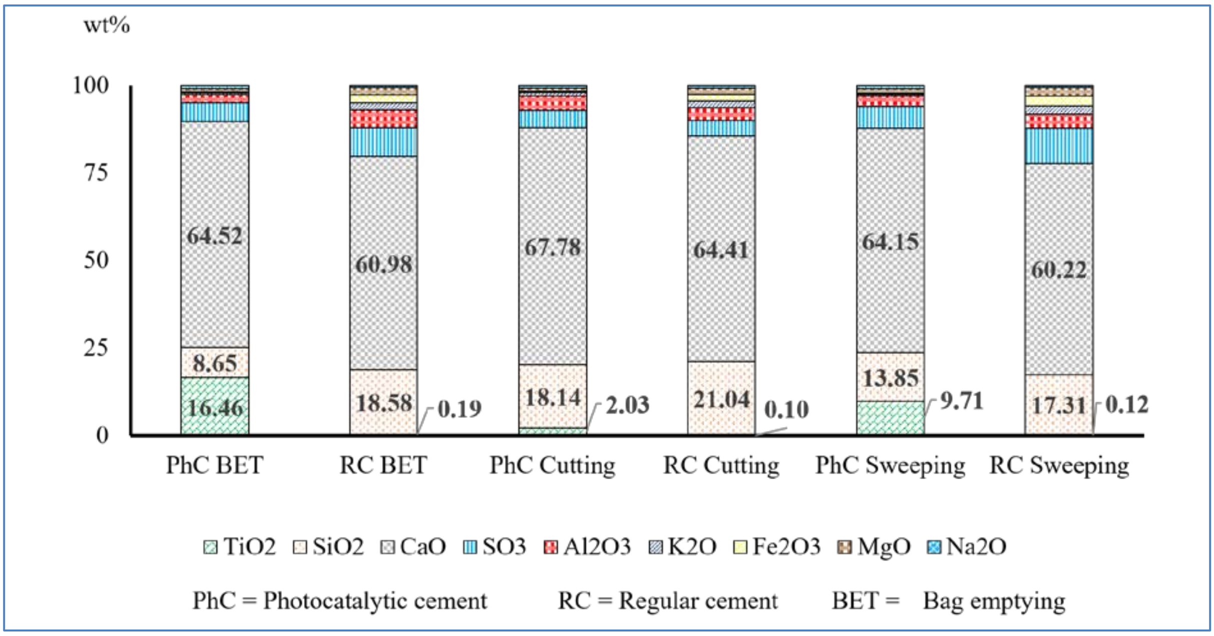


Figure 10: Elemental composition analysis from (SEM-EDX) given in percent for each substance from cement working activities

Cement powder samples were analyzed with X-ray diffraction and the phase analyses are shown in Table 2. Tricalcium silicate ($Ca_3SiO_5$) and dicalcium silicate ($Ca_2SiO_4$) were the most abundant elements in both cement types. Photocatalytic cement contained 2.6 wt% of nano $TiO_2$ in two different forms: anatase (1.8 wt%) and rutile (0.8 wt%).

Table2: Cement powder phase analysis by X-ray diffraction

| Mineral | Chemical formula | Bulk material (wt%) | |
|---|---|---|---|
| | | **Photocatalytic Cement** | **Regular Cement** |
| Tricalcium silicate (alite) | $Ca_3SiO_5$ | 61.4 | 58.2 |
| Dicalcium silicate (belite) | $Ca_2SiO_4$ | 14.2 | 15.6 |
| Tricalcium aluminate | $Ca_3Al_2O_4$ | 2.3 | 6.9 |
| Tetracalcium aluminoferrite | $Ca_4Al_nFe_{2-n}O_7$ | 3.4 | 5.7 |
| Calcite | CaCO3 | 10.1 | 7.9 |
| Anhydrite | $CaCO_3$ | 2.5 | 2.7 |
| Gypsum | $CaSO. 2H_2O$ | 1.4 | 1.1 |
| Portlandite | $Ca(OH)_2$ | 1.3 | 1 |
| Lime | CaO | 0.5 | 0.7 |
| Quartz | $SiO_2$ | 0.3 | 0.2 |
| Titanium dioxide | $TiO_2$ | | |
| • Anatase | | 1.80 | 0.00 |
| • Rutile | | 0.80 | 0.00 |

We found crystalline silica only during concrete (cement + sand) cutting for photocatalytic and regular cement with the following concentrations 2.5 and 3.5 mg/m$^3$, respectively. When only cement was used (no sand), the crystalline silica concentrations were always below the detection limit (LOD = 5 µg / sample).

***Field sampling at the construction sites***

During our study, we discovered that authorities in both Switzerland and Thailand discourage the use of photocatalytic cement due to the lack of information related to health effects associated with this exposure. The photocatalytic cement is already on the European and US market, but we were unable to find the amounts sold per year. We were thus not able to give an estimate for the number of workers potentially exposed, or to identify companies that use these products. Consequently, we collected samples in the construction industry among workers using only regular cement.

We collected the Swiss samples from July to September. The temperatures ranged during collection from 20 °C to 25 °C, and relative humidity was 50-60%. We sampled the Thai workers from November to December, and the temperatures were between 30-35 °C, and the relative humidity was 60-70%.

GMs and GSDs for size number distributions and number concentrations obtained at the Swiss construction sites are shown in figure 11A and 11B. Mean airborne particle number concentrations over 2 hours was 46,000 pt/cm$^3$, GMD was 49 nm and GSD was 2.4. Peak nanoparticle concentrations measured with the DiSCmini were for construction (n=5) 4.9 x 10$^5$ pt/cm$^3$. Polishing (n= 5) was double (9.9 x 10$^5$ pt/cm$^3$), and drilling activity (n=5) was slightly above (6.5 x 10$^5$ pt/cm$^3$). Figure 11C shows peak nanoparticle concentrations for the three activities separately in the same graph.

The mean mass concentration for inhalable dust was more than threefold greater for Switzerland (7.08 mg/m$^3$, SD±3.02) compared to Thailand (2.22 mg/m$^3$, SD±1.61) (Figure 11D). This was also true for respirable dust (Switzerland had 4.00 mg/m$^3$, SD±2.31 and Thailand 1.19 mg/m$^3$, SD±1.15).

Mass particle size distributions (Figure 11D) were quite different between the two country-specific construction sites. The Swiss construction site had a peak mass concentration of 2.22 mg/m$^3$ (SD±0.61) at 1.55 µm, while in Thailand the peak was just a fraction of this (0.57 mg/m$^3$ SD±0.46) and for smaller particles (0.93 µm).

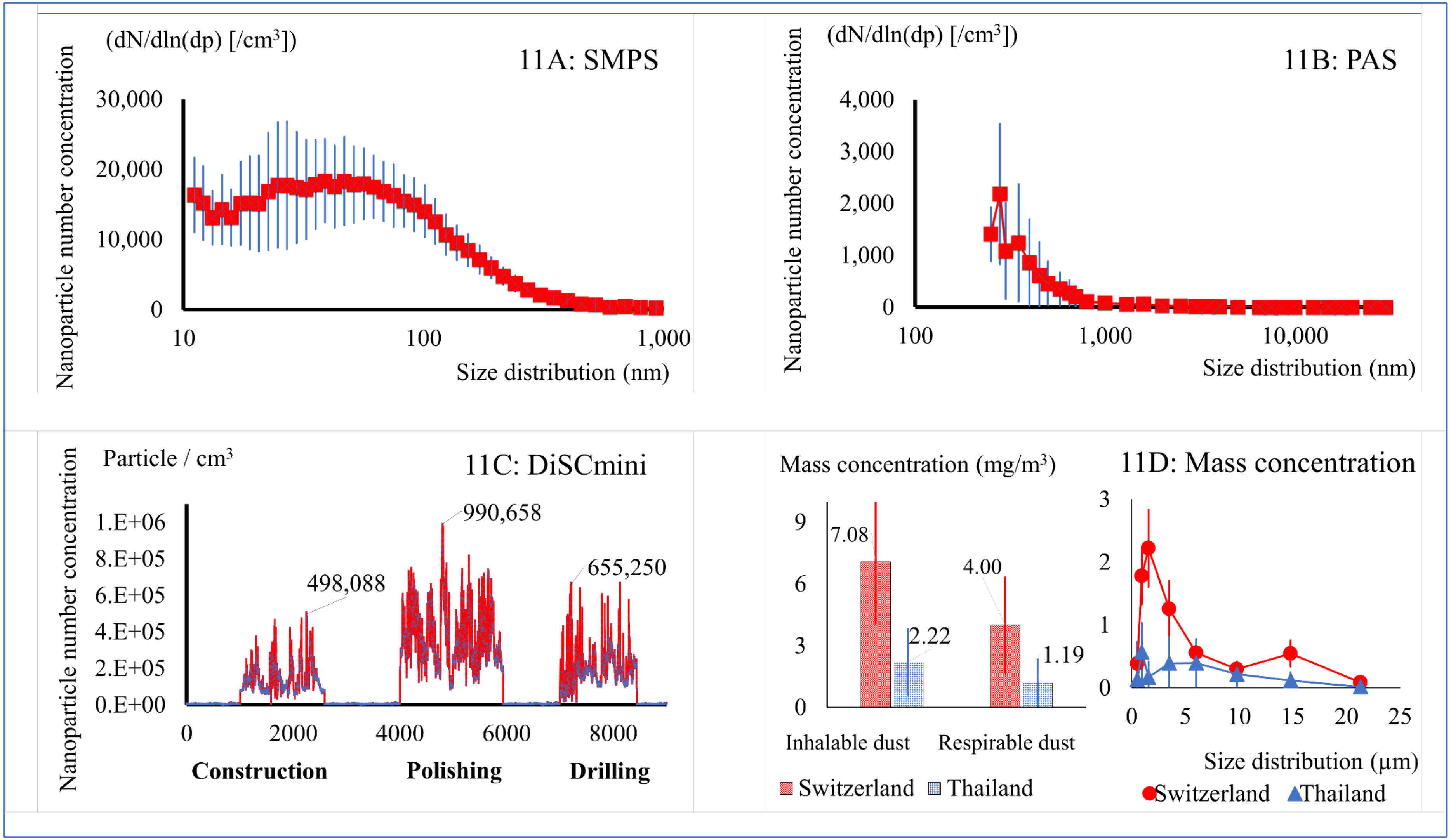


Figure 11: **<u>Construction sampling:</u>** nanoparticle mass and number size distributions and concentrations in construction

## 4. Discussion

In experiments with photocatalytic cement, we observed much larger mass-fractions of airborne particle-bound $TiO_2$ during sweeping (9.7 wt%) and during bag emptying (16.5 wt%) than what we found in the bagged cement (2 wt%). This shows that nano $TiO_2$ was easily airborne during activities with cement powder. It is in agreement with our previous dustiness study conducted with the same cement type where we observed nano $TiO_2$ to become airborne far easier than the remainder of the cement powder (Batsungnoen et al., 2019). Both nano $TiO_2$ crystalline phases, anatase and rutile, were identified in the photocatalytic cement (Table 2). It is important to understand what proportion of the nanomaterial additive that is airborne when assessing workers' exposures to nano cement. We analyzed the cement powder sampled directly from the bag shipped by the manufacturer with XRD. We characterized the composition of both the photocatalytic and the regular cement powders. These results are given in Table 2 and show that photocatalytic cement contained 2.6% TiO2. XRD analysis need a minimum of 3 g of sample. Unfortunately, we cannot analyze the dust collected with air sampling with XRD because air samples contain far less than the required amount. Due to this limitation, we confirmed the chemical composition in a few aerosol samples collected during cement working activities with SEM-EDX. We focused on a single dot with a 300 nm dimeter in the SEM-EDX images which showed this particle to be 82% $TiO_2$.

The work activity and the form in which the nano-additive is present also seem to play an important role. Notably, photocatalytic cement concrete cutting resulted in similar proportions of nano $TiO_2$ (2 wt%) in airborne nanoparticles as in bagged cement material. This suggests that the nano-additive was well bound to the matrix during the cutting, and consequently, the nano $TiO_2$ particles were released in the aerosol as a part of the concrete particles. We cannot visualize chemically bound particles, but rely on dispersion as a measure of the degree to which particles clump together into agglomerates or aggregates. We measured dispersion as the particle size distribution and the width of a particle size distribution. We observed small particles on the boundary of larger particles on the TEM image obtained during bag emptying (Fig. 5) and sweeping (Fig. 9) photocatalytic cement. We did not observe these small particles in the TEM images obtained for the same activities with regular cement. Consequently, we conclude that these smaller particles are mainly $TiO_2$ nanoparticles as this was the only difference between photocatalytic and regular cement as well as the SEM-EDX analysis. The $TiO_2$ nanoparticles agglomerated to the larger particle and are held together by weak bonds (e.g., van der Waals forces or physical entanglement). TEM images obtained from air sampling during concrete cutting (Fig. 7) showed only 2% $TiO_2$. We observed that these particles were embedded in larger concrete particles resembling an aggregate, which are generally held together by covalent bonds. Covalent bonds between $TiO_2$ and $SiO_2$, $CaCO_3$ and $SO_3$, have previously been shown by FTIR analysis (Zouzelka and Rathousky, 2017; Yang et al., 2018). We hypothesize that the nano $TiO_2$ in the dry cement powder is not chemically bound as we could observe primary nanoparticles in the TEM image for bag-emptying (Figures 5A and 5A) and sweeping (9A and 9B). We believe that nanoparticles were bound to the concrete surface when water was added, as we observed no primary nanoparticles for cutting either for regular or photocatalytic cement (Figure 7).

Inhaling nano $TiO_2$ has been associated with respiratory problems in animals (Kwon et al., 2012). An association between photocatalytic cement and respiratory problems is not known as no such studies are available. We can hypothesize that an association between photocatalytic cement exposure and respiratory problems is possible given that nano $TiO_2$ is released from photocatalytic cement. The nano $TiO_2$ concentrations in our experiments were low ($10^3$ particles/$cm^3$ range) compared to the respiratory study in rats that showed nano $TiO_2$ to be toxic at particle number concentration in the $10^6$ range (Kwon et al., 2012). The study exposed the rats to only nano $TiO_2$ therefore it is difficult to extrapolate to possible health effects from exposure to a mixture of cement and nano $TiO_2$ particles. Complexing the matter further, the lung injury induced by nano $TiO_2$ depended on dimension, size distribution, concentration, crystal phase, agglomeration, surface coating, chemical, and physical properties (Noël et al., 2012; Wang and Fan, 2014).

Both photocatalytic and regular cement had 99 % of the airborne particles with sizes less than 3.5 µm in all working activities; and can thus be deposited and diffuse into the respiratory tract especially in the alveoli (Oberdörster et al., 2005; ICRP, 1994; Sha et al., 2015; Tedja et al., 2011). The mean size of airborne cement particles during simulated working activities was 200-350 nm, which were far greater than what we found at the construction sites (mean size was 49 nm). This was surprising, and possibly not related to the cement but rather to the diesel truck picking up the concrete walls, since diesel operated vehicles often emit particles in the 50 nm size range (Xue et al., 2015).

World-wide, only few occupational exposure limits (OELs) exist for nano $TiO_2$. The US Occupational Safety and Health Administration (OSHA) and NIOSH recommend a nano $TiO_2$ exposure limit for 8 hours to be (NIOSH, 2011; OSHA, 2013):

- particle size >100 nm OEL= 2.4 mg/m$^3$
- particle size <100 nm OEL= 0.3 mg/m$^3$

In addition, the French Agency for Food, Environmental and Occupational Health & Safety (ANSES) recommends a toxicity reference value (TRV) for inhaled $TiO_2$ nanoparticles with particle sizes from 25 nm (P25) of 120 mg/m$^3$ (ANSES, 2019).

Our work activity simulation showed airborne mass concentrations for photocatalytic cement bag emptying (2 min) of 15 mg/m$^3$ thereof 16.5% $TiO_2$ (from the elemental composition analysis), which gave 2.5 mg/m$^3$ $TiO_2$. Assuming different bag emptying work scenarios and that exposure increased linearly with 2.50 mg/m$^3$ with each bag emptying. Emptying four consecutive bags would then give a total of 10 mg/m$^3$ $TiO_2$ (2.5 mg/m$^3$ $TiO_2$ x 4 bags). This averages out over 4 hours to be 2.50 mg/m$^3$ (10 mg/m$^3$ $TiO_2$ / 4 hours). We observed that workers emptied 2-4 bags during the morning as well as the afternoon shifts in Thailand. Thus, workers worked eight hours per day and emptied eight bags per day (four in the morning and four in the afternoon). Emptying eight bags will generate (2.5 $TiO_2$ mg/m$^3$/bag x 8 bags) 20 mg/m$^3$ $TiO_2$. Averaging this over the workday gives and upper range of 2.5 mg/m$^3$ $TiO_2$ (20 mg/m$^3$ $TiO_2$ / 8 hours/day). This time weighted average is just above the OEL for particle sizes >100 nm. We compared our results with this OEL since our GM particle size diameter was 322 nm. To reduce the airborne dust concentrations, we could recommend that workers should empty less than 8 bags during a shift, but that would not be cost effective. Another strategy would be to reduce the airborne particles that lingers in the air post-bag emptying as we observed in the simulations (Figure 4C). The workers would empty one bag, add water, and then mix, and repeat this procedure four times. This would bring the dust concentrations down to background within 15 min thus the average over the shift would not exceed 2.5 mg/m$^3$ $TiO_2$. Consequently, the morning exposure would be 2.5 mg/m$^3$ $TiO_2$ and same in the afternoon, which gives a total exposure of (2.5 mg/m$^3$ $TiO_2$ + 2.5 mg/m$^3$ $TiO_2$) 5 mg/m$^3$ $TiO_2$ per day averaged over 8 hours would be 0.62 mg/m$^3$ $TiO_2$ (5 mg/m$^3$ $TiO_2$ / 8 hours). These values are based on our exposure chamber simulations and would of course be altered by worksite specific elements such as factors affecting the dispersion like wind and openness of the space as well as factors affecting release and agglomeration such as rain and humidity. In our simulation study, bag emptying generated the greatest amount of airborne nano $TiO_2$ thus this work activity is of greatest concern. In Switzerland, cement arrived at the worksite already mixed with water thereby reducing this exposure among construction workers. Another approach would be that the producers develop a formula that would add nano $TiO_2$ as a liquid dispersion, thereby reducing the potential for aerosolizing these particles.

Cement dust is regulated in Thailand and Switzerland as particulates not otherwise regulated (PNOR). The Thai OEL for PNOR dust is 15 mg/m$^3$ for inhalable and 5 mg/m$^3$ for respirable dust. In Switzerland, the OELs are slightly lower; 10 mg/m$^3$ and 3 mg/m$^3$ for inhalable and respirable dust, respectively. Thai construction workers were not exposed above the Thai OELs, while the Swiss construction workers were exceeding the Swiss OEL for respirable dust. The jobs performed were similar among the Swiss and Thai construction workers, but the difference was that the Swiss construction workers used powerful machine tools, in particularly during concrete polishing and drilling, while the Thai construction workers worked with small hand-held hammer drills. Power tools have shown to generate more dust compared to manual tools such as drilling concrete, which generated the highest exposures for quartz and respirable dust among construction workers (Deurssen van et al., 2014). Moreover, Qi and colleagues (Qi, Echt, and Gressel, 2017) reported that concentrations of airborne particles during fiber cement cutting increased with the power of the tools used. The main factors associated with particle generation were number of blade teeth, blade rotating speed, and cutting feed rate (Qi, Echt, and Gressel, 2017). We found comparable result in our work activity simulation, where cutting concrete blocks using power tools generated high particle concentrations (Figure 6).

We confirmed that calcium dioxides made up 62 wt% of the airborne particles generated during work activity simulation; the same concentration as in cement (Meo, 2004). This was observed irrespective of cement type and working activities. If we assume 62% of the total particle concentration in the Swiss construction (GM 7.08 mg/m$^3$) as CaO, we get 4.38 mg/m$^3$ CaO

(7.08 mg/$m^3$ CaO x 62%). This estimate was twice the Swiss OEL (2 mg/$m^3$). The Thai OEL for CaO is more than double of the Swiss OEL, i.e., 5 mg/$m^3$. Performing the same estimate for CaO concentration for the Thai workers (GM 2.22 mg/$m^3$), gave 1.37 mg/$m^3$ (2.22 mg/$m^3$ CaO x 62%), which was below both Swiss and Thai OELs. Although, the Swiss construction workers were below the PNOR OEL, exposure reduction measures are still needed as they exceed the OEL for CaO. Although, both countries' OELs were established to protect against upper respiratory tract inflammation produced by CaO's alkaline properties (TOXNET, 2014; NJDHSS, 2003), the countries' feasibility assessments for respecting the limit resulted in different values.

The second most abundant airborne particles were $SiO_2$. CaO and $SiO_2$ were chemically bound to tricalcium silicate ($Ca_3SiO_5$) and dicalcium silicate ($Ca_2SiO_4$) in the cement. Although, we quantified 0.2-0.3 wt% crystalline $SiO_2$ in cement (Table 2), only the respirable fraction of the airborne dust during concrete cutting was present as crystalline $SiO_2$. Thus, respiratory crystalline $SiO_2$ originated from the sand and not from the cement as previously reported by others (McLean et al., 2017). The levels of crystalline silica observed were very high, well above the 8-hour OEL levels, which suggests that for dusty work activities with concrete, the greatest risk comes from crystalline silica in sand rather than from nano-additives.

Sweeping with a broom generated inhalable and respirable dust greater than the Swiss and Thai OELs during simulation (Figure 1C, Figure 8) but not in the field (Figure 3C, Figure 11 includes sweeping with other job activities). The field samples were likely lower because the work place was generously ventilated (some jobs were performed outside) while the simulations were performed in an exposure chamber (10 $m^3$) without ventilation. Although, the simulations were not able to generate field concentrations, it gave us a relative ranking of the particle exposure that we observed in the field: very high exposure during cutting (41-75 mg/m$^3$, Figure 6D), and much lower and similar concentrations for bag emptying (11-15 mg/m$^3$, Figure 4D) and sweeping (11-15 mg/m$^3$, Figure 8D). Other researchers have also found that sweeping cement is associated with higher airborne particle concentrations (GM 0.79-1.2 mg/m$^3$) compared to other cement production jobs such as laboratory, foreman and administration (GM 0.42-0.45 mg/m$^3$) (Notø et al., 2015). In Notø and colleagues's very large study comprising 24 cement plants in eight countries, they found 63% of the variability to be explained by plant differences. This could also be true for the differences in airborne particle concentrations we observed between Switzerland and Thailand; however, due to the limited number of samples in our study, we cannot calculate this. One study specifically reported concentrations during cleaning using brooms at two cement plants in Ethiopia (Zeleke et al., 2011). They confirmed significantly greater exposures to total and respirable dust in these cleaners compared to other production worker at the same plants.

Sweeping photocatalytic cement produced 31% more inhalable airborne particles (Figure 8D) than regular cement. This increase in mass is probably not explained by the slight increase in airborne particles less than 5 µm as this would not significantly add mass. Rather particles around 15 µm would contribute to the increase in mass observed. Why we have a greater mass concentration in photocatalytic cement compared to regular cement, we can only speculate. Perhaps the addition of nano $TiO_2$ to the cement contributes to agglomeration of particles of smaller size than if absent, thus the particles generated will be airborne over a longer time. We have not found any scientific publications describing or refuting such a postulation.

Cleaning using other methods than a broom would reduce the cement exposures among Thai construction workers, while Swiss construction workers will need other protective measures to reduce exposures. Exposures to airborne cement particles in the construction industry also depends on duration, environment (temperature, humidity and wind), space (indoor, outdoor), workplace sizes, machine tool use, material type, control measures, and use of personal protective equipment (PPE). We observed that Thai construction workers did not use respiratory protective equipment (RPE) while Swiss construction workers did. Thai construction workers were not comfortable using RPE because it was both hot and humid. Control measures need to be implemented for the Swiss construction workers to not only comply with the Swiss OEL regulations, but to reduce the risk of developing COPD. Local exhaust ventilation (LEV) in construction were shown to be effective in reducing respirable dust in both the work and adjacent area (Kokkonen et al., 2019).

The protection measures needed for workers working with photocatalytic cement, especially during dry cement work, should be similar to recommendations made for nano $TiO_2$ exposures. Wet processes to reduce airborne dust exposures should be recommended if possible. Several international bodies have recommended ways to reduce nano particle exposures using engineering controls such as enclosed process chambers with negative pressure and local exhaust ventilation (LEV) installed with high-efficiency particulate air (HEPA) filters (NIOSH, 2011; NIOSH, 2012; NIOSH, 2013; OSHA, 2013; Goede et al., 2018). Where enclosure of the source is not possible other alternatives should be considered such as portable capture hood, wet or dry vacuum machine equipped with a HEPA filter. Administrative control strategies can also be implemented such as adjust work schedules, education, training, good general hygiene, good housekeeping, and medical surveillance (NIOSH, 2011; NIOSH, 2012; NIOSH, 2013; OSHA 2013). More specifically, OSHA and NIOSH recommend using: RPE, protective clothing, nitrile or chemically impervious gloves, and goggles. The RPE types recommended are N100, R100, and P100 for US (OSHA, 2013; OSHA, 2011; NIOSH, 2014) and P3 and filtering face piece (FFP3) for Europe (EN 143 and EN 149) (Goede et al., 2018; Rengasamy et al., 2009).

**5. Conclusion**

The airborne nano $TiO_2$ concentration was far greater than the labeled 2 wt% in the photocatalytic cement bag during simulation, increasing to 9.7 wt% during sweeping and 16.5 wt% during bag emptying. Work activities studied in the exposure chamber such as sweeping and bag emptying gave rise to nano $TiO_2$ air concentrations while concrete cutting did not. Thai and Swiss construction workers using regular cement had different exposure profiles. Thai workers were mostly exposed during sweeping and Swiss workers during drilling and polishing cement blocks. Both photocatalytic and regular cement had a GMD less than 3.5 μm thus will be able to penetrate into the lung. Emerging health risks associated with nano $TiO_2$ has yet to be assessed for construction workers using photocatalytic cement. We recommend workers using photocatalytic cement to use protection measures similar to recommendations made for nano $TiO_2$ exposures.

**6. Conflict of interest**

The authors declare no conflict of interest.

## 7. Acknowledgements

Funding was received from Center for Primary Care and Public Health (Unisanté), Department of Occupational and Environmental Health (formerly known as Institute for Work and Health, IST), Switzerland, the Royal Thai Government, and the Ministry of Science and Technology, Thailand. We greatly appreciate help from Dr. Nicolas Concha Lozano for the morphology, crystalline silica analysis, and elemental composition analysis. We would like to thank Ms. Nicole Charriere, Mr. Benoit Allaz, Mr. Nicolas Sambiagio, Mr. Timothée Ndarugendamwo, Mr. Elvar Oskarsson, Mr. Antoine Milon and Mr. Yannick Rodari for all practical laboratory and field support. We also thank the Laboratory of Construction Materials (LCM), at Swiss Federal Institute of Technology Lausanne (EPFL) for the x-ray diffraction characterization. We thank Italcementi group for sending us a free sample.

## 8. References

Aitken, R.J., K.S. Creely, and C.L. Tran. 2004. "Nanoparticles: An Occupational Hygiene Review." Research Reports. http://www.hse.gov.uk/research/rrhtm/rr274.htm.

ANSES. 2019. "Titanium Dioxide in Nanoparticle Form: ANSES Defines a Toxicity Reference Value (TRV) for Chronic Inhalation Exposure." French Agency for Food, Environmental and Occupational Health & Safety. https://www.anses.fr/en/content/titanium-dioxide-nanoparticle-form-anses-defines-toxicity-reference-value-trv-chronic.

Arenberg, Mary R., and Yuji Arai. 2020. "The Effects of Oxyanion Adsorption on Reactive Oxygen Species Generation by Titanium Dioxide." Clays and Clay Minerals. https://doi.org/10.1007/s42860-019-00039-8.

Banerjee, Swagata, Dionysios D. Dionysiou, and Suresh C. Pillai. 2015. "Self-Cleaning Applications of TiO2 by Photo-Induced Hydrophilicity and Photocatalysis." Applied Catalysis B: Environmental 176–177 (October): 396–428. https://doi.org/10.1016/j.apcatb.2015.03.058.

Batsungnoen, Kiattisak, Nancy B. Hopf, Guillaume Suárez, and Michael Riediker. 2019. "Characterization of Nanoparticles in Aerosolized Photocatalytic and Regular Cement." Aerosol Science and Technology 53 (5): 540–48. https://doi.org/10.1080/02786826.2019.1578334.

Carp, O., C. L. Huisman, and A. Reller. 2004. "Photoinduced Reactivity of Titanium Dioxide." Progress in Solid State Chemistry 32 (1–2): 33–177. https://doi.org/10.1016/j.progsolidstchem.2004.08.001.

Chen, Jun, and Chi-sun Poon. 2009. "Photocatalytic Construction and Building Materials: From Fundamentals to Applications." Building and Environment 44 (9): 1899–1906. https://doi.org/10.1016/j.buildenv.2009.01.002.

Dalton, J. S, P. A Janes, N. G Jones, J. A Nicholson, K. R Hallam, and G. C Allen. 2002. “Photocatalytic Oxidation of NOx Gases Using TiO2: A Surface Spectroscopic Approach.” Environmental Pollution 120 (2): 415–22. https://doi.org/10.1016/S0269-7491(02)00107-0.

Deurssen, Erik van, Anjoeka Pronk, Suzanne Spaan, Henk Goede, Erik Tielemans, Dick Heederik, and Tim Meijster. 2014. “Quartz and Respirable Dust in the Dutch Construction Industry: A Baseline Exposure Assessment as Part of a Multidimensional Intervention Approach.” The Annals of Occupational Hygiene 58 (6): 724–38. https://doi.org/10.1093/annhyg/meu021.

Diesen, Veronica, and Mats Jonsson. 2014. “Formation of H2O2 in TiO2 Photocatalysis of Oxygenated and Deoxygenated Aqueous Systems: A Probe for Photocatalytically Produced Hydroxyl Radicals.” The Journal of Physical Chemistry C 118 (19): 10083–87. https://doi.org/10.1021/jp500315u.

Ding, Yaobo, Thomas A. J. Kuhlbusch, Martie Van Tongeren, Araceli Sánchez Jiménez, Ilse Tuinman, Rui Chen, Iñigo Larraza Alvarez, et al. 2017. “Airborne Engineered Nanomaterials in the Workplace—a Review of Release and Worker Exposure during Nanomaterial Production and Handling Processes.” Journal of Hazardous Materials, SI:Environmental Nanotechnol, 322 (January): 17–28. https://doi.org/10.1016/j.jhazmat.2016.04.075.

Edwin G. Foulke. 2008. Preventing Skin Problems from Working with Portland Cement. Occupational Safety and Health Administration, OSHA. https://www.osha.gov/Publications/OSHA-3351-portland-cement.pdf.

Eom, Sang-Yong, Eun-Bi Cho, Moo-Kyung Oh, Sun-Seog Kweon, Hae-Sung Nam, Yong-Dae Kim, and Heon Kim. 2017. “Increased Incidence of Respiratory Tract Cancers in People Living near Portland Cement Plants in Korea.” International Archives of Occupational and Environmental Health 90 (8): 859–64. https://doi.org/10.1007/s00420-017-1244-9.

Falck, G. C. M., H. K. Lindberg, S. Suhonen, M. Vippola, E. Vanhala, J. Catalán, K. Savolainen, and H. Norppa. 2009. “Genotoxic Effects of Nanosized and Fine TiO2.” Human & Experimental Toxicology 28 (6–7): 339–52. https://doi.org/10.1177/0960327109105163.

Friedlander, Sheldon K., and David Y. H. Pui. 2003. “National Science Foundation Workshop Report on Emerging Issues in Nanoparticle Aerosol Science and Technology (NAST).” Workshop Report. http://www.eng.uc.edu/~beaucag/Classes/MorphologyofComplexMaterials/NSFAerosolPar%20Report.pdf.

Fujishima, Akira, and Xintong Zhang. 2006. “Titanium Dioxide Photocatalysis: Present Situation and Future Approaches.” Comptes Rendus Chimie, Conversion photochimique et stockage de l’énergie solaire, 9 (5): 750–60. https://doi.org/10.1016/j.crci.2005.02.055.

Geiser, Marianne, and Wolfgang G. Kreyling. 2010. “Deposition and Biokinetics of Inhaled Nanoparticles.” Particle and Fibre Toxicology 7: 2. https://doi.org/10.1186/1743-8977-7-2.

Ghosh, Manosij, Maumita Bandyopadhyay, and Anita Mukherjee. 2010. “Genotoxicity of Titanium Dioxide (TiO2) Nanoparticles at Two Trophic Levels: Plant and Human Lymphocytes.” Chemosphere 81 (10): 1253–62. https://doi.org/10.1016/j.chemosphere.2010.09.022.

Goede, Henk, Yvette Christopher-de Vries, Eelco Kuijpers, and Wouter Fransman. 2018. “A Review of Workplace Risk Management Measures for Nanomaterials to Mitigate Inhalation and Dermal Exposure.” Annals of Work Exposures and Health. https://doi.org/10.1093/annweh/wxy032.

Guillemin, Michel. 1975. “Mise Au Point et Utilisation d’une Cabine d’expérimentation.” Archives Des Maladies Professionnelles de Medecine Du Travail et de Securite Sociale (Paris) (Arch. Mal. Prof.) 36: 421–28.

IARC. 1997. IARC Monographs on the Evaluation of Carcinogenic Risk to Human Silica, Some Silicates, Coal Dust and Para-Aramid Fibrils. Vol. 68. World health organization, International Agency for Research on Cancer. http://monographs.iarc.fr/ENG/Monographs/vol68/.

IARC. 2012. Silica Dust Crystalline in the Form of Quartz or Cristobalite. World health organization, International Agency for Research on Cancer. https://monographs.iarc.fr/ENG/Monographs/vol100C/mono100C-14.pdf.

IARC. 2017. IARC Monographs on the Evaluation of Carcinogenic Risk to Human; List of Classification. Vol. 1–120. World health organization, International Agency for Research on Cancer. http://monographs.iarc.fr/ENG/Classification/latest_classif.php.

ICRP. 1994. “Human Respiratory Tract Model for Radiological Protection. A Report of a Task Group of the International Commission on Radiological Protection.” Annals of the ICRP 24 (1–3): 1–482.

ILO. 2014. “Safety and Health in the Construction Sector- Overcoming the Challenges.” Event. October 2, 2014. http://www.ilo.org/empent/Eventsandmeetings/WCMS_310993/lang--en/index.htm.

Jimenez-Relinque, E., J. R. Rodriguez-Garcia, A. Castillo, and M. Castellote. 2015. “Characteristics and Efficiency of Photocatalytic Cementitious Materials: Type of Binder, Roughness and Microstructure.” Cement and Concrete Research 71 (May): 124–31. https://doi.org/10.1016/j.cemconres.2015.02.003.

Kaewamatawong, Theerayuth, Natsuko Kawamura, Mina Okajima, Masumi Sawada, Takehito Morita, and Akinori Shimada. 2005. “Acute Pulmonary Toxicity Caused by Exposure to Colloidal Silica: Particle Size Dependent Pathological Changes in Mice.” Toxicologic Pathology 33 (7): 745–51. https://doi.org/10.1080/01926230500416302.

Kokkonen, Anna, Markku Linnainmaa, Arto Säämänen, Tomi Kanerva, Jouni Sorvari, Mikko Kolehmainen, Vuokko Lappalainen, and Pertti Pasanen. 2019. “Control of Dust Dispersion From an Enclosed Renovation Site Into Adjacent Areas by Using Local Exhaust Ventilation.” Annals of Work Exposures and Health. https://doi.org/10.1093/annweh/wxz016.

Kreyling, Wolfgang G, Stephanie Hirn, and Carsten Schleh. 2010. “Nanoparticles in the Lung.” Nature Biotechnology 28 (12): 1275–76. https://doi.org/10.1038/nbt.1735.

Kwon, Soonjin, Young-Su Yang, Hyo-Seon Yang, Jinsoo Lee, Min-Sung Kang, Byoung-seok Lee, Kyuhong Lee, and Chang-Woo Song. 2012. “Nasal and Pulmonary Toxicity of Titanium Dioxide Nanoparticles in Rats.” Toxicological Research 28 (4): 217–24. https://doi.org/10.5487/TR.2012.28.4.217.

Lan, Yucheng, Yalin Lu, and Zhifeng Ren. 2013. “Mini Review on Photocatalysis of Titanium Dioxide Nanoparticles and Their Solar Applications.” Nano Energy 2 (5): 1031–45. https://doi.org/10.1016/j.nanoen.2013.04.002.

Lee, Jaesang, Shaily Mahendra, and Pedro J. J. Alvarez. 2010. “Nanomaterials in the Construction Industry: A Review of Their Applications and Environmental Health and Safety Considerations.” ACS Nano 4 (7): 3580–90. https://doi.org/10.1021/nn100866w.

Lim, Tak Hyoung, Sang Mun Jeong, Sang Done Kim, and Janos Gyenis. 2000. “Photocatalytic Decomposition of NO by TiO2 Particles.” Journal of Photochemistry and Photobiology A: Chemistry 134 (3): 209–17. https://doi.org/10.1016/S1010-6030(00)00265-3.

Long, Thomas C., Navid Saleh, Robert D. Tilton, Gregory V. Lowry, and Bellina Veronesi. 2006. “Titanium Dioxide (P25) Produces Reactive Oxygen Species in Immortalized Brain Microglia (BV2): Implications for Nanoparticle Neurotoxicity.” Environmental Science & Technology 40 (14): 4346–52.

Ma, Baoguo, Hainan Li, Junpeng Mei, Xiangguo Li, and Fangjie Chen. 2015. “Effects of Nano-TiO2 on the Toughness and Durability of Cement-Based Material.” Advances in Materials Science and Engineering. https://doi.org/10.1155/2015/583106.

Ma, Hongbo, Amanda Brennan, and Stephen A. Diamond. 2012. “Photocatalytic Reactive Oxygen Species Production and Phototoxicity of Titanium Dioxide Nanoparticles Are Dependent on the Solar Ultraviolet Radiation Spectrum.” Environmental Toxicology and Chemistry 31 (9): 2099–2107. https://doi.org/10.1002/etc.1916.

Maciejewska, A., and G. Bielichowska-Cybula. 1991. “[Biological effect of cement dust].” Medycyna Pracy 42 (4): 281–89.

McLaughlin, J. K., W. H. Chow, and L. S. Levy. 1997. “Amorphous Silica: A Review of Health Effects from Inhalation Exposure with Particular Reference to Cancer.” Journal of Toxicology and Environmental Health 50 (6): 553–66. https://doi.org/10.1080/15287399709532054.

McLean, David, Bill Glass, Andrea ’t Mannetje, and Jeroen Douwes. 2017. “Exposure to Respirable Crystalline Silica in the Construction Industry-Do We Have a Problem?” The New Zealand Medical Journal 130 (1466): 78–82.

Meo, Sultan A. 2004. “Health Hazards of Cement Dust.” Saudi Medical Journal 25 (9): 1153–59.

Merget, R., T. Bauer, H. U. Küpper, S. Philippou, H. D. Bauer, R. Breitstadt, and T. Bruening. 2002. “Health Hazards Due to the Inhalation of Amorphous Silica.” Archives of Toxicology 75 (11–12): 625–34.

Moghadam, Somayeh Rahimi, Siavosh Abedi, Mahdi Afshari, Ehsan Abedini, and Mahmood Moosazadeh. 2017. “Decline in Lung Function among Cement Production Workers: A Meta-Analysis.” Reviews on Environmental Health 32 (4): 333–341. https://doi.org/10.1515/reveh-2017-0017.

Napierska, Dorota, Leen CJ Thomassen, Dominique Lison, Johan A Martens, and Peter H Hoet. 2010. “The Nanosilica Hazard: Another Variable Entity.” Particle and Fibre Toxicology 7 (December): 39. https://doi.org/10.1186/1743-8977-7-39.

NIOSH. 1998. “NIOSH Manual of Analytical Methods 0600: Particulate Not Otherwise Regulated, Respirable.” The National Institute for Occupational Safety and Health (NIOSH). https://www.cdc.gov/niosh/docs/2003-154/method-cas0.html.

NIOSH. 2003. “NIOSH Manual of Analytical Methods 7602: Silica, Crystalline by IR (KBr Pellet).” The National Institute for Occupational Safety and Health (NIOSH). https://www.cdc.gov/niosh/docs/2003-154/method-cas1.html.

NIOSH. 2009. Approaches to Safe Nanotechnology Managing the Health and Safety Concerns Associated with Engineered Nanomaterials. U.S. Department of Health and Human Services, Centers for Disease Control and Prevention, National Institute for Occupational Safety and Health. http://www.cdc.gov/niosh/docs/2009-125/pdfs/2009-125.pdf.

NIOSH. 2011. Occupational Exposure to Titanium Dioxide. U.S. Department of Health and Human Services, Centers for Disease Control and Prevention, National Institute for Occupational Safety and Health.

NIOSH. 2012. General Safe Practices for Working with Engineered Nanomaterials in Research Laboratories. U.S. Department of Health and Human Services, Centers for Disease Control and Prevention, National Institute for Occupational Safety and Health. http://www.cdc.gov/niosh/docs/2012-147/pdfs/2012-147.pdf.

NIOSH. 2013. Current Strategies for Engineering Controls in Nanomaterial Production and Downstream Handling Processes. U.S. Department of Health and Human Services, Centers for Disease Control and Prevention, National Institute for Occupational Safety and Health. http://www.cdc.gov/niosh/docs/2014-102/pdfs/2014-102.pdf.

NIOSH. 2014. "NIOSH Guide to the Selection and Use of Particulate Respirators, Certified Under 42 CFR 84." U.S. Department of Health and Human Services, Centers for Disease Control and Prevention, National Institute for Occupational Safety and Health. http://www.cdc.gov/niosh/docs/96-101/.

NIOSH. 2018. "NIOSH Pocket Guide to Chemical Hazards: Silica, Amorphous." The National Institute for Occupational Safety and Health (NIOSH). https://www.cdc.gov/index.htm.

NJDHSS. 2003. “Hazardous Substances Fact Sheet: Calcium Oxide.” New Jersey Department of Health and Senior Services. https://nj.gov/health/eoh/rtkweb/documents/fs/0325.pdf.

Noël, A., K. Maghni, Y. Cloutier, C. Dion, K. J. Wilkinson, S. Hallé, R. Tardif, and G. Truchon. 2012. “Effects of Inhaled Nano-TiO2 Aerosols Showing Two Distinct Agglomeration States on Rat Lungs.” Toxicology Letters 214 (2): 109–19. https://doi.org/10.1016/j.toxlet.2012.08.019.

Nordby, K.-C., A. K. M. Fell, H. Notø, W. Eduard, M. Skogstad, Y. Thomassen, A. Bergamaschi, J. Kongerud, and H. Kjuus. 2011. “Exposure to Thoracic Dust, Airway Symptoms and Lung Function in Cement Production Workers.” The European Respiratory Journal 38 (6): 1278–86. https://doi.org/10.1183/09031936.00007711.

Notø, Hilde, Karl-Christian Nordby, Helge Kjuus, Øivind Skare, Yngvar Thomassen, and Wijnand Eduard. 2015. “Exposure to Thoracic Aerosol in a Prospective Lung Function Study of Cement Production Workers.” The Annals of Occupational Hygiene 59 (1): 4–24. https://doi.org/10.1093/annhyg/meu080.

Oberdörster, Günter, Eva Oberdörster, and Jan Oberdörster. 2005. “Nanotoxicology: An Emerging Discipline Evolving from Studies of Ultrafine Particles.” Environmental Health Perspectives 113 (7): 823–39.

OSHA. 2011. “Respiratory Protection. - 1910.134.” U.S. Department of Labor, Occupational Safety and Health Administration. https://www.osha.gov/pls/oshaweb/owadisp.show_document?p_table=STANDARDS&p_id=12716.

OSHA. 2013. “Working Safely with Nanomaterials.” U.S. Department of Labour, Occupational Safety and Health Administration. https://www.osha.gov/Publications/OSHA_FS-3634.pdf.

OSHA. 2018. “Occupational Exposure Limits (OELs).” Occupational Safety and Health Administration. https://www.osha.gov/dsg/annotated-pels/tablez-1.html.

Ostiguy, C., G. Lapointe, L. Ménard, Y. Cloutier, M. Trottier, M. Boutin, M. Antoun, and C. Normand. 2006. “Nanoparticles - Actual Knowledge about Occupational Health and Safety Risks and Prevention Measures.” Research Reports. https://www.irsst.qc.ca/en/publications-tools/publication/i/100189/n/nanoparticles-current-knowledge-about-occupational-health-and-safety-risks-and-prevention-measures-r-470.

Paz, Y., Z. Luo, L. Rabenberg, and A. Heller. 1995. “Photooxidative Self-Cleaning Transparent Titanium Dioxide Films on Glass.” Journal of Materials Research 10 (11): 2842–48. https://doi.org/10.1557/JMR.1995.2842.

Penrose, Beris. 2014. “Occupational Exposure to Cement Dust: Changing Opinions of a Respiratory Hazard.” Health and History 16 (1): 25–44.

Qi, Chaolong, Alan Echt, and Michael G. Gressel. 2017. “The Generation Rate of Respirable Dust from Cutting Fiber Cement Siding Using Different Tools.” Annals of Work Exposures and Health 61 (2): 218–25. https://doi.org/10.1093/annweh/wxw010.

Rengasamy, Samy, Benjamin C. Eimer, and Ronald E. Shaffer. 2009. “Comparison of Nanoparticle Filtration Performance of NIOSH-Approved and CE-Marked Particulate Filtering Facepiece Respirators.” The Annals of Occupational Hygiene 53 (2): 117–28. https://doi.org/10.1093/annhyg/men086.

Ringen, Knut, John Dement, Laura Welch, Xiuwen Sue Dong, Eula Bingham, and Patricia S. Quinn. 2014. “Risks of a Lifetime in Construction. Part II: Chronic Occupational Diseases.” American Journal of Industrial Medicine 57 (11): 1235–45. https://doi.org/10.1002/ajim.22366.

Sayes, Christie M., Rajeev Wahi, Preetha A. Kurian, Yunping Liu, Jennifer L. West, Kevin D. Ausman, David B. Warheit, and Vicki L. Colvin. 2006. “Correlating Nanoscale Titania Structure with Toxicity: A Cytotoxicity and Inflammatory Response Study with Human Dermal Fibroblasts and Human Lung Epithelial Cells.” Toxicological Sciences 92 (1): 174–85. https://doi.org/10.1093/toxsci/kfj197.

Sha, Baoyong, Wei Gao, Xingye Cui, Lin Wang, and Feng Xu. 2015. “The Potential Health Challenges of TiO2 Nanomaterials.” Journal of Applied Toxicology: JAT, July. https://doi.org/10.1002/jat.3193.

Shi, Hongbo, Ruth Magaye, Vincent Castranova, and Jinshun Zhao. 2013. “Titanium Dioxide Nanoparticles: A Review of Current Toxicological Data.” Particle and Fibre Toxicology 10 (April): 15. https://doi.org/10.1186/1743-8977-10-15.

Shinohara, Naohide, Yutaka Oshima, Toshio Kobayashi, Nobuya Imatanaka, Makoto Nakai, Takayuki Ichinose, Takeshi Sasaki, Kenji Kawaguchi, Guihua Zhang, and Masashi Gamo. 2015. “Pulmonary Clearance Kinetics and Extrapulmonary Translocation of Seven Titanium Dioxide Nano- and Submicron Materials Following Intratracheal Administration in Rats.” Nanotoxicology 9 (8): 1050–58. https://doi.org/10.3109/17435390.2015.1015644.

Soutar, C. A., A. Robertson, B. G. Miller, A. Searl, and J. Bignon. 2000. “Epidemiological Evidence on the Carcinogenicity of Silica: Factors in Scientific Judgement.” Annals of Occupational Hygiene 44 (1): 3–14. https://doi.org/10.1093/annhyg/44.1.3.

Tedja, Roslyn, Christopher Marquis, May Lim, and Rose Amal. 2011. “Biological Impacts of TiO2 on Human Lung Cell Lines A549 and H1299: Particle Size Distribution Effects.” Journal of Nanoparticle Research 13 (9): 3801–13. https://doi.org/10.1007/s11051-011-0302-6.

TOXNET. 2014. “Calcium Oxide.” Toxicology data network, US National Library of Medicine. https://toxnet.nlm.nih.gov/cgi-bin/sis/search2/r?dbs+hsdb:@term+@DOCNO+1615.

Wang, Jiangxue, Chunying Chen, Ying Liu, Fang Jiao, Wei Li, Fang Lao, Yufeng Li, et al. 2008. “Potential Neurological Lesion after Nasal Instillation of TiO2 Nanoparticles in the Anatase and Rutile Crystal Phases.” Toxicology Letters 183 (1–3): 72–80. https://doi.org/10.1016/j.toxlet.2008.10.001.

Wang, Jiangxue, and Yubo Fan. 2014. “Lung Injury Induced by TiO2 Nanoparticles Depends on Their Structural Features: Size, Shape, Crystal Phases, and Surface Coating.” International Journal of Molecular Sciences 15 (12): 22258–78. https://doi.org/10.3390/ijms151222258.

WHO. 2010. IARC Monographs on the Evaluation of Carcinogenic Risks to Humans: Carbon Black, Titanium Dioxide, and Talc. Vol. 93. World health organization, International Agency for Research on Cancer. http://monographs.iarc.fr/ENG/Monographs/vol93/mono93.pdf.

Xue, Chengbin, Wen Luo, and Xiang liang Yang. 2015. “A Mechanism for Nano-Titanium Dioxide-Induced Cytotoxicity in HaCaT Cells under UVA Irradiation.” Bioscience, Biotechnology, and Biochemistry 79 (8): 1384–90. https://doi.org/10.1080/09168451.2015.1023248.

Xue, Jian, Yang Li, Xiaoliang Wang, Thomas D. Durbin, Kent C. Johnson, Georgios Karavalakis, Akua Asa-Awuku, et al. 2015. “Comparison of Vehicle Exhaust Particle Size Distributions Measured by SMPS and EEPS During Steady-State Conditions.” Aerosol Science and Technology 49 (10): 984–96. https://doi.org/10.1080/02786826.2015.1088146.

Yang, C. Y., C. C. Huang, H. F. Chiu, J. F. Chiu, S. J. Lan, and Y. C. Ko. 1996. "Effects of Occupational Dust Exposure on the Respiratory Health of Portland Cement Workers." Journal of Toxicology and Environmental Health 49 (6): 581–88.

Yang, Lu, Amer Hakki, Fazhou Wang, and Donald E. Macphee. 2018. "Photocatalyst Efficiencies in Concrete Technology: The Effect of Photocatalyst Placement." Applied Catalysis B: Environmental 222 (March): 200–208. https://doi.org/10.1016/j.apcatb.2017.10.013.

Zeleke, Zeyede K., Bente E. Moen, and Magne Bråtveit. 2011. "Excessive Exposure to Dust among Cleaners in the Ethiopian Cement Industry." Journal of Occupational and Environmental Hygiene 8 (9): 544–50. https://doi.org/10.1080/15459624.2011.601711.

Zhi Ge, and Zhili Gao. 2008. "Applications of Nanotechnology and Nanomaterials in Construction." First International Conference on Construction In Developing Countries (ICCIDC–I). http://www.neduet.edu.pk/Civil/ICCIDC-I/Conference%20Proceedings/Papers/025.pdf.

Zhu, W., P. J. M. Bartos, and A. Porro. 2004. "Application of Nanotechnology in Construction." Materials and Structures 37 (9): 649–58. https://doi.org/10.1007/BF02483294.

Zouzelka, Radek, and Jiri Rathousky. 2017. "Photocatalytic Abatement of NOx Pollutants in the Air Using Commercial Functional Coating with Porous Morphology." Applied Catalysis B: Environmental 217 (November): 466–76. https://doi.org/10.1016/j.apcatb.2017.06.009.

# CHAPTER VII

# REACTIVE OXYGEN SPECIES (ROS) MEASUREMENT

**Accepted for publication in the Journal of Nanoparticle Research**

Accepted date: 5 June 2020

## Article topic

## Airborne reactive oxygen species (ROS) is associated with nano TiO2 concentrations in aerosolized cement particles during simulated work activities

**Kiattisak Batsungnoen[1,2]**, Michael Riediker[3], Nancy B Hopf[1] and Guillaume Suárez[1]

1. Center for Primary Care and Public Health (Unisante), University of Lausanne, Switzerland. (Kiattisak.Batsungnoen@unisante.ch, Nancy.Hopf@unisante.ch, Guillaume.Suarez@unisante.ch)
2. Institute of Public Health, Suranaree University of Technology, Thailand (kiattisak@sut.ac.th)
3. Swiss Centre for Occupational and Environmental Health (SCOEH), Winterthur, Switzerland. (michael.riediker@alumni.ethz.ch)

**Corresponding author:**

Guillaume Suárez, PhD

**Keywords:** photocatalytic cement, nano cement, nano $TiO_2$ exposure, reactive oxygen species (ROS), ROS exposure

**Abstract**

Photocatalytic cement is self-cleaning due to the addition of titanium dioxide ($TiO_2$) nanoparticles, which react with sunlight (UV) and produce reactive oxygen species (ROS). Construction workers using photocatalytic cement are exposed not only to cement particles that are irritants but also to nano $TiO_2$ and UV, both carcinogens, as well as the generated ROS. Quantifying ROS generated from added nano $TiO_2$ in photocatalytic cement is necessary to efficiently assess combined health risks.

We designed and built an experimental setup to generate, under controlled environmental conditions (*i.e.* temperature, relative humidity, UV irradiance) both regular and photocatalytic cement aerosols. In addition, cement working activities – namely bag emptying and concrete cutting – were simulated in an exposure chamber while continuously measuring particles size distribution/concentration with a scanning mobility particle sizer (SMPS). ROS production was measured with a newly developed photonic sensing system based on a colorimetric assay.

ROS production generated from the photocatalytic cement aerosol exposed to UV ($3.3 \cdot 10^{-9}$ nmol/pt) was significantly higher than for regular cement aerosol, either UV-exposed ($0.5 \cdot 10^{-9}$ nmol/pt) or not ($1.1 \cdot 10^{-9}$ nmol/pt). Quantitatively, the level of photocatalytic activity measured for nano $TiO_2$-containing cement aerosol was in good agreement with the one obtained with only nano $TiO_2$ aerosol at similar experimental conditions of temperature and relative humidity (around 60 %). As a consequence, we recommend that exposure reduction strategies, in addition to cement particle exposures, also consider nano $TiO_2$ and *in situ* generated ROS, in particular if the work is done in sunny environments.

## Introduction

Nanotechnology – the study of matter in nano range from 1 to 100 nanometers - is widely used to improve materials' properties especially strength, weight, and insulation. In the construction sector, photocatalytic cement has been introduced for its self-cleaning properties (Lan et al., 2013; Carp et al., 2004; Banerjee et al., 2015) related to the photocatalytic activity of titanium dioxide nanoparticles (nano $TiO_2$) (Hernández-Rodríguez et al., 2019; Feng et al., 2013; Folli et al., 2010). This cement is composed of regular cement made up of fine inorganic particles such as CaO, $SiO_2$, $Fe_2O_3$, and MgO (Meo, 2004; Batsungnoen et al., 2019) and nano $TiO_2$.

It is well known that inhalation of particulate matter (PM) is associated with pulmonary and cardiovascular diseases (e.g. COPD, asthma, lung cancer) (Risom et al., 2005; Aust et al., 2002; Schins et al., 2004; Ghio and Devlin, 2001; Knaapen et al., 2004; Upadhyay et al., 2003; Upadhyay et al., 2003; Park et al., 2018). In addition IARC has PM as a group 1 carcinogen (IARC, 2017) and $TiO_2$ as possibly carcinogenic to humans (2B) (IARC, 2015). Numerous studies have shown that nano $TiO_2$ is genotoxic and cytotoxic (NIOSH, 2009; Sayes et al., 2006), especially for the lung bronchial epithelial cells (Sha et al., 2015;Lee et al., 2010) but can also translocate to other organs via the blood circulation (Wang et al., 2008; Kreyling et al., 2010; Geiser and Kreyling, 2010; Shi et al., 2013).

Cell toxicity associated with nano $TiO_2$ exposure is related to reactive oxygen species (ROS) generation, which may lead to oxidative stress, lipid peroxidation, and nucleic acids alteration (Wang and Fan, 2014; Shi et al., 2013; Panieri and Santoro, 2016; Liou and Storz, 2010). ROS such as hydroxyl radical, superoxide anion radical, hydrogen peroxide ($H_2O_2$) and singlet oxygen play a mechanistic role in many human diseases, including cancer (Waris and Ahsan, 2006; Brieger et al., 2012), especially in the initiation and progression of multistage carcinogenesis (Waris & Ahsan, 2006). Elevated ROS levels have also been associated with various inflammation-related human diseases (Alfadda & Sallam, 2012).

ROS are also generated outside of the body, and has to be considered together with the endogenous ROS exposure generated through the metabolic response. Environmental ROS generation is especially relevant when airborne nano $TiO_2$ particulates are exposed to UV (Vernez et al., 2017). Due to its electronic energy band gap nano $TiO_2$ behaves as a semi-conductor: UV-excited electrons (ē) reach the conductance band while a hole ($h^+$) forms at the valence energy level. The resulting $\bar{e}/\ h^+$ pair reacts with molecular oxygen ($O_2$) and water giving rise to a series of ROS formation. They react readily with organic materials (e.g. bacteria and mold), giving them a particularly efficient biocide property (Li et al., 2014; Lan et al., 2013; Li, 2004; Zhi Ge and Zhili Gao, 2008; Chen and Poon, 2009; Lee et al., 2010).

Photocatalytic cement exposure among outdoor construction workers may thus have direct exposures to ROS as secondary airborne toxicant (exogenous ROS) from UV activation of nano $TiO_2$. Concentrations of exogenous ROS has not yet been assessed for these workers, consequently, potential health risks associated to this exposure are currently unknown.

Airborne ROS can be quantified using a photonic detection device that was developed at our laboratory and which relies on the formation of a colorimetric complex (Fe(III)-orange xylenol) due to the oxidation of the probe solution containing reduced iron form (Fe(II)) by ROS (Laulagnet et al., 2015). The use of multiscattering absorbance enhancement (MAE) strategy as photonic core principle for the device enabled sensitive ROS determination (Suárez et al., 2013) (Suárez et al., 2014).

The main objective of the present study was to quantify amount of ROS generated from airborne cement and photocatalytic particles at constant relative humidity of about 60% under controlled conditions:

i) Laboratory aerosolization with photocatalytic and regular cements equipped with a UV lamp;

ii) Exposure chamber set-up where two construction activities (cement bag emptying and concrete cutting) were simulated with both cement types separately.

## 2. Materials and Method

**Materials:** Photocatalytic cement was obtained from ESSROC (TX-Active®, Italcementi group, Nazareth, US) while regular cement defined as Portland cement CEM I (CE number 266-043-4), was purchased from Jura cement (Wildegg, Switzerland). The ROS-detection reagent – so-called FOX solution – was freshly prepared by mixing ammonium iron (Fe(II)) sulfate (260 µM), xylenol orange (130 µM) and D-sorbitol (100 mM) into sulfuric acid (25 mM). The solution was kept in a fumed glass flask (100 mL). UV exposure was achieved using a solar light simulator (LS-1000 Solar Simulator Solar Light Co., Glenside, PA, USA). Jet-nebulizer system (1-jet Collison Mesa Labs, Butler, NJ; USA) was used to maintain controlled aerosol humidity to 60%. Ecolog TH1 device enabled monitoring of both temperature and humidity during the aerosol generation (ELPRO-BUCHS AG, Buchs, Switzerland). System airflows were monitored using digital mass flow meters (Vögtlin Instruments AG, flow technology, Aesch BL, Switzerland). Concrete was made by mixing cement and water (2:1). Concrete cutting was operated with a circular saw (diameter 230 mm) and at maximum rated speed (6,600 RPM) (PWS 20-230 J, BOSCH, Leinfelden-Echterdingen, Germany).

## Methods

**Generation of cement aerosols:** Airborne particles of both photocatalytic and regular cements were generated using an aerosolization system previously described by Ding and Riediker 2015 and 2016 (Ding and Riediker, 2015; Ding and Riediker, 2016). Two grams of cement were loaded into a glass funnel and dry air blown upwards through the funnel with 2 L/min. The experimental set-up is shown in Fig 1.

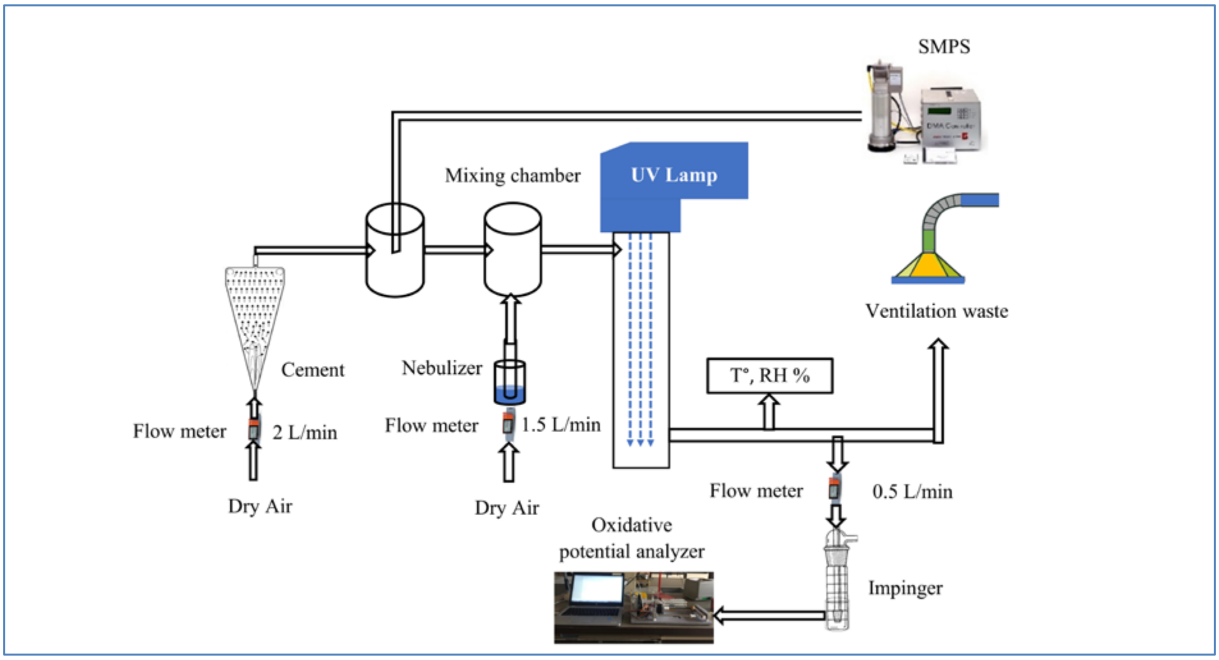


Fig 1: Set-up of cement powder experiment. Cement powder gets aerosolized in the glass funnel (2 L/min) by a gentile airstream (Ding and Riediker, 2015; Ding and Riediker, 2016). The main air stream was split into one leading to the SMPS for measuring particle number concentration (11-1083 nm), and a second driving the aerosol to the mixing chamber. The particles were mixed with humid air and transported into the UV-exposure cylinder (solar simulator lamp). Temperature and humidity were monitored after the air passed through the UV-cylinder. The airborne particles were captured in an impinger filled with FOX solution and the associated ROS production analyzed with the oxidative potential analyzer system (Laulagnet et al., 2015; Vernez et al., 2017).

**Control of environmental conditions:** The airborne particles produced in the funnel were transported directly into a mixing chamber by shear force and mixed with humid air originated from a nebulizer. The nebulizer flowrate was 1.5 L/min, which maintained the relative humidity at 60%. Downstream, the aerosol was driven into the exposure cylinder where they were exposed to UV radiation for 2.7 min (average residence time in the cylinder). The UV radiation light source was equipped with solar UV filters to reproduce the UV-A and UV-B spectrum. The lamp produced an irradiance intensity of 785 $W/m^2$ in the cylinder, corresponding to 12 folds the terrestrial irradiance. The airborne particles exiting the cylinder were captured in an impinger (25 mL) filled with FOX solution (5ml). Temperature and relative humidity were monitored continuously during the run.

**Working activities:** two construction activities, cement bag emptying and concrete cutting, were simulated in an exposure chamber (10 $m^3$) with either photocatalytic or regular cement. Prior to the simulation activities, the ventilation system (80 $m^3/h$) was running for two hours in order to reduce background particles, and during simulation, the ventilation system was off. The operator simulating the construction activity wore a respirator (N100, P3, or FFP3), a chemical suit, nitrile gloves, goggles, safety shoes, and hearing protection. Bag emptying activity was performed by turning an open cement bag (25 kg) upside-down, pouring it into a plastic container (diameter x Height : 60 x 40 cm), and shaking until the cement bag was empty. The concrete cutting activity was performed by using a circular saw for 10 seconds cutting a prepared concrete block (size 25 x 36 x 6 cm). The aerosolized cement particles were sampled in the operator's breathing zone with an impinger (25 mL) containing Fox solution (5 mL) and operating at a flow rate of 0.5 L/min. Each experimental construction activity was repeated in triplicate by a single operator, as shown in Fig 2.

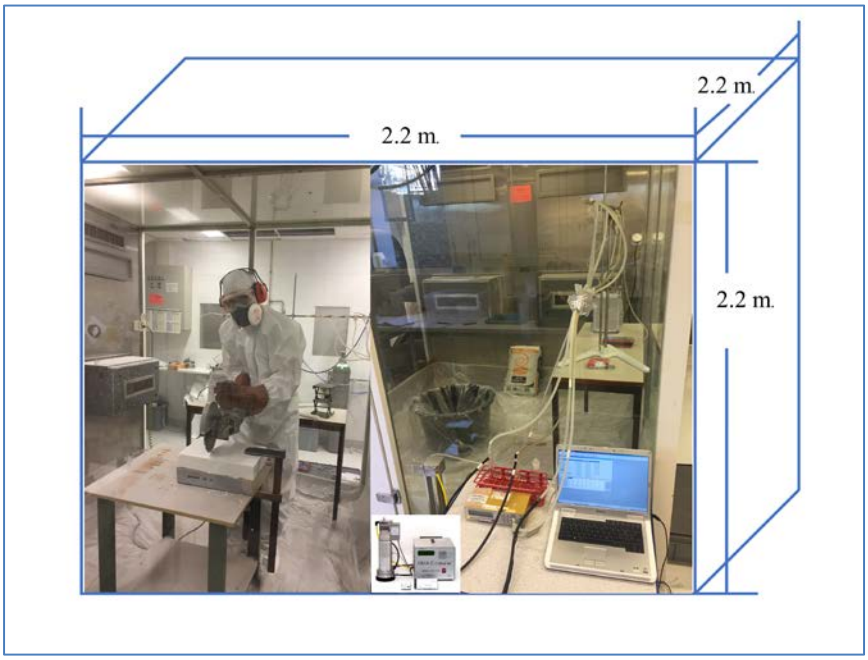


Fig 2: Experimental setup to characterize work-generated particle emissions.Two activities, bag emptying and concrete cutting, were reproduced experimentally in the exposure cabin. Workers were wearing whole body protection with personal protective equipment (PPE): dust protection cloth, rubber gloves, goggles, safety shoes, ears muff and respirator.

**ROS analysis:** ROS concentration – also defined as oxidative potential – was determined using a photonic system developed by our laboratory and based on multiscattering-enhanced absorbance strategy (Laulagnet et al., 2015; Vernez et al., 2017). In brief, air samples are bubbled through an impinger filled FOX solution (5 mL), which is the reaction medium. In the presence of ROS the Fe(II) undergoes oxidized into Fe(III) that forms a complex with orange xylenol absorbing light at 580 nm. The color change is measured via the use of a narrow emission led (580 nm) coupled to a photodetector both driven through a microcontroller board (Arduino Uno) The multiscattering regime occurring in the photonic cell due to the combination of rough aluminium cavity and inner Teflon housing enables dramatic lengthening of the optical path and improved analytical sensitivity. The ROS sensor response was calibrated with $H_2O_2$ and ROS values expressed as $H_2O_2$ equivalents.

**Particles measurements:** The size distribution and number concentration of airborne nanoparticles in the size range between 11 and 1,083 nm were measured by scanning mobility particle sizer (SMPS) (model SMPS+C model 5400, Grimm Aerosol Technik GmbH & Co. KG, Ainring, Germany). For morphology determination, the particles were collected onto Transmission Electron Microscopy (TEM) grids (Quantifoil R1/4, Quantifoil Micro Tools GmbH, Germany) using a mini particle sampler (MPS) (Ecomesure, Sacly, France) operating at a sampling flow rate of 0.3 L/min. The TEM grids were transferred to a transmission electron microscope (TEM) (TEM CM-100 (JEOL, USA) at 80 kV).

**Statistical analysis:** Means and standard deviations for nanoparticle size and distribution as well as ROS concentrations were compared by two-sample t-test using STATA version 15.

## 3. Results

The ROS detection system developed by our group enabled us to quantify hydrogen peroxide ($H_2O_2$) and hydroxyl radicals ($OH^{\bullet}$). Quantitative determination of the aerosol reactivity expressed – once normalized by total particle number concentration – in nanomoles of $H_2O_2$ equivalents per particle (nmol/pt) was possible by combining accurate aerosol generation and sensitive ROS detection.

The average size distribution from aerosolized photocatalytic cement in the experimental set-up was around $2{\cdot}10^5$ pt/cm$^3$, with a geometric mean diameter (GMD) of 285 nm and a geometric standard deviation (GSD) of 1.65 nm. Regular cement aerosol had a particle number concentration of $1{\cdot}10^5$ pt/cm$^3$ with GMD and GSD of 376 and 1.74 nm, respectively (Fig 3A). The TEM images confirmed that photocatalytic cement aerosols contained agglomerates from pristine nanoparticles with primary size around 50 nm (Fig 3B).

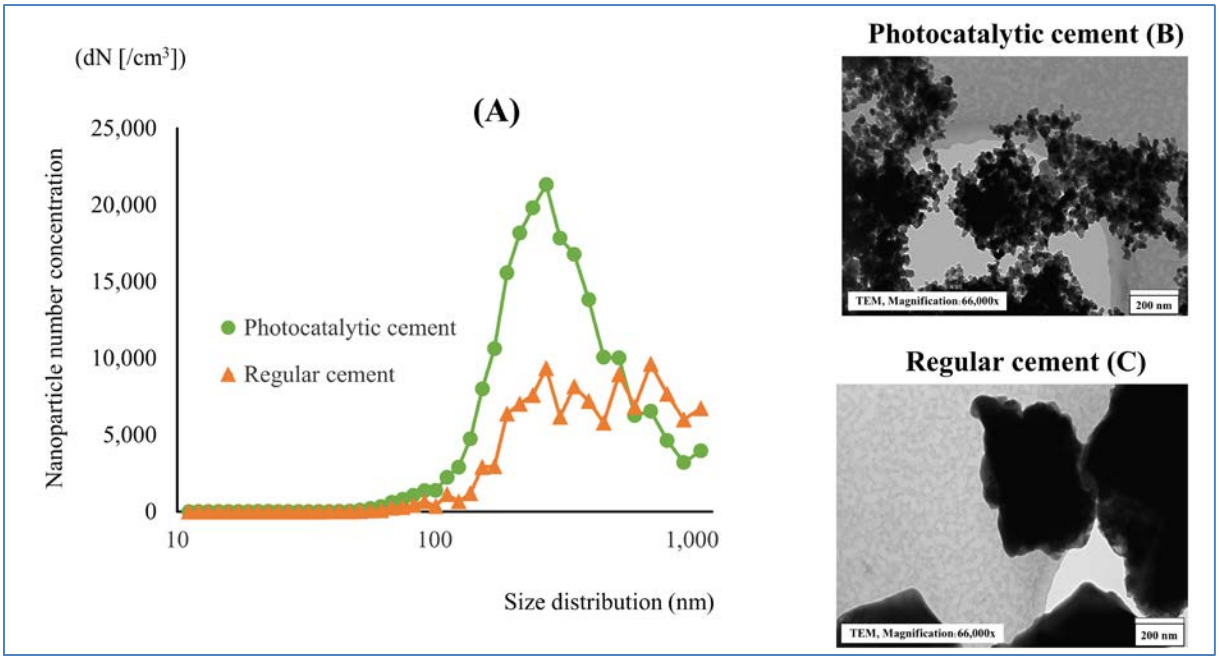


Fig 3: (A) Airborne nanoparticle size distribution expressed in number concentration (dN [/cm3]) obtained by SMPS for photocatalytic cement (solid circles) and regular cement (solid triangles) in the range size between 11 and 1,083 nm. TEM images of (B) photocatalytic cement and (C) regular cement; (Magnification: 66,000x).

In complement, the aerosol ROS generation calculated in the present study indicate that the aerosolized photocatalytic cement exposed to UV irradiance ($3.3{\cdot}10^{-9}$ nmol/pt) is significantly more reactive in terms of produced $H_2O_2$ equivalents than regular cement exposed to UV ($0.5{\cdot}10^{-9}$ nmol/pt) or not ($1.1{\cdot}10^{-9}$ nmol/pt). ROS generation for non-UV exposed cement aerosols were $1.6{\cdot}10^{-9}$ nmol/pt and $1.1{\cdot}10^{-9}$ nmol/pt for photocatalytic and regular cement, respectively (Table1). In good agreement with prior study (Vernez et al., 2017), the results herein obtained clearly indicate that the presence of nano $TiO_2$ in the photocatalytic cement do increase its chemical reactivity in terms of ROS generation prompt to act as secondary toxicants.

Table 1: ROS concentration originated from airborne aerosols of photocatalytic and regular cement, with and without UV irradiance

| | **ROS concentration (nmol/pt)** | **$TiO_2$ content (wt%) *** | **Avg. particle concentration (pt/cm$^3$)** | **Distribution interval (nm)** |
|---|---|---|---|---|
| Photocatalytic cement exposed UV | $3.34 \cdot 10^{-9}$ (SD. = $1.32 \cdot 10^{-9}$) | 37.35 | 214,482 | 100 - 930 |
| Photocatalytic cement non-exposed UV | $1.58 \cdot 10^{-9}$ (SD. = $0.11 \cdot 10^{-9}$) | 37.35 | 182,996 | 100 - 930 |
| | Average particle concentration (pt/cm$^3$) | | 198,739 | |
| | | | | |
| Regular cement exposed UV | $0.51 \cdot 10^{-9}$ (SD. = $0.20 \cdot 10^{-9}$) | 0.16 | 139,132 | 550 – 1,000** |
| Regular cement non-exposed UV | $1.12 \cdot 10^{-9}$ (SD. = $0.54 \cdot 10^{-9}$) | 0.16 | 76,616 | 550 – 1,000** |
| | Average particle concentration (pt/cm$^3$) | | 107,874 | |

* From Batsungnoen et al., 2019

** Top range detection limit for SMPS measurements

The effect of UV irradiance on nano $TiO_2$ is manifest in the fact that ROS generation from photocatalytic cement doubled in the presence of UV irradiance. As expected, ROS production from photocatalytic cement exposed to UV was significantly higher than regular cement with or without UV (fig 4). There was no significant difference in ROS generation between regular cement exposed and not to UV light.

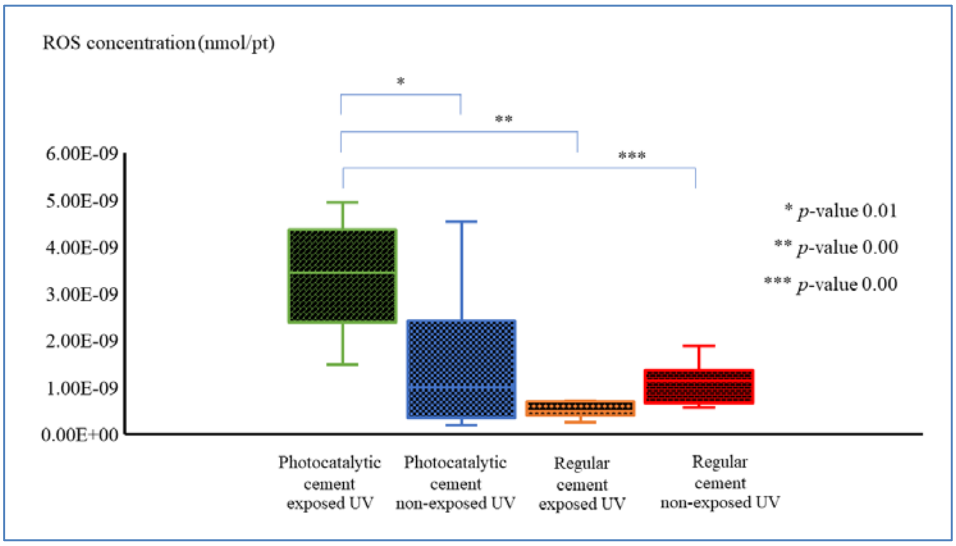


Fig 4: Box plot showing the normalized ROS production (nmol/pt) originated from photocatalytic and regular cement airborne particles.

Simulated construction work activities performed in exposure chamber to evaluate airborne ROS levels show that for bag emptying activity, the measured ROS production was significantly greater ($p$-value = 0.04) for photocatalytic ($4.6 \cdot 10^{-10}$ nmol/ pt) than for regular cement ($1.5 \cdot 10^{-10}$ nmol/pt) during bag emptying (Fig 5).

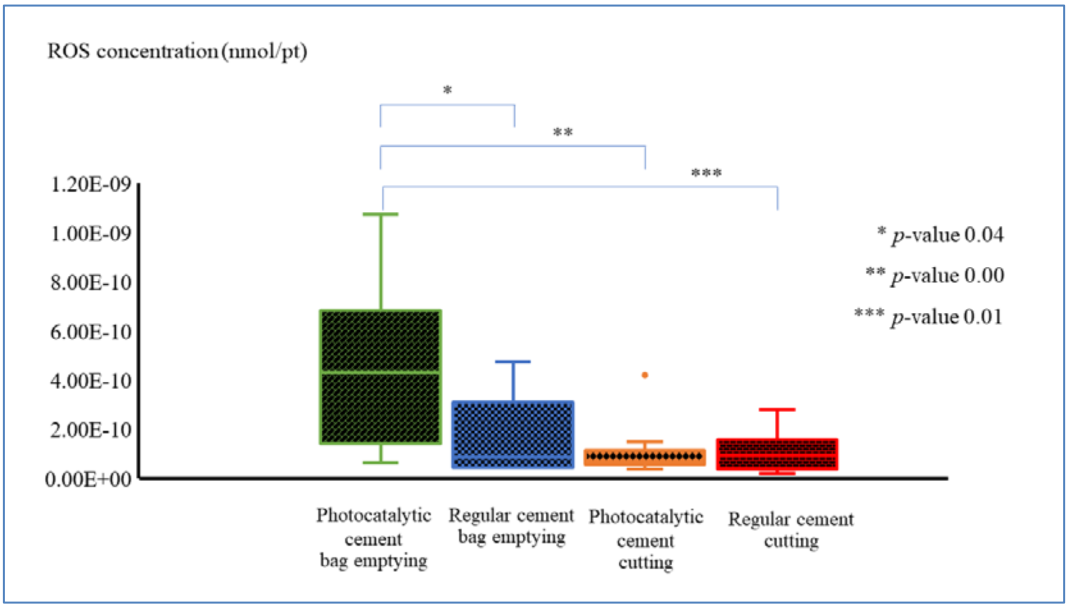


Fig 5: The ROS production from cement bag emptying and concrete cutting.

In the case of concrete cutting no significant difference was observed between photocatalytic and regular cement, with ROS reactivities of $1.1 \cdot 10^{-10}$ and $1.1 \cdot 10^{-10}$ nmol/pt, respectively (Table 2)

Table 2: ROS concentration originated from aerosols generated during cement bag emptying and concrete cutting activities

| | ROS concentration (nmol/pt) | $TiO_2$ content (wt%) | Avg. particle concentration (pt/cm$^3$) | Distribution interval (nm) |
|---|---|---|---|---|
| Photocatalytic cement bag emptying | $4.60 \cdot 10^{-10}$ (SD. = $3.47 \cdot 10^{-10}$) | 16.46 | 3,715 | 240 - 1,000* |
| Regular cement bag emptying | $1.58 \cdot 10^{-10}$ (SD. = $1.81 \cdot 10^{-10}$) | 0.19 | 3,662 | 240 - 1,000* |
| | | | | |
| Photocatalytic concrete cutting | $1.10 \cdot 10^{-10}$ (SD. = $1.09 \cdot 10^{-10}$) | 2.03 | 10,549 | 150 - 1,000* |
| Regular concrete cutting | $1.12 \cdot 10^{-10}$ (SD. = $1.01 \cdot 10^{-8}$) | 0.10 | 19,143 | 150 - 1,000* |

* Top range detection limit for SMPS measurements

## 4. Discussion

Airborne photocatalytic cement particles are a potential source of ROS that is further enhanced in the presence of UV irradiance, and is mainly attributed to the presence of nano $TiO_2$ on the airborne particles (Batsungnoen et al., 2019b). The photo-induced mechanism that triggers the production of ROS – mainly in the form of $H_2O_2$ – at the surface of $TiO_2$ is well established (Kakinoki et al., 2004) (Ghadiry et al., 2016) and has recently been demonstrated for nano $TiO_2$ airborne particles in our prior study (Vernez et al., 2017). The results obtained herein, clearly indicate that the presence of nano $TiO_2$ in the photocatalytic cement increase its chemical reactivity in terms of ROS generation, which is in good agreement with this prior study (Vernez et al., 2017).

In the absence of UV irradiance the ROS generation associated to photocatalytic cement aerosol is not significantly different than the one obtained with regular cement, exposed or not. However, the large interval observed in the ROS production by photocatalytic aerosol without UV exposure might be attributed to the activation of nano $TiO_2$ by visible light during experimental measurements (Etacheri et al., 2015). Consequently, indoor construction workers using photocatalytic cement under artificial light might have greater exposures to ROS compared to workers using regular cement, although to a far lesser extent than outdoor workers.

The low reactivity observed with regular cement particles could potentially be originated from redox reactions in which transition metal in its composition – namely iron oxide (2 % $Fe_2O_3$) – are prone to take part (Batsungnoen et al., 2019b). While many studies have demonstrated the ability of iron oxides particles – such as $Fe_2O_3$ and to a greater extent $Fe_3O_4$ – to activate $H_2O_2$ into highly reactive hydroxyl radical via their so-called peroxidase-like behavior (Gao et al., 2017; Pham et al., 2012), to our knowledge, the contribution of iron oxide in the generation of exogenous ROS by Portland cement particles was not yet reported.

In the case of work activities, the ROS production observed during bag emptying with photocatalytic cement was three-fold greater than the one measured with regular cement. Again, even in the absence of UV irradiance, this photocatalytic activity may be attributed to the visible light energy present in the experimental setup, though nano-$TiO_2$ can produce ROS also under dark conditions (Kakinoki et al., 2004). More interestingly, one can notice that in the case of concrete cutting no significant difference is shown between photocatalytic and regular concretes, while in parallel the corresponding $TiO_2$ contents in the generated aerosols are relatively low (max. 2 %) as shown in Table 2. The different $TiO_2$ content observed depending on the work activity is explained by the fact that bag emptying process favors the smaller size fraction to remain airborne (16.5 % of $TiO_2$ detected airborne), while the larger cement powder particles will sediment rapidly. In contrast, aerosols created from cement concrete cutting roughly reflects the initial composition of the initial cement powder in the bag (2.0 % nano-$TiO_2$) because the $TiO_2$ has become part of the cement matrix and is no longer present as individual nano- $TiO_2$ particles. It is worthily to notice that the ROS concentration measured during bag emptying using photocatalytic cement was in the same order of magnitude than the value obtained in prior work with pure nano $TiO_2$ once normalized by $TiO_2$ content (Vernez et al., 2017).

Finally, health effects related to airborne nano $TiO_2$ exposure in photocatalytic cement should integrate its reactivity – in the presence of environmental UV/vis irradiance – by considering the associated ROS products as secondary airborne toxicants. In terms of toxic effects, ROS are associated to various metabolic/pathological paths such as oxidative stress, inflammation, genotoxicity, cytotoxicity, DNA damage and cancer (Li et al., 2014; Brieger et al., 2012; Scherz-Shouval and Elazar, 2011; Jaeger et al., 2012; Yin et al., 2012; Jaeger et al., 2012; Wang and Fan, 2014).

## 5. Conclusion

The combination of an efficient aerosol generation setup coupled with a solar simulation lamp and a sensitive photonic detection device made it possible to assess the production of ROS by photocatalytic and regular cement aerosols. As expected, the presence of nano $TiO_2$ in photocatalytic cement has a strong impact on the ability of the corresponding aerosol to produce exogenous airborne ROS in the presence of UV light. Moreover, the level of ROS generated during work activities was found to be linked to the amount of airborne nano $TiO_2$ present in the cement aerosol. Thus, concrete cutting activities appears to be considerably less problematic in terms of ROS production than bag emptying for which the nano $TiO_2$ content in the aerosol reaches 16 %. Considering the photoreactivity of aerosolized photocatalytic cement under UV irradiance and the high content of airborne nano $TiO_2$ generated during bag emptying, worker protection procedures should not only consider nano $TiO_2$ exposure but also its ability to produce ROS as secondary airborne potential toxicants. Providing the specific reactivity of its aerosol under environmental conditions, photocatalytic cement should not only be considered as a novel promising material but also as a potential new hazard in construction sites.

**Conflict of interest**

The authors declare no conflict of interest.

## 6. Acknowledgements

The Center for Primary Care and Public Health (Unisanté), Department of Occupational and Environmental Health (formerly known as Institute for Work and Health, IST), Switzerland, Royal Thai Government and the ministry of science and technology, Thailand funded this study. We greatly appreciated help from Dr. Nicolas Concha Lozano for morphology study, Mr. Timothee Ndarugendamwo for laboratory assistant and ROS analysis, Ms. Nicole Charrier Mr. Benoit Allaz, Mr. Nicolas Sambiagio, Mr. Elvar Oskarsson, Mr. Antoine Milon and Mr. Yannick Rodari for all practical laboratory support. We thank Italcementi group for sending us free sample.

## 7. References


Alfadda, A. A., & Sallam, R. M. (2012). Reactive Oxygen Species in Health and Disease [Research article]. BioMed Research International. https://doi.org/10.1155/2012/936486

Aust, A. E., Ball, J. C., Hu, A. A., Lighty, J. S., Smith, K. R., Straccia, A. M., Veranth, J. M., & Young, W. C. (2002). Particle characteristics responsible for effects on human lung epithelial cells. Research Report (Health Effects Institute), 110, 1–65; discussion 67-76.

Banerjee, S., Dionysiou, D. D., & Pillai, S. C. (2015). Self-cleaning applications of TiO2 by photo-induced hydrophilicity and photocatalysis. Applied Catalysis B: Environmental, 176–177, 396–428. https://doi.org/10.1016/j.apcatb.2015.03.058

Batsungnoen, K., Hopf, N. B., Suárez, G., & Riediker, M. (2019). Characterization of nanoparticles in aerosolized photocatalytic and regular cement. Aerosol Science and Technology, 53(5), 540–548. https://doi.org/10.1080/02786826.2019.1578334

Brieger, K., Schiavone, S., Miller, F. J., & Krause, K.-H. (2012). Reactive oxygen species: From health to disease. Swiss Medical Weekly, 142, w13659. https://doi.org/10.4414/smw.2012.13659

Carp, O., Huisman, C. L., & Reller, A. (2004). Photoinduced reactivity of titanium dioxide. Progress in Solid State Chemistry, 32(1–2), 33–177. https://doi.org/10.1016/j.progsolidstchem.2004.08.001

Chen, J., & Poon, C. (2009). Photocatalytic construction and building materials: From fundamentals to applications. Building and Environment, 44(9), 1899–1906. https://doi.org/10.1016/j.buildenv.2009.01.002

Ding, Y., & Riediker, M. (2015). A system to assess the stability of airborne nanoparticle agglomerates under aerodynamic shear. Journal of Aerosol Science, 88, 98–108. https://doi.org/10.1016/j.jaerosci.2015.06.001

Ding, Y., & Riediker, M. (2016). A System to Create Stable Nanoparticle Aerosols from Nanopowders. JoVE (Journal of Visualized Experiments), 113, e54414–e54414. https://doi.org/10.3791/54414

Etacheri, V., Di Valentin, C., Schneider, J., Bahnemann, D., & Pillai, S. C. (2015). Visible-light activation of TiO2 photocatalysts: Advances in theory and experiments. Journal of Photochemistry and Photobiology C: Photochemistry Reviews, 25, 1–29. https://doi.org/10.1016/j.jphotochemrev.2015.08.003

Feng, D., Xie, N., Gong, C., Leng, Z., Xiao, H., Li, H., & Shi, X. (2013). Portland Cement Paste Modified by TiO2 Nanoparticles: A Microstructure Perspective. Industrial & Engineering Chemistry Research, 52(33), 11575–11582. https://doi.org/10.1021/ie4011595

Folli, A., Pochard, I., Nonat, A., Jakobsen, U. H., Shepherd, A. M., & Macphee, D. E. (2010). Engineering Photocatalytic Cements: Understanding TiO2 Surface Chemistry to Control and Modulate Photocatalytic Performances. Journal of the American Ceramic Society, 93(10), 3360–3369. https://doi.org/10.1111/j.1551-2916.2010.03838.x

Gao, L., Fan, K., & Yan, X. (2017). Iron Oxide Nanozyme: A Multifunctional Enzyme Mimetic for Biomedical Applications. Theranostics, 7(13), 3207–3227. https://doi.org/10.7150/thno.19738

Geiser, M., & Kreyling, W. G. (2010). Deposition and biokinetics of inhaled nanoparticles. Particle and Fibre Toxicology, 7, 2. https://doi.org/10.1186/1743-8977-7-2

Ghadiry, M., Gholami, M., Choon Kong, L., Wu Yi, C., Ahmad, H., & Alias, Y. (2016). Nano-Anatase TiO2 for High Performance Optical Humidity Sensing on Chip. Sensors, 16(1), 39. https://doi.org/10.3390/s16010039

Ghio, A. J., & Devlin, R. B. (2001). Inflammatory lung injury after bronchial instillation of air pollution particles. American Journal of Respiratory and Critical Care Medicine, 164(4), 704–708. https://doi.org/10.1164/ajrccm.164.4.2011089

Hernández-Rodríguez, M. J., Santana Rodríguez, R., Darias, R., González Díaz, O., Pérez Luzardo, J. M., Doña Rodríguez, J. M., & Pulido Melián, E. (2019). Effect of TiO2 Addition on Mortars: Characterization and Photoactivity. Applied Sciences, 9(13), 2598. https://doi.org/10.3390/app9132598

IARC. (2015). Agents Classified by the IARC Monographs (Vols. 1–114). World health organization, International Agency for Research on Cancer. http://monographs.iarc.fr/ENG/Classification/

IARC. (2017). IARC Monographs on the evaluation of carcinogenic risk to human; List of classification (Vols. 1–120). World health organization, International Agency for Research on Cancer. http://monographs.iarc.fr/ENG/Classification/latest_classif.php

Jaeger, A., Weiss, D. G., Jonas, L., & Kriehuber, R. (2012). Oxidative stress-induced cytotoxic and genotoxic effects of nano-sized titanium dioxide particles in human HaCaT keratinocytes. Toxicology, 296(1), 27–36. https://doi.org/10.1016/j.tox.2012.02.016

Kakinoki, K., Yamane, K., Teraoka, R., Otsuka, M., & Matsuda, Y. (2004). Effect of Relative Humidity on the Photocatalytic Activity of Titanium Dioxide and Photostability of Famotidine. Journal of Pharmaceutical Sciences, 93(3), 582–589. https://doi.org/10.1002/jps.10575

Knaapen, A. M., Borm, P. J. A., Albrecht, C., & Schins, R. P. F. (2004). Inhaled particles and lung cancer. Part A: Mechanisms. International Journal of Cancer, 109(6), 799–809. https://doi.org/10.1002/ijc.11708

Kreyling, W. G., Hirn, S., & Schleh, C. (2010). Nanoparticles in the lung. Nature Biotechnology, 28(12), 1275–1276. https://doi.org/10.1038/nbt.1735

Lan, Y., Lu, Y., & Ren, Z. (2013). Mini review on photocatalysis of titanium dioxide nanoparticles and their solar applications. Nano Energy, 2(5), 1031–1045. https://doi.org/10.1016/j.nanoen.2013.04.002

Laulagnet, A., Sauvain, J. J., Concha-Lozano, N., Riediker, M., & Suárez, G. (2015). Sensitive Photonic System to Measure Oxidative Potential of Airborne Nanoparticles and ROS Levels in Exhaled Air. Procedia Engineering, 120, 632–636. https://doi.org/10.1016/j.proeng.2015.08.659

Lee, J., Mahendra, S., & Alvarez, P. J. J. (2010). Nanomaterials in the Construction Industry: A Review of Their Applications and Environmental Health and Safety Considerations. ACS Nano, 4(7), 3580–3590. https://doi.org/10.1021/nn100866w

Li, G. (2004). Properties of high-volume fly ash concrete incorporating nano-SiO2. Cement and Concrete Research, 34(6), 1043–1049. https://doi.org/10.1016/j.cemconres.2003.11.013

Li, M., Yin, J.-J., Wamer, W. G., & Lo, Y. M. (2014). Mechanistic characterization of titanium dioxide nanoparticle-induced toxicity using electron spin resonance. Journal of Food and Drug Analysis, 22(1), 76–85. https://doi.org/10.1016/j.jfda.2014.01.006

Liou, G.-Y., & Storz, P. (2010). Reactive oxygen species in cancer. Free Radical Research, 44(5), 479–496. https://doi.org/10.3109/10715761003667554

Meo, S. A. (2004). Health hazards of cement dust. Saudi Medical Journal, 25(9), 1153–1159.

NIOSH. (2009). Approaches to Safe Nanotechnology Managing the Health and Safety Concerns Associated with Engineered Nanomaterials. U.S. Department of Health and Human Services, Centers for Disease Control and Prevention, National Institute for

Occupational Safety and Health. http://www.cdc.gov/niosh/docs/2009-125/pdfs/2009-125.pdf

Panieri, E., & Santoro, M. M. (2016). ROS homeostasis and metabolism: A dangerous liason in cancer cells. Cell Death & Disease, 7(6), e2253. https://doi.org/10.1038/cddis.2016.105

Park, J., Park, E. H., Schauer, J. J., Yi, S.-M., & Heo, J. (2018). Reactive oxygen species (ROS) activity of ambient fine particles (PM2.5) measured in Seoul, Korea. Environment International, 117, 276–283. https://doi.org/10.1016/j.envint.2018.05.018

Pham, A. L.-T., Doyle, F. M., & Sedlak, D. L. (2012). Kinetics and efficiency of H2O2 activation by iron-containing minerals and aquifer materials. Water Research, 46(19), 6454–6462. https://doi.org/10.1016/j.watres.2012.09.020

Risom, L., Møller, P., & Loft, S. (2005). Oxidative stress-induced DNA damage by particulate air pollution. Mutation Research/Fundamental and Molecular Mechanisms of Mutagenesis, 592(1), 119–137. https://doi.org/10.1016/j.mrfmmm.2005.06.012

Sayes, C. M., Wahi, R., Kurian, P. A., Liu, Y., West, J. L., Ausman, K. D., Warheit, D. B., & Colvin, V. L. (2006). Correlating Nanoscale Titania Structure with Toxicity: A Cytotoxicity and Inflammatory Response Study with Human Dermal Fibroblasts and Human Lung Epithelial Cells. Toxicological Sciences, 92(1), 174–185. https://doi.org/10.1093/toxsci/kfj197

Scherz-Shouval, R., & Elazar, Z. (2011). Regulation of autophagy by ROS: Physiology and pathology. Trends in Biochemical Sciences, 36(1), 30–38. https://doi.org/10.1016/j.tibs.2010.07.007

Schins, R. P. F., Lightbody, J. H., Borm, P. J. A., Shi, T., Donaldson, K., & Stone, V. (2004).

Inflammatory effects of coarse and fine particulate matter in relation to chemical and biological constituents. Toxicology and Applied Pharmacology, 195(1), 1–11. https://doi.org/10.1016/j.taap.2003.10.002

Sha, B., Gao, W., Cui, X., Wang, L., & Xu, F. (2015). The potential health challenges of TiO2 nanomaterials. Journal of Applied Toxicology: JAT. https://doi.org/10.1002/jat.3193

Shi, H., Magaye, R., Castranova, V., & Zhao, J. (2013). Titanium dioxide nanoparticles: A review of current toxicological data. Particle and Fibre Toxicology, 10, 15. https://doi.org/10.1186/1743-8977-10-15

Suárez, G., Santschi, C., Plateel, G., Martin, O. J. F., & Riediker, M. (2014). Absorbance enhancement in microplate wells for improved-sensitivity biosensors. Biosensors & Bioelectronics, 56, 198–203. https://doi.org/10.1016/j.bios.2013.12.063

Suárez, G., Santschi, C., Slaveykova, V. I., & Martin, O. J. F. (2013). Sensing the dynamics of oxidative stress using enhanced absorption in protein-loaded random media. Scientific Reports, 3, 3447. https://doi.org/10.1038/srep03447

Upadhyay, D., Panduri, V., Ghio, A., & Kamp, D. W. (2003). Particulate Matter Induces Alveolar Epithelial Cell DNA Damage and Apoptosis. American Journal of Respiratory Cell and Molecular Biology, 29(2), 180–187. https://doi.org/10.1165/rcmb.2002-0269OC

Vernez, D., Sauvain, J.-J., Laulagnet, A., Otaño, A. P., Hopf, N. B., Batsungnoen, K., & Suárez, G. (2017). Airborne nano-TiO2 particles: An innate or environmentally-induced toxicity? Journal of Photochemistry and Photobiology A: Chemistry, 343, 119–125. https://doi.org/10.1016/j.jphotochem.2017.04.022

Wang, J., Chen, C., Liu, Y., Jiao, F., Li, W., Lao, F., Li, Y., Li, B., Ge, C., Zhou, G., Gao, Y., Zhao, Y., & Chai, Z. (2008). Potential neurological lesion after nasal instillation of TiO2 nanoparticles in the anatase and rutile crystal phases. Toxicology Letters, 183(1–3), 72–80. https://doi.org/10.1016/j.toxlet.2008.10.001

Wang, J., & Fan, Y. (2014). Lung Injury Induced by TiO2 Nanoparticles Depends on Their Structural Features: Size, Shape, Crystal Phases, and Surface Coating. International Journal of Molecular Sciences, 15(12), 22258–22278. https://doi.org/10.3390/ijms151222258

Waris, G., & Ahsan, H. (2006). Reactive oxygen species: Role in the development of cancer and various chronic conditions. Journal of Carcinogenesis, 5, 14. https://doi.org/10.1186/1477-3163-5-14

Yin, J.-J., Liu, J., Ehrenshaft, M., Roberts, J. E., Fu, P. P., Mason, R. P., & Zhao, B. (2012). Phototoxicity of nano titanium dioxides in HaCaT keratinocytes—Generation of reactive oxygen species and cell damage. Toxicology and Applied Pharmacology, 263(1), 81–88. https://doi.org/10.1016/j.taap.2012.06.001

Zhi Ge, & Zhili Gao. (2008). Applications of Nanotechnology and Nanomaterials in Construction. First International Conference on Construction In Developing Countries (ICCIDC–I). http://www.neduet.edu.pk/Civil/ICCIDC-I/Conference%20Proceedings/Papers/025.pdf

# CHAPTER VIII

# SUMMARY OF THE MAIN RESULTS

## 8.1 Characterization of nanoparticles in laboratory aerosolized

In aerosolized system the nanoparticles size range between 11 and 1,083 nm and fine particle from 250 to 32,000 nm were measured with SMPS and PAS respectively. The SMPS showed average number concentration of photocatalytic cement was 14,900 pt/cm3 and 9,700 pt/cm3 for regular cement. Photocatalytic cement had a geometric mean diameter (GMD) of 249 nm and geometric standard deviation (GSD) of 2 nm and 417 nm (GSD 2 nm) for regular cement.

Two-sample t-test with 95% confident showed mean nanoparticle size for the photocatalytic cement was significantly smaller than for regular cement ($p$-value < 0.0005). Furthermore, the particle number concentration for photocatalytic cement was significantly greater than for regular cement particles ($p$-value < 0.0005).

Particle size distributions measured with SMPS combined with PAS showed photocatalytic cement contained nanoparticles around 4.7 % in aerosolized, while regular cement only contained 0.4 %. Both of cement types had over 90 percent of the particle count in the size range less than 1µm.

Elemental composition analysis showed the majority of the particle material found in both regular and photocatalytic cement was CaO. The second most abundant particle material was silica (SiO2). CaO in photocatalytic bagged was 62.4 wt%, while this only made up 31.2 wt% in the aerosolized form. $TiO_2$ in photocatalytic cement showed the 2.0 wt% in bags powder and increased to 37.4 wt% in the aerosolized particles.

Morphology study by TEM and SEM images confirmed that photocatalytic cement consisted of two distinct particle types that differed in morphology and in size (c.a. 50 nm and > 200 nm, respectively magnification with focus on particles of around 50 nm size). The regular cement contained only coarse particles size around 1µm.

### 8.2 Working activities in exposure chamber and construction site sampling

***Cement bag emptying***

Photocatalytic cement, bag emptying generated 3,715 pt/cm$^3$ giving a GMD of 322 nm and a GSD of 2.90 nm; and 3,662 pt/cm$^3$, GMD 227 nm and GSD 3.31 nm for regular cement. Both cement types had a single peak at 692 nm: the modal values were 3,216 pt/cm$^3$ for photocatalytic and 1,419 pt/cm$^3$ for regular cement**.** Photocatalytic cement had a higher number concentration than regular cement across the entire size range. Irrespective of cement type, 99% of the cumulative particle number in sizes below 3.5 µm during bag emptying.

Mass particle fraction, inhalable dust mass concentration was 15.16 (SD± 3.12) mg/m$^3$ and respirable dust was 13.34 (SD±1.36) mg/m$^3$ for photocatalytic cement during bag emptying. Inhalable and respirable dust mass concentrations for regular cement, respectively during bag emptying with 10.74 (SD±3.70) mg/m$^3$ for inhalable dust and 6.75 (SD±1.97) mg/m$^3$ for respirable dust. Mass particles size distribution showed a peak concentration of 10.67 (SD±5.09) mg/m$^3$ at 1.55 µm for photocatalytic cement. Regular cement had a mass concentration less than half 3.99 (SD±1.70) mg/m$^3$) of photocatalytic cement and at a smaller size (0.93 µm).

Airborne photocatalytic cement particles were both nanoparticles and fine particles as visualized with TEM. The particle boundary layer showed a much greater number of small particles (size around 50 nm) compared to regular cement. The presence of nano-sized spherical particles only found in the photocatalytic cement might possibly be attributed to nano $TiO_2$. The regular cement contained only coarse particles (particles size around 1 µm) as shown in figure 5C and figure 5D.

***Concrete block cutting***

SMPS showed mean particle number concentration during cutting concrete blocks made with photocatalytic cement was 10,549 pt/cm$^3$, GMD of 287 nm and GSD of 2.22 nm. Cutting blocks made with regular cement gave 19,143 pt/cm$^3$, GMD 345 nm and GSD 1.96 nm. The size distributions were similar; increasing at particle size 137.8 and fluctuating between 277.8 and 930.5 nm. The peak number concentration was about double for regular cement (12,629 pt/cm$^3$) at 348.9 nm compared to the peak for photocatalytic cement (5,875 pt/cm$^3$) at 271.8 nm. Irrespective of cement type, concrete cutting had 99% of cumulative particle number in sizes below 3.5 µm

Inhalable photocatalytic cement concrete dust mass concentrations during cutting were double (75.10 mg/m$^3$, SD±7.92) compared to regular cement concrete cutting (40.95 mg/m$^3$, SD± 4.16). Respirable dust concentrations were somewhat similar for photocatalytic cement (57.99 mg/m$^3$, SD± 11.96) and regular cement concrete cutting (42.01 mg/m$^3$, SD± 3.52). Photocatalytic and regular cement concrete cutting had the same peak mass concentrations at 1.55 µm with 19.90 (SD± 5.06) and 14.54 (SD±4.79) mg/m$^3$, respectively.

Particle morphology for airborne photocatalytic and regular cement during cutting sampled with a TEM grid. The morphology for fine particles generated during concrete cutting were similar for the two cement types. The presence of nano $TiO_2$ spherical particles was not observed for photocatalytic cement concrete cutting.

***Cement sweeping***

Nanoparticle size distributions and number concentrations measured during sweeping with SMPS showed photocatalytic cement mean particle number concentrations of 1,895 pt/cm$^3$, GMD of 194 nm and GSD of 3 nm. The same particle number concentrations (2,272 pt/cm$^3$) was observed for regular cement but for larger particles (GMD 283 nm and GSD 3 nm). Sweeping had a particles peak size of 692 nm with number concentrations double for photocatalytic (1,024 pt/cm$^3$) compared to regular (517 pt/cm$^3$) cement. Cement sweeping had 99% of cumulative particle number in sizes below 3.5 µm.

Inhalable dust concentrations were 30% greater (15.19 (SD± 2.35) mg/m$^3$ for photocatalytic compared to regular cement (10.53 (SD± 1.60) mg/m$^3$). Respirable dust concentrations for photocatalytic cement were about double the concentration (9.52 (SD± 2.99) mg/m$^3$) of regular cement (4.98 (SD± 1.98) mg/m$^3$). Photocatalytic and regular cement during sweeping had the same peak at 1.55 µm with 5.26 (SD± 2.33) and 3.86 (SD±1.47) mg/m$^3$, respectively.

Airborne photocatalytic cement contained two distinct types of nanoparticles as well as coarse particles. The presence of nano-ranged spherical particles was only observed for photocatalytic cement and could possibly be attributed to nano $TiO_2$. The regular cement contained mostly coarse particles (particles size around 1 µm).

### *Elemental composition analysis*

Elemental compositions were analyzed by SEM-EDX and the results for both cement types by working activities. Calcium oxide (CaO) and silicon dioxide ($SiO_2$) were the elemental substances detected in greatest quantity. Photocatalytic cement (bag sample) contained around 2 wt% nano $TiO_2$. Regular cement (bag sample) contained no detectable nano $TiO_2$. Photocatalytic cement bag emptying and sweeping had the highest airborne nano $TiO_2$ concentration 16.5 wt% and 9.7 wt%, respectively. Photocatalytic cement concrete cutting contained 2.0 wt % nano $TiO_2$, which was the same concentration found in the bag sample. None of the airborne aerosol samples collected during activities with regular cement contained nano $TiO_2$.

Cement powder samples were analyzed with X-ray diffraction and the phase analyses are shown in Table 2. Tricalcium silicate ($Ca_3SiO_5$) and dicalcium silicate ($Ca_2SiO_4$) were the most abundant elements in both cement types. Photocatalytic cement contained 2.6 wt% of nano $TiO_2$ in two different forms: anatase (1.8 wt%) and rutile (0.8 wt%).

We found crystalline silica only during concrete (cement + sand) cutting for photocatalytic and regular cement with the following concentrations 2.5 and 3.5 mg/m$^3$, respectively. When only cement was used (no sand), the crystalline silica concentrations were always below the detection limit (LOD = 5 µg / sample).

The mass concentration of nano $TiO_2$ in photocatalytic cement was calculated from element composition and inhalable dust mass concentration (sampled on the filter). Our work activity simulation showed airborne $TiO_2$ mass concentrations for photocatalytic cement bag emptying

2.50 mg/m$^3$, concrete cutting 1.53 mg/m$^3$, and sweeping 1.48 mg/m$^3$, respectively, for particles size >100 nm.

***Field sampling at the construction sites***

No stationary nano sampling instruments were readily available in Thailand, and we could not ship them from Switzerland as the SMPS has a radioactive source. Consequently, no direct-reading instruments were used during the Thai sampling campaign. SMPS showed mean airborne particle number concentrations over 2 hours was 46,000 pt/cm$^3$, GMD was 49 nm and GSD was 2.4 nm. Peak nanoparticle concentrations measured with the DiSC were for construction (n= 5) 498,088 pt/cm$^3$. Polishing (n= 5) was double (990,658 pt/cm$^3$), and drilling activity (n=5) was slightly above (655,259 pt/cm$^3$).

The mean mass concentration for inhalable dust was more than threefold greater for Switzerland (7.08 mg/m$^3$, SD±3.02) compared to Thailand (2.22 mg/m$^3$, SD±1.61. This was also true for respirable dust (Switzerland had 4.00 mg/m$^3$, SD±2.31 and Thailand 1.19 mg/m$^3$, SD±1.15).

Mass particles size distributions were quite different between the two country-specific construction sites. The Swiss construction site had a peak mass concentration of 2.22 mg/m$^3$ (SD±0.61) at 1.55 µm, while in Thailand the peak was a fraction of this (0.57 mg/m$^3$ SD±0.46) and for smaller particles (0.93 µm).

## 8.3 Reactive oxygen species (ROS) production from cement particle

Photocatalytic cement aerosol exposed to UV irradiance showed a significant increase in ROS activity ($3.3 \cdot 10^{-9}$ nmol/pt) in comparison to regular cement exposed to UV ($0.5 \cdot 10^{-9}$ nmol/pt). Aerosol non-exposed UV the ROS production due to photocatalytic and regular cements were $1.58 \cdot 10^{-9}$ nmol/pt and $1.12 \cdot^{-9}$nmol/pt, respectively.

In addition, ROS production from photocatalytic cement exposed to UV was significantly higher than regular cement both exposed and non-exposed to UV with 95% confident ($p$-value $< 0.05$). In the case of regular cement, the effect of UV exposure on the ROS production was found to be not statistically significant.

Photocatalytic cement bag emptying contained significantly more nano $TiO_2$ (16.46 %) than the one issued from concrete block cutting (2.03 %). ROS production from bag emptying activity were found to be significantly greater ($p$-value = 0.04) for photocatalytic ($4.6 \cdot 10^{-10}$ nmol/ pt) than for regular cement ($1.5 \cdot 10^{-10}$ nmol/ pt). In the case of concrete cutting no significant difference was observed between photocatalytic and regular cement, with ROS reactivities of $1.1 \cdot 10^{-10}$ nmol/and $1.12 \cdot 10^{-10}$ nmol/pt, respectively.

# CHAPTER IX

# DISCUSSION

Aerosolized photocatalytic cement had a greater concentration of nanoscale particles compared to aerosolized regular cement. The morphology results confirmed that (1) the photocatalytic cement contained nanoparticles and (2) $TiO_2$ is a constituent of the photocatalytic cement aerosol. Taken together, this suggests that nano $TiO_2$ can be easily mobilized from photocatalytic cement powder when aerosolized. This can be expected if the nano $TiO_2$ particles are not chemically bound to the larger cement particles.

It is important to note that the $TiO_2$ content in photocatalytic bagged cement powder was only 2 % while reaching 37 % in the aerosolized form. In stable conditions, the aerosolized photocatalytic cement contained about 5% of airborne nanoparticle numbers, presumably $TiO_2$. It is likely that a part of the airborne nano$TiO_2$ was present in the form of agglomerates as seen previously by (Ding & Riediker, 2015).

From the measured ROS activities, it appears that airborne particles produced from photocatalytic cement are a potential source of ROS that is further enhanced in the presence of UV irradiance. As expected, since it is known that $TiO_2$ produce free radicals when exposed to UV. When nano $TiO_2$ expose to UV light or illuminated light source wave length of 280 - 400 nm with energy higher than its electron band gap (3.1-4.3 electron volt) can production hydroxyl radicals, superoxide radical and hydrogen peroxide ($H_2O_2$) (M. Li et al., 2014; Lan et al., 2013; Sayes et al., 2006; Lee et al., 2010; Long et al., 2006). Nano $TiO_2$ exposed UV light giving electrons(ē) and holes (h+). Electrons from conduction band react with molecule of oxygen ($O_2$) in air become superoxide free radical ($O_2^{\bullet -}$). At the same time, holes (h+) from valence band reacts with hydroxyl ion ($OH^-$) from water ($H_2O$) or humidity become hydroxyl radical ($OH^•$) free radical. By product, superoxide radical ($O_2^{•-}$) reacts with $H^+$ which is isolate from molecule of water to produce hydroperoxyl radical ($OH_2^•$). In addition, ($OH_2^•$) combined to other molecule of ($OH_2^•$) given hydrogen peroxide ($H_2O_2$). Moreover, ($O_2^{•-}$) also combined with other molecule of ($O_2^{•-}$) and $2H^+$ from molecule of water given $H_2O_2$ (Jedsukontorn et al., 2016) (Dodd & Jha, 2011; Chen & Poon, 2009; Lan et al., 2013). However, in regular cement UV light not significant effect to increasing ROS because in regular cement had no photocatalysis behavior material. Therefore, UV and $TiO_2$ are the most important factors to increasing ROS in photocatalytic cement. In addition, recent study has shown that airborne nano $TiO_2$ had exhibit a high photocatalytic behavior under environmental outdoor conditions. Humidity and UV irradiance are the most important factor to increasing of ROS from nano $TiO_2$. The optimization of ROS generation were 80 percent of humidity has been confirmed (Vernez et al., 2017).

On the other hand, in different working activity, photocatalytic cement bag emptying had significantly ROS higher than regular cement bag emptying and concrete block cutting. Because in photocatalytic cement bag emptying had higher nano $TiO_2$ than other work activities. Therefore, nano $TiO_2$ in photocatalytic cement can indicate photocatalysis property. Moreover, the estimated ROS concentration from photocatalytic cement bag emptying is similar concentration to Vernez et al., 2017 study with pure $TiO_2$ (Vernez et al., 2017). Therefore, nano TiO2 was the main important factors to generation of ROS concentration.

In addition, this statement highlights a new dimension in the risks associated with airborne nano $TiO_2$ exposure from photocatalytic cement which is the production of ROS that potentially act as secondary toxicants. ROS is important factor link to genotoxicity, cytotoxicity, inflammation, DNA damage and cancer (M. Li et al., 2014; Brieger et al., 2012; Scherz-Shouval & Elazar, 2011; Jaeger et al., 2012; Yin et al., 2012; Jaeger et al., 2012; Wang & Fan, 2014).

In working simulation with photocatalytic cement, we observed much larger mass-fractions of airborne particle-bound $TiO_2$ during sweeping (9.7 wt%) and during bag emptying (16.5 wt%) than what we found in the bagged cement (2 wt%). This shows that nano $TiO_2$ was easily airborne during activities with cement powder (Batsungnoen et al., 2019a).

Photocatalytic cement concrete block cutting resulted in similar proportions of nano $TiO_2$ (2 wt%) in airborne nanoparticles as in bagged cement material. This suggests that the nano-additive was well bound to the matrix so that during the cutting, the nano $TiO_2$ was released into the aerosol as a part of the concrete particles. Indeed, studies on the chemical nature of concrete nano-additive compounds found that nano $TiO_2$ particles were chemically bound to the concrete surface specifically to $SiO_2$, carbonate ($CaCO_3$), and sulfate ($SO_3$) compounds (Zouzelka & Rathousky, 2017; L. Yang et al., 2018).

Inhaling nano $TiO_2$ has been associated with respiratory problems (Kwon et al., 2012). An association between photocatalytic cement and respiratory problems is not known as no such studies are available. Complexing the matter further, lung injury induced by nano $TiO_2$ depended on dimension, size distribution, concentration, crystal phase, agglomeration, surface coating, and chemical and physical properties (Noël et al., 2012; Wang & Fan, 2014).

Both photocatalytic and regular cement had 99 % of the airborne particles with sizes less than 3.5 µm in all working activities; and can thus be deposited and diffused into the respiratory tract especially in the alveoli (Oberdörster et al., 2005; ICRP, 1994; Sha et al., 2015; Tedja et al., 2011).

Our work activity simulation showed airborne mass concentrations for photocatalytic cement bag emptying (2 min) of 15 mg/m$^3$ thereof 2.50 mg/m$^3$ for nano $TiO_2$ particles >100 nm over two hours. We observed that workers emptied 2-4 bags during the morning as well as the afternoon shifts in Thailand. This scenario would lead to 2.50 mg/m$^3$ for 8-h or at the OEL (particle size >100 nm OEL= 2.4 mg/m3) (NIOSH, 2011a; OSHA, 2013). To reduce the airborne dust concentrations, we recommended that the workers empty one bag, add water, and then mix, and repeat this procedure four times. Another approach would be that the producers develops a formula that would allow adding nano $TiO_2$ in the form of a liquid dispersion, thereby strongly reducing the potential for aerosolization.

The jobs performed were similar among the Swiss and Thai construction workers, but the difference was that the Swiss construction workers used powerful machine tools, in particularly during concrete polishing and drilling, while the Thai construction workers worked with small hand-held hammer drills. The mean mass concentration for inhalable dust was more than threefold greater for Switzerland (7.08 mg/m$^3$, SD±3.02) for 8-hr TWA 1.77 mg/m$^3$ compared to Thailand (2.22 mg/m$^3$, SD±1.61) for 8-hr TWA 0.55 mg/m$^3$. This was also true for respirable dust (Switzerland had 4.00 mg/m$^3$, SD±2.31 and Thailand 1.19 mg/m$^3$, SD±1.15). Power tools have shown to generate more dust compared to manual tools such as drilling concrete generated the highest exposures for quartz and respirable dust among construction workers (Deurssen van et al., 2014). Moreover, Qi and colleagues (Qi et al., 2017) reported that concentrations of airborne particles during fiber cement cutting increased with the power of the tools used. The main factors associated with particle generation were number of blade teeth, blade rotating speed, and cutting feed rate (Qi et al., 2017). We found comparable result in our work activity simulation, where cutting concrete blocks using power tools generated high particle concentrations.

Exposure to regular cement is associated with lung function decline at elevated exposures (Karl-Christian Nordby et al., 2016). In addition, cement dust as such has been associated with impaired lung function, inflammation, bronchitis, chronic obstructive pulmonary disease, restrictive lung disease, and pneumoconiosis (Eom et al., 2017; Maciejewska & Bielichowska-Cybula, 1991; Meo, 2004; Penrose, 2014).

The majority of the particle material found in both regular and photocatalytic cement was CaO. Inhaled CaO dust can cause inflammation in the upper respiratory tract due to its alkalinity (TOXNET, 2014; NJDHSS, 2003).

The second most abundant particle material was silica ($SiO_2$). Exposure to crystalline silica can lead to health effects such as silicosis, tuberculosis, chronic bronchitis, COPD and lung cancer (IARC, 1997; Merget et al., 2002; Kaewamatawong et al., 2005; Napierska et al., 2010). Amorphous silica is associated with reversible inflammation, granuloma formation and emphysema (McLaughlin et al., 1997; Merget et al., 2002; Kaewamatawong et al., 2005). Only the respiratory fraction of the airborne dust during concrete cutting was crystalline $SiO_2$ present. Thus, respiratory crystalline $SiO_2$ originates from the sand and not from the cement as previously reported by others (McLean et al., 2017). The levels of crystalline silica observed were very high, well above the 8-hour OEL levels, which suggests that for dusty work activities with cement, the greatest risk comes from crystalline silica in sand rather than from nano-additives.

None of these toxicological and epidemiological assessments were made with nano-sized particles. We therefore concluded that exposures to these nano-sized particles could lead to unexplained effects on human health, and consequently, safety and environmental burden should not be neglected (Maynard et al., 2006; Oberdörster et al., 2005).

The inhalation pathway is considered the major route of nanoparticle exposure, and the lungs and pleura are the major primary targets for adverse effects (Ken Donaldson & Poland, 2012; Oberdörster et al., 2005). It is difficult to say how nano $TiO_2$ might change health hazards already associated with cement exposure, but this should be considered when assessing exposure risks among cement workers.

Sweeping with a broom was generated inhalable, and respirable dust. In addition, sweeping with photocatalytic cement produced nano $TiO_2$. Other researcher have also found that cleaning cement is associated with higher airborne particle concentrations compared to other cement production jobs such as laboratory, foreman and administration (H. Notø et al., 2015). One study specifically reported concentrations during cleaning using brooms at two cement plants in Ethiopia (Zeleke et al., 2011). They confirmed significantly greater exposures to total and respirable dust in cleaners compared to other production worker at these cement plants. Therefore, cleaning using other methods than a broom would reduce the cement exposures among Thai construction workers.

Exposures to airborne cement particles in the construction industry also depends on duration, environment (temperature, humidity and wind), space (indoor, outdoor), workpiece sizes, machine tool use, material type, control measures, and use of personal protective equipment (PPE). We observed that Thai construction workers did not use respiratory protective equipment (RPE) while Swiss construction workers did. Thai construction workers were not comfortable using RPE because it was both hot and humid. Control measures need to be implemented for the Swiss construction workers to not only comply with the swiss OEL regulations, but to reduce the risk of developing COPD. Local exhaust ventilation (LEV) in construction were shown to be effective in reducing respirable dust in both the work and adjacent area (Kokkonen et al., 2019).

The protection measures needed for workers working with photocatalytic cement, especially during dry cement work, should be similar to recommendations made for nano $TiO_2$ exposures. Wet processes to reduce airborne dust exposures should be recommended if possible. Several international bodies have recommended ways to reduce nano particle exposures using engineering controls such as enclosed process chambers with negative pressure and local exhaust ventilation (LEV) installed with high-efficiency particulate air (HEPA) filters (NIOSH, 2011a; NIOSH, 2012; NIOSH, 2013; OSHA, 2013; Goede et al., 2018). Where enclosure of the source is not possible other alternatives should be considered such as portable capture hood, wet or dry vacuum machine equipped with a HEPA filter. Another suggestion would to be manufacture nano $TiO_2$ as a paste that can be added to the cement powder with the water. Administrative control strategies can also be implemented such as adjust work schedules, education, training, good general hygiene, good housekeeping, and medical surveillance (NIOSH, 2011a; NIOSH, 2012; NIOSH, 2013; OSHA, 2013). More specifically, OSHA and NIOSH recommend using: RPE, protective clothing, nitrile or chemically impervious gloves, and goggles. The RPE types recommended are N100, R100, and P100 for US (OSHA, 2013; OSHA, 2011; NIOSH, 2014) and P3 and filtering face piece (FFP3) for Europe (EN 143 and EN 149) (Goede et al., 2018; Rengasamy et al., 2009). Perhaps new modern comfortable, cheap hoods with positive pressure and air condition could be designed for worker construction industry to reduce a particles exposure and heat.

# CHAPTER X

# CONCLUSION

The photocatalytic cement had significantly smaller particle size distribution than the regular cement in an aerosolized experimental system. As expected, the cement particle concentration was significantly greater for the photocatalytic compared to regular cement, but regular cement also produced nanosized particles.

The comparative approach between photocatalytic and regular cement aerosols confirmed the origin of the airborne ROS produced from nano $TiO_2$ photocatalytic activity. Considering both the photoreactivity of aerosolized photocatalytic cement under UV irradiance and the high content of airborne nano $TiO_2$ generated during bag emptying activity highlight the potential risks for construction workers. Nano $TiO_2$ and UV irradiance are the most important factors to increasing ROS concentration in photocatalytic cement. In Thailand construction worker work outside with sunny environment and high humidity. Therefore, worker protection procedures should not only consider nano $TiO_2$ exposure but also its ability to produce ROS as secondary airborne potential toxicants.

The airborne nano $TiO_2$ concentration was far greater than the labeled 2 wt% in the photocatalytic cement bag, increasing to 9.7 wt% during sweeping and 16.5wt% during bag emptying. This suggests that nano $TiO_2$ can be easily mobilized from photocatalytic cement powder when aerosolized. Work activities studied in the exposure chamber such as sweeping and bag emptying gave rise to nano $TiO_2$ air concentrations while concrete cutting did not.

Both photocatalytic and regular cement had a GMD less than 3.5 µm thus will be able to penetrate deep into the lung especially in alveoli.

Thai workers were exposed to cement particles mainly during sweeping and Swiss workers during drilling and polishing cement blocks. Nano $TiO_2$ air concentrations cannot readily be extrapolated from the fraction in the bag, especially cement powder handling will require nanoparticle targeted exposure assessments. Exposure to nano $TiO_2$ adds to the already known particle-related health concerns among construction workers.

Finally, the recommendation for workers who using photocatalytic cement to use protection measures similar to recommendations made for nano $TiO_2$ exposures.

## REFERENCES


ACGIH. (2015). *TLVs and BEIs*. The American Conference of Governmental Industrial Hygienists, (ACGIH).

AIHA. (2015). *Personal Protective Equipment for Engineered Nanoparticles Personal Protective Equipment for Engineered Nanoparticles*. American Industrial Hygiene Association. https://www.aiha.org/government-affairs/Documents/PPE%20for%20ENP_FINAL.pdf

Aitken, R. J., Creely, K. S., & Tran, C. L. (2004). *Nanoparticles: An occupational hygiene review* [Research Reports]. http://www.hse.gov.uk/research/rrhtm/rr274.htm

Alfadda, A. A., & Sallam, R. M. (2012). *Reactive Oxygen Species in Health and Disease* [Research article]. BioMed Research International. https://doi.org/10.1155/2012/936486

Anjilvel, S., & Asgharian, B. (1995). A Multiple-Path Model of Particle Deposition in the Rat Lung. *Fundamental and Applied Toxicology*, *28*(1), 41–50. https://doi.org/10.1006/faat.1995.1144

ANSES. (2019). *Titanium dioxide in nanoparticle form: ANSES defines a toxicity reference value (TRV) for chronic inhalation exposure*. French Agency for Food, Environmental and Occupational Health & Safety. https://www.anses.fr/en/content/titanium-dioxide-nanoparticle-form-anses-defines-toxicity-reference-value-trv-chronic

Arenberg, M. R., & Arai, Y. (2020). The Effects of Oxyanion Adsorption on Reactive Oxygen Species Generation by Titanium Dioxide. *Clays and Clay Minerals*. https://doi.org/10.1007/s42860-019-00039-8

Asgharian, B., Hofmann, W., & Bergmann, R. (2001). Particle Deposition in a Multiple-Path Model of the Human Lung. *Aerosol Science and Technology*, *34*(4), 332–339. https://doi.org/10.1080/02786820119122

Ashraf, M. A., Peng, W., Zare, Y., & Rhee, K. Y. (2018). Effects of Size and Aggregation/Agglomeration of Nanoparticles on the Interfacial/Interphase Properties and Tensile Strength of Polymer Nanocomposites. *Nanoscale Research Letters*, *13*(1), 214. https://doi.org/10.1186/s11671-018-2624-0

ASTM. (2010). *E2456-06, Standard Terminology Relating to Nanotechnology*. www.astm.org

Aust, A. E., Ball, J. C., Hu, A. A., Lighty, J. S., Smith, K. R., Straccia, A. M., Veranth, J. M., & Young, W. C. (2002). Particle characteristics responsible for effects on human lung epithelial cells. *Research Report (Health Effects Institute)*, *110*, 1–65; discussion 67-76.

Baan, R. A. (2007). Carcinogenic Hazards from Inhaled Carbon Black, Titanium Dioxide, and Talc not Containing Asbestos or Asbestiform Fibers: Recent Evaluations by an IARC Monographs Working Group. *Inhalation Toxicology*, *19*(sup1), 213–228. https://doi.org/10.1080/08958370701497903

Banerjee, S., Dionysiou, D. D., & Pillai, S. C. (2015). Self-cleaning applications of TiO2 by photo-induced hydrophilicity and photocatalysis. *Applied Catalysis B: Environmental*, *176–177*, 396–428. https://doi.org/10.1016/j.apcatb.2015.03.058

Batsungnoen, K., Hopf, N. B., Suárez, G., & Riediker, M. (2019a). Characterization of nanoparticles in aerosolized photocatalytic and regular cement. *Aerosol Science and Technology*, *53*(5), 540–548. https://doi.org/10.1080/02786826.2019.1578334

Batsungnoen, K., Hopf, N. B., Suárez, G., & Riediker, M. (2019b). Characterization of nanoparticles in aerosolized photocatalytic and regular cement. *Aerosol Science and Technology*, *53*(5), 540–548. https://doi.org/10.1080/02786826.2019.1578334

Bello, D., Wardle, B. L., Yamamoto, N., Guzman deVilloria, R., Garcia, E. J., Hart, A. J., Ahn, K., Ellenbecker, M. J., & Hallock, M. (2009). Exposure to nanoscale particles and fibers during machining of hybrid advanced composites containing carbon nanotubes. *Journal of Nanoparticle Research, 11*(1), 231–249. https://doi.org/10.1007/s11051-008-9499-4

Brieger, K., Schiavone, S., Miller, F. J., & Krause, K.-H. (2012). Reactive oxygen species: From health to disease. *Swiss Medical Weekly*, *142*, w13659. https://doi.org/10.4414/smw.2012.13659

Broekhuizen, P. van, Broekhuizen, F. van, Cornelissen, R., & Reijnders, L. (2011). Use of nanomaterials in the European construction industry and some occupational health aspects thereof. *Journal of Nanoparticle Research*, *13*(2), 447–462. https://doi.org/10.1007/s11051-010-0195-9

Carp, O., Huisman, C. L., & Reller, A. (2004). Photoinduced reactivity of titanium dioxide. *Progress in Solid State Chemistry*, *32*(1–2), 33–177. https://doi.org/10.1016/j.progsolidstchem.2004.08.001

Chen, J., & Poon, C. (2009). Photocatalytic construction and building materials: From fundamentals to applications. *Building and Environment*, *44*(9), 1899–1906. https://doi.org/10.1016/j.buildenv.2009.01.002

Dalton, J. S., Janes, P. A., Jones, N. G., Nicholson, J. A., Hallam, K. R., & Allen, G. C. (2002). Photocatalytic oxidation of NOx gases using TiO2: A surface spectroscopic approach. *Environmental Pollution*, *120*(2), 415–422. https://doi.org/10.1016/S0269-7491(02)00107-0

Deurssen van, E., Pronk, A., Spaan, S., Goede, H., Tielemans, E., Heederik, D., & Meijster, T. (2014). Quartz and Respirable Dust in the Dutch Construction Industry: A Baseline Exposure Assessment as Part of a Multidimensional Intervention Approach. *The Annals of Occupational Hygiene, 58*(6), 724–738. https://doi.org/10.1093/annhyg/meu021

Diebold, U. (2003). The surface science of titanium dioxide. *Surface Science Reports*, *48*(5–8), 53–229. https://doi.org/10.1016/S0167-5729(02)00100-0

Diesen, V., & Jonsson, M. (2014). Formation of H2O2 in TiO2 Photocatalysis of Oxygenated and Deoxygenated Aqueous Systems: A Probe for Photocatalytically Produced Hydroxyl Radicals. *The Journal of Physical Chemistry C*, *118*(19), 10083–10087. https://doi.org/10.1021/jp500315u

Ding, Y., Kuhlbusch, T. A. J., Van Tongeren, M., Jiménez, A. S., Tuinman, I., Chen, R., Alvarez, I. L., Mikolajczyk, U., Nickel, C., Meyer, J., Kaminski, H., Wohlleben, W., Stahlmecke, B., Clavaguera, S., & Riediker, M. (2017). Airborne engineered nanomaterials in the workplace—A review of release and worker exposure during nanomaterial production and handling processes. *Journal of Hazardous Materials*, *322*, 17–28. https://doi.org/10.1016/j.jhazmat.2016.04.075

Ding, Y., & Riediker, M. (2015). A system to assess the stability of airborne nanoparticle agglomerates under aerodynamic shear. *Journal of Aerosol Science*, *88*, 98–108. https://doi.org/10.1016/j.jaerosci.2015.06.001

Ding, Y., & Riediker, M. (2016). A System to Create Stable Nanoparticle Aerosols from Nanopowders. *JoVE (Journal of Visualized Experiments)*, *113*, e54414–e54414. https://doi.org/10.3791/54414

Dodd, N. J. F., & Jha, A. N. (2011). Photoexcitation of Aqueous Suspensions of Titanium Dioxide Nanoparticles: An Electron Spin Resonance Spin Trapping Study of Potentially Oxidative Reactions. *Photochemistry and Photobiology*, *87*(3), 632–640. https://doi.org/10.1111/j.1751-1097.2011.00897.x

Donaldson, K, Stone, V., Seaton, A., & MacNee, W. (2001). Ambient particle inhalation and the cardiovascular system: Potential mechanisms. *Environmental Health Perspectives*, *109*(Suppl 4), 523–527.

Donaldson, Ken, & Poland, C. A. (2012). Inhaled nanoparticles and lung cancer—What we can learn from conventional particle toxicology. *Swiss Medical Weekly*, *142*(2526). https://doi.org/10.4414/smw.2012.13547

Eastlake, A. C., Beaucham, C., Martinez, K. F., Dahm, M. M., Sparks, C., Hodson, L. L., & Geraci, C. L. (2016). Refinement of the Nanoparticle Emission Assessment Technique into the Nanomaterial Exposure Assessment Technique (NEAT 2.0). *Journal of Occupational and Environmental Hygiene*, *13*(9), 708–717. https://doi.org/10.1080/15459624.2016.1167278

Edwin G. Foulke. (2008). *Preventing Skin Problems from Working with Portland Cement*. Occupational Safety and Health Administration, OSHA. https://www.osha.gov/Publications/OSHA-3351-portland-cement.pdf

Eom, S.-Y., Cho, E.-B., Oh, M.-K., Kweon, S.-S., Nam, H.-S., Kim, Y.-D., & Kim, H. (2017). Increased incidence of respiratory tract cancers in people living near Portland cement plants in Korea. *International Archives of Occupational and Environmental Health*, *90*(8), 859–864. https://doi.org/10.1007/s00420-017-1244-9

Etacheri, V., Di Valentin, C., Schneider, J., Bahnemann, D., & Pillai, S. C. (2015). Visible-light activation of TiO2 photocatalysts: Advances in theory and experiments. *Journal of Photochemistry and Photobiology C: Photochemistry Reviews*, *25*, 1–29. https://doi.org/10.1016/j.jphotochemrev.2015.08.003

Falck, G. C. M., Lindberg, H. K., Suhonen, S., Vippola, M., Vanhala, E., Catalán, J., Savolainen, K., & Norppa, H. (2009). Genotoxic effects of nanosized and fine TiO2. *Human & Experimental Toxicology*, *28*(6–7), 339–352. https://doi.org/10.1177/0960327109105163

Fell, A. K. M., & Nordby, K. C. (2017). Association between exposure in the cement production industry and non-malignant respiratory effects: A systematic review. *BMJ Open*, *7*(4), e012381. https://doi.org/10.1136/bmjopen-2016-012381

Feng, D., Xie, N., Gong, C., Leng, Z., Xiao, H., Li, H., & Shi, X. (2013). Portland Cement Paste Modified by TiO2 Nanoparticles: A Microstructure Perspective. *Industrial & Engineering Chemistry Research*, *52*(33), 11575–11582. https://doi.org/10.1021/ie4011595

Folli, A., Pochard, I., Nonat, A., Jakobsen, U. H., Shepherd, A. M., & Macphee, D. E. (2010). Engineering Photocatalytic Cements: Understanding TiO2 Surface Chemistry to Control and Modulate Photocatalytic Performances. *Journal of the American Ceramic Society*, *93*(10), 3360–3369. https://doi.org/10.1111/j.1551-2916.2010.03838.x

Fonseca, A. S., Viitanen, A.-K., Koivisto, A. J., Kangas, A., Huhtiniemi, M., Hussein, T., Vanhala, E., Viana, M., Querol, X., & Hämeri, K. (2015). Characterization of Exposure to Carbon Nanotubes in an Industrial Setting. *The Annals of Occupational Hygiene*, *59*(5), 586–599. https://doi.org/10.1093/annhyg/meu110

Friedlander, S. K., & Pui, D. Y. H. (2003). *National Science Foundation Workshop Report on Emerging issues in nanoparticle aerosol science and technology (NAST)* [Workshop Report]. http://www.eng.uc.edu/~beaucag/Classes/MorphologyofComplexMaterials/NSFAerosolPar%20Report.pdf

Friedrichs, S., & Schulte, J. (2007). Environmental, health and safety aspects of nanotechnology—Implications for the R&D in (small) companies. *Science and Technology of Advanced Materials*, *8*(1), 12–18. https://doi.org/10.1016/j.stam.2006.11.020

FSO. (2017). *Full-time job equivalent per sector, Switzerland* [Labour statistics]. Federal Statistical Office, Swiss Confederation. https://www.bfs.admin.ch/bfs/en/home/statistics/industry-services/businesses-employment/jobs-statistics/jobs.assetdetail.3243521.html

Fujishima, A., & Zhang, X. (2006). Titanium dioxide photocatalysis: Present situation and future approaches. *Comptes Rendus Chimie*, *9*(5), 750–760. https://doi.org/10.1016/j.crci.2005.02.055

Gao, L., Fan, K., & Yan, X. (2017). Iron Oxide Nanozyme: A Multifunctional Enzyme Mimetic for Biomedical Applications. *Theranostics*, *7*(13), 3207–3227. https://doi.org/10.7150/thno.19738

Gaté, L., Disdier, C., Cosnier, F., Gagnaire, F., Devoy, J., Saba, W., Brun, E., Chalansonnet, M., & Mabondzo, A. (2017). Biopersistence and translocation to extrapulmonary organs of titanium dioxide nanoparticles after subacute inhalation exposure to aerosol in adult and elderly rats. *Toxicology Letters*, *265*, 61–69. https://doi.org/10.1016/j.toxlet.2016.11.009

Geiser, M., & Kreyling, W. G. (2010). Deposition and biokinetics of inhaled nanoparticles. *Particle and Fibre Toxicology*, *7*, 2. https://doi.org/10.1186/1743-8977-7-2

Ghadiry, M., Gholami, M., Choon Kong, L., Wu Yi, C., Ahmad, H., & Alias, Y. (2016). Nano-Anatase TiO2 for High Performance Optical Humidity Sensing on Chip. *Sensors*, *16*(1), 39. https://doi.org/10.3390/s16010039

Ghio, A. J., & Devlin, R. B. (2001). Inflammatory lung injury after bronchial instillation of air pollution particles. *American Journal of Respiratory and Critical Care Medicine*, *164*(4), 704–708. https://doi.org/10.1164/ajrccm.164.4.2011089

Ghosh, M., Bandyopadhyay, M., & Mukherjee, A. (2010). Genotoxicity of titanium dioxide ($TiO_2$) nanoparticles at two trophic levels: Plant and human lymphocytes. *Chemosphere*, *81*(10), 1253–1262. https://doi.org/10.1016/j.chemosphere.2010.09.022

Goede, H., Christopher-de Vries, Y., Kuijpers, E., & Fransman, W. (2018). A Review of Workplace Risk Management Measures for Nanomaterials to Mitigate Inhalation and Dermal Exposure. *Annals of Work Exposures and Health*. https://doi.org/10.1093/annweh/wxy032

Guillemin, M. (1975). Mise au point et utilisation d'une cabine d'expérimentation. *Archives Des Maladies Professionnelles de Medecine Du Travail et de Securite Sociale (Paris) (Arch. Mal. Prof.)*, *36*, 421–428.

Hämeri, K., Lähde, T., Hussein, T., Koivisto, J., & Savolainen, K. (2009). Facing the key workplace challenge: Assessing and preventing exposure to nanoparticles at source. *Inhalation Toxicology*, *21*(sup1), 17–24. https://doi.org/10.1080/08958370902942525

Hanaor, D. A. H., & Sorrell, C. C. (2011). Review of the anatase to rutile phase transformation. *Journal of Materials Science*, *46*(4), 855–874. https://doi.org/10.1007/s10853-010-5113-0

He, M., & Dhaniyala, S. (2013). A multiple charging correction algorithm for scanning electrical mobility spectrometer data. *Journal of Aerosol Science*, *61*, 13–26. https://doi.org/10.1016/j.jaerosci.2013.03.007

Hernández-Rodríguez, M. J., Santana Rodríguez, R., Darias, R., González Díaz, O., Pérez Luzardo, J. M., Doña Rodríguez, J. M., & Pulido Melián, E. (2019). Effect of $TiO_2$ Addition on Mortars: Characterization and Photoactivity. *Applied Sciences*, *9*(13), 2598. https://doi.org/10.3390/app9132598

Huang, Z., Maness, P.-C., Blake, D. M., Wolfrum, E. J., Smolinski, S. L., & Jacoby, W. A. (2000). Bactericidal mode of titanium dioxide photocatalysis. *Journal of

*Photochemistry and Photobiology A: Chemistry*, *130*(2), 163–170. https://doi.org/10.1016/S1010-6030(99)00205-1

IARC. (1997). *IARC monographs on the evaluation of carcinogenic risk to human silica, some silicates, coal dust and para-aramid fibrils* (Vol. 68). World health organization, International Agency for Research on Cancer. http://monographs.iarc.fr/ENG/Monographs/vol68/

IARC. (2012). *Silica dust crystalline in the form of quartz or cristobalite*. World health organization, International Agency for Research on Cancer. https://monographs.iarc.fr/ENG/Monographs/vol100C/mono100C-14.pdf

IARC. (2015). *Agents Classified by the IARC Monographs* (Vols. 1–114). World health organization, International Agency for Research on Cancer. http://monographs.iarc.fr/ENG/Classification/

IARC. (2017). *IARC Monographs on the evaluation of carcinogenic risk to human; List of classification* (Vols. 1–120). World health organization, International Agency for Research on Cancer. http://monographs.iarc.fr/ENG/Classification/latest_classif.php

ICRP. (1994). Human respiratory tract model for radiological protection. A report of a Task Group of the International Commission on Radiological Protection. *Annals of the ICRP*, *24*(1–3), 1–482.

ILO. (1999). *Safety, health and welfare on construction sites: A training manual* (2nd ed.). International Labour Organization.

ILO. (2014, October 2). *Safety and Health in the Construction Sector- Overcoming the Challenges* [Event]. http://www.ilo.org/empent/Eventsandmeetings/WCMS_310993/lang--en/index.htm

ISO/TS 27687. (2008). *ISO/TS 27687: Nanotechnologies*. International Organization for Standardization. https://www.iso.org/obp/ui/#iso:std:iso:ts:27687:ed-1:v2:en

Jaeger, A., Weiss, D. G., Jonas, L., & Kriehuber, R. (2012). Oxidative stress-induced cytotoxic and genotoxic effects of nano-sized titanium dioxide particles in human HaCaT keratinocytes. *Toxicology*, *296*(1), 27–36. https://doi.org/10.1016/j.tox.2012.02.016

Jedsukontorn, T., Meeyoo, V., Saito, N., & Hunsom, M. (2016). Effect of electron acceptors H2O2 and O2 on the generated reactive oxygen species 1O2 and OH in TiO2-catalyzed photocatalytic oxidation of glycerol. *Chinese Journal of Catalysis*, *37*(11), 1975–1981. https://doi.org/10.1016/S1872-2067(16)62519-6

Jeff Thomas, & Hamlin Jennings. (2008). *Mineral and Oxide Composition of Portland Cement*. Northwestern University. http://iti.northwestern.edu/cement/monograph/Monograph3_6.html

Jimenez-Relinque, E., Rodriguez-Garcia, J. R., Castillo, A., & Castellote, M. (2015). Characteristics and efficiency of photocatalytic cementitious materials: Type of binder, roughness and microstructure. *Cement and Concrete Research*, *71*, 124–131. https://doi.org/10.1016/j.cemconres.2015.02.003

Kaewamatawong, T., Kawamura, N., Okajima, M., Sawada, M., Morita, T., & Shimada, A. (2005). Acute Pulmonary Toxicity Caused by Exposure to Colloidal Silica: Particle Size Dependent Pathological Changes in Mice. *Toxicologic Pathology*, *33*(7), 745–751. https://doi.org/10.1080/01926230500416302

Kakinoki, K., Yamane, K., Teraoka, R., Otsuka, M., & Matsuda, Y. (2004). Effect of Relative Humidity on the Photocatalytic Activity of Titanium Dioxide and Photostability of Famotidine. *Journal of Pharmaceutical Sciences*, *93*(3), 582–589. https://doi.org/10.1002/jps.10575

Knaapen, A. M., Borm, P. J. A., Albrecht, C., & Schins, R. P. F. (2004). Inhaled particles and lung cancer. Part A: Mechanisms. *International Journal of Cancer*, *109*(6), 799–809. https://doi.org/10.1002/ijc.11708

Kokkonen, A., Linnainmaa, M., Säämänen, A., Kanerva, T., Sorvari, J., Kolehmainen, M., Lappalainen, V., & Pasanen, P. (2019). Control of Dust Dispersion From an Enclosed Renovation Site Into Adjacent Areas by Using Local Exhaust Ventilation. *Annals of Work Exposures and Health*. https://doi.org/10.1093/annweh/wxz016

Kreyling, W. G., Hirn, S., & Schleh, C. (2010). Nanoparticles in the lung. *Nature Biotechnology*, *28*(12), 1275–1276. https://doi.org/10.1038/nbt.1735

Kwon, S., Yang, Y.-S., Yang, H.-S., Lee, J., Kang, M.-S., Lee, B., Lee, K., & Song, C.-W. (2012). Nasal and Pulmonary Toxicity of Titanium Dioxide Nanoparticles in Rats. *Toxicological Research*, *28*(4), 217–224. https://doi.org/10.5487/TR.2012.28.4.217

Lan, Y., Lu, Y., & Ren, Z. (2013). Mini review on photocatalysis of titanium dioxide nanoparticles and their solar applications. *Nano Energy*, *2*(5), 1031–1045. https://doi.org/10.1016/j.nanoen.2013.04.002

Laulagnet, A., Sauvain, J. J., Concha-Lozano, N., Riediker, M., & Suárez, G. (2015). Sensitive Photonic System to Measure Oxidative Potential of Airborne Nanoparticles and ROS Levels in Exhaled Air. *Procedia Engineering*, *120*, 632–636. https://doi.org/10.1016/j.proeng.2015.08.659

Lee, J., Mahendra, S., & Alvarez, P. J. J. (2010). Nanomaterials in the Construction Industry: A Review of Their Applications and Environmental Health and Safety Considerations. *ACS Nano*, *4*(7), 3580–3590. https://doi.org/10.1021/nn100866w

Li, G. (2004). Properties of high-volume fly ash concrete incorporating nano-SiO2. *Cement and Concrete Research*, *34*(6), 1043–1049. https://doi.org/10.1016/j.cemconres.2003.11.013

Li, M., Yin, J.-J., Wamer, W. G., & Lo, Y. M. (2014). Mechanistic characterization of titanium dioxide nanoparticle-induced toxicity using electron spin resonance. *Journal of Food and Drug Analysis*, *22*(1), 76–85. https://doi.org/10.1016/j.jfda.2014.01.006

Lim, T. H., Jeong, S. M., Kim, S. D., & Gyenis, J. (2000). Photocatalytic decomposition of NO by TiO2 particles. *Journal of Photochemistry and Photobiology A: Chemistry*, *134*(3), 209–217. https://doi.org/10.1016/S1010-6030(00)00265-3

Liou, G.-Y., & Storz, P. (2010). Reactive oxygen species in cancer. *Free Radical Research*, *44*(5), 479–496. https://doi.org/10.3109/10715761003667554

Liu, M. (2013). *Coating Technology of Nuclear Fuel Kernels: A Multiscale View*. https://doi.org/10.5772/55651

Long, T. C., Saleh, N., Tilton, R. D., Lowry, G. V., & Veronesi, B. (2006). Titanium dioxide (P25) produces reactive oxygen species in immortalized brain microglia (BV2): Implications for nanoparticle neurotoxicity. *Environmental Science & Technology*, *40*(14), 4346–4352.

Ma, B., Li, H., Mei, J., Li, X., & Chen, F. (2015). Effects of Nano-TiO2 on the Toughness and Durability of Cement-Based Material. *Advances in Materials Science and Engineering*. https://doi.org/10.1155/2015/583106

Ma, H., Brennan, A., & Diamond, S. A. (2012). Photocatalytic reactive oxygen species production and phototoxicity of titanium dioxide nanoparticles are dependent on the solar ultraviolet radiation spectrum. *Environmental Toxicology and Chemistry*, *31*(9), 2099–2107. https://doi.org/10.1002/etc.1916

Maciejewska, A., & Bielichowska-Cybula, G. (1991). [Biological effect of cement dust]. *Medycyna Pracy*, *42*(4), 281–289.

Matsunaga, T., Tomoda, R., Nakajima, T., & Wake, H. (1985). Photoelectrochemical sterilization of microbial cells by semiconductor powders. *FEMS Microbiology Letters*, *29*(1), 211–214.

Maynard, A. D., Aitken, R. J., Butz, T., Colvin, V., Donaldson, K., Oberdörster, G., Philbert, M. A., Ryan, J., Seaton, A., Stone, V., Tinkle, S. S., Tran, L., Walker, N. J., & Warheit, D. B. (2006, November 15). *Safe handling of nanotechnology* [Comments and Opinion]. Nature. https://doi.org/10.1038/444267a

McLaughlin, J. K., Chow, W. H., & Levy, L. S. (1997). Amorphous silica: A review of health effects from inhalation exposure with particular reference to cancer. *Journal of Toxicology and Environmental Health*, *50*(6), 553–566. https://doi.org/10.1080/15287399709532054

McLean, D., Glass, B., ’t Mannetje, A., & Douwes, J. (2017). Exposure to respirable crystalline silica in the construction industry-do we have a problem? *The New Zealand Medical Journal*, *130*(1466), 78–82.

Meo, S. A. (2004). Health hazards of cement dust. *Saudi Medical Journal*, *25*(9), 1153–1159.

Merget, R., Bauer, T., Küpper, H. U., Philippou, S., Bauer, H. D., Breitstadt, R., & Bruening, T. (2002). Health hazards due to the inhalation of amorphous silica. *Archives of Toxicology*, *75*(11–12), 625–634.

Methner, M., Hodson, L., & Geraci, C. (2010). Nanoparticle Emission Assessment Technique (NEAT) for the Identification and Measurement of Potential Inhalation Exposure to Engineered Nanomaterials—Part A. *Journal of Occupational and Environmental Hygiene*, *7*(3), 127–132. https://doi.org/10.1080/15459620903476355

Michael Chusid. (2017). *Self-Cleaning Concrete*. Concrete Decor. http://www.concretedecor.net/index.cfm/decorativeconcretearticles/vol-5-no-4-augustseptember-2005/self-cleaning-concrete/

Miller, F. J., Asgharian, B., Schroeter, J. D., & Price, O. (2016). Improvements and additions to the Multiple Path Particle Dosimetry model. *Journal of Aerosol Science, 99*, 14–26. https://doi.org/10.1016/j.jaerosci.2016.01.018

Moghadam, S. R., Abedi, S., Afshari, M., Abedini, E., & Moosazadeh, M. (2017). Decline in lung function among cement production workers: A meta-analysis. *Reviews on Environmental Health*, *32*(4), 333–341. https://doi.org/10.1515/reveh-2017-0017

Nano werk. (2015). *Nanotechnology in the Construction Industry*. http://www.nanowerk.com/nanotechnology-in-construction-industry.php

Napierska, D., Thomassen, L. C., Lison, D., Martens, J. A., & Hoet, P. H. (2010). The nanosilica hazard: Another variable entity. *Particle and Fibre Toxicology, 7*, 39. https://doi.org/10.1186/1743-8977-7-39

NIA. (2017). *Powdered titanium dioxide (TiO2) to be classified as carcinogen by inhalation*. The Nanotechnology Industries Association. http://nanotechia.org/news/powdered-titanium-dioxide-tio2-be-classified-carcinogen-inhalation

Nichols, G., Byard, S., Bloxham, M. J., Botterill, J., Dawson, N. J., Dennis, A., Diart, V., North, N. C., & Sherwood, J. D. (2002). A review of the terms agglomerate and aggregate with a recommendation for nomenclature used in powder and particle characterization. *Journal of Pharmaceutical Sciences*, *91*(10), 2103–2109. https://doi.org/10.1002/jps.10191

NIOSH. (1998). *NIOSH Manual of Analytical Methods 0600: Particulate not otherwise regulated, respirable*. The National Institute for Occupational Safety and Health (NIOSH). https://www.cdc.gov/niosh/docs/2003-154/method-cas0.html

NIOSH. (2003). *NIOSH Manual of Analytical Methods 7602: Silica, crystalline by IR (KBr pellet)*. The National Institute for Occupational Safety and Health (NIOSH). https://www.cdc.gov/niosh/docs/2003-154/method-cas1.html

NIOSH. (2009). *Approaches to Safe Nanotechnology Managing the Health and Safety Concerns Associated with Engineered Nanomaterials*. U.S. Department of Health and Human Services, Centers for Disease Control and Prevention, National Institute for Occupational Safety and Health. http://www.cdc.gov/niosh/docs/2009-125/pdfs/2009-125.pdf

NIOSH. (2011a). *Occupational Exposure to Titanium Dioxide*. U.S. Department of Health and Human Services, Centers for Disease Control and Prevention, National Institute for Occupational Safety and Health.

NIOSH. (2011b). *Portland cement*. National Institute for Occupational Safety and Health. https://www.cdc.gov/niosh/pel88/65997-15.html

NIOSH. (2012). *General Safe Practices for Working with Engineered Nanomaterials in Research Laboratories*. U.S. Department of Health and Human Services, Centers for Disease Control and Prevention, National Institute for Occupational Safety and Health. http://www.cdc.gov/niosh/docs/2012-147/pdfs/2012-147.pdf

NIOSH. (2013). *Current Strategies for Engineering Controls in Nanomaterial Production and Downstream Handling Processes*. U.S. Department of Health and Human Services, Centers for Disease Control and Prevention, National Institute for Occupational Safety and Health. http://www.cdc.gov/niosh/docs/2014-102/pdfs/2014-102.pdf

NIOSH. (2014). *NIOSH Guide to the Selection and Use of Particulate Respirators, Certified Under 42 CFR 84*. U.S. Department of Health and Human Services, Centers for Disease Control and Prevention, National Institute for Occupational Safety and Health. http://www.cdc.gov/niosh/docs/96-101/

NIOSH. (2018). *NIOSH pocket guide to chemical hazards: Silica, amorphous*. The National Institute for Occupational Safety and Health (NIOSH). https://www.cdc.gov/index.htm

NIST. (2015). *Safety Data Sheet of Titanium Dioxide Nanomaterial*. National Institute of Standards and Technology. https://www-s.nist.gov/srmors/msds/1898-MSDS.pdf?CFID=36999612&CFTOKEN=ad5bfee85cf1516a-78FD69CB-F49A-0335-2137AF2FA89B4D5F

NJDHSS. (2003). *Hazardous substances fact sheet: Calcium Oxide*. New Jersey Department of Health and Senior Services. https://nj.gov/health/eoh/rtkweb/documents/fs/0325.pdf

Noël, A., Maghni, K., Cloutier, Y., Dion, C., Wilkinson, K. J., Hallé, S., Tardif, R., & Truchon, G. (2012). Effects of inhaled nano-TiO2 aerosols showing two distinct agglomeration states on rat lungs. *Toxicology Letters*, *214*(2), 109–119. https://doi.org/10.1016/j.toxlet.2012.08.019

Nordby, Karl-Christian, Notø, H., Eduard, W., Skogstad, M., Fell, A. K., Thomassen, Y., Skare, Ø., Bergamaschi, A., Pietroiusti, A., Abderhalden, R., Kongerud, J., & Kjuus, H. (2016). Thoracic dust exposure is associated with lung function decline in cement production workers. *The European Respiratory Journal*, *48*(2), 331–339. https://doi.org/10.1183/13993003.02061-2015

Nordby, K.-C., Fell, A. K. M., Notø, H., Eduard, W., Skogstad, M., Thomassen, Y., Bergamaschi, A., Kongerud, J., & Kjuus, H. (2011). Exposure to thoracic dust, airway symptoms and lung function in cement production workers. *The European Respiratory Journal*, *38*(6), 1278–1286. https://doi.org/10.1183/09031936.00007711

Notø, H., Nordby, K.-C., Kjuus, H., Skare, Ø., Thomassen, Y., & Eduard, W. (2015). Exposure to thoracic aerosol in a prospective lung function study of cement production workers. *The Annals of Occupational Hygiene*, *59*(1), 4–24. https://doi.org/10.1093/annhyg/meu080

Notø, H. P., Nordby, K.-C., & Eduard, W. (2016). Relationships between Personal Measurements of 'Total' Dust, Respirable, Thoracic, and Inhalable Aerosol Fractions in the Cement Production Industry. *Annals of Occupational Hygiene*, mev093. https://doi.org/10.1093/annhyg/mev093

Oberdörster, G., Oberdörster, E., & Oberdörster, J. (2005). Nanotoxicology: An emerging discipline evolving from studies of ultrafine particles. *Environmental Health Perspectives*, *113*(7), 823–839.

OSHA. (1999). *Nanotechnology Safety and Health Topic*. Occupational Safety and Health Administration. https://www.osha.gov/dsg/nanotechnology/nanotechnology.html

OSHA. (2002). *Crystalline Silica Exposure" Health Hazard Information for Construction Employees*. https://www.osha.gov/Publications/osha3177.pdf

OSHA. (2011). *Respiratory Protection. - 1910.134*. U.S. Department of Labor, Occupational Safety and Health Administration. https://www.osha.gov/pls/oshaweb/owadisp.show_document?p_table=STANDARDS&p_id=12716

OSHA. (2013). *Working Safely with Nanomaterials*. U.S. Department of Labour, Occupational Safety and Health Administration. https://www.osha.gov/Publications/OSHA_FS-3634.pdf

OSHA. (2018). *Occupational exposure limits (OELs)*. Occupational Safety and Health Administration. https://www.osha.gov/dsg/annotated-pels/tablez-1.html

Ostiguy, C., Lapointe, G., Ménard, L., Cloutier, Y., Trottier, M., Boutin, M., Antoun, M., & Normand, C. (2006). *Nanoparticles—Actual Knowledge about Occupational Health and Safety Risks and Prevention Measures* [Research Reports].

https://www.irsst.qc.ca/en/publications-tools/publication/i/100189/n/nanoparticles-current-knowledge-about-occupational-health-and-safety-risks-and-prevention-measures-r-470

Panieri, E., & Santoro, M. M. (2016). ROS homeostasis and metabolism: A dangerous liason in cancer cells. *Cell Death & Disease*, *7*(6), e2253. https://doi.org/10.1038/cddis.2016.105

Park, J., Park, E. H., Schauer, J. J., Yi, S.-M., & Heo, J. (2018). Reactive oxygen species (ROS) activity of ambient fine particles (PM2.5) measured in Seoul, Korea. *Environment International*, *117*, 276–283. https://doi.org/10.1016/j.envint.2018.05.018

Paz, Y., Luo, Z., Rabenberg, L., & Heller, A. (1995). Photooxidative self-cleaning transparent titanium dioxide films on glass. *Journal of Materials Research*, *10*(11), 2842–2848. https://doi.org/10.1557/JMR.1995.2842

PCA. (2013). *World Cement Consumption*. The Portland Cement Association. http://www.cement.org/

Penrose, B. (2014). Occupational exposure to cement dust: Changing opinions of a respiratory hazard. *Health and History*, *16*(1), 25–44.

Pham, A. L.-T., Doyle, F. M., & Sedlak, D. L. (2012). Kinetics and efficiency of H2O2 activation by iron-containing minerals and aquifer materials. *Water Research*, *46*(19), 6454–6462. https://doi.org/10.1016/j.watres.2012.09.020

Plitzko, S. (2009). Workplace exposure to engineered nanoparticles. *Inhalation Toxicology*, *21*(sup1), 25–29. https://doi.org/10.1080/08958370902962317

Qi, C., Echt, A., & Gressel, M. G. (2017). The Generation Rate of Respirable Dust from Cutting Fiber Cement Siding Using Different Tools. *Annals of Work Exposures and Health*, *61*(2), 218–225. https://doi.org/10.1093/annweh/wxw010

Rengasamy, S., Eimer, B. C., & Shaffer, R. E. (2009). Comparison of Nanoparticle Filtration Performance of NIOSH-approved and CE-Marked Particulate Filtering Facepiece Respirators. *The Annals of Occupational Hygiene*, *53*(2), 117–128. https://doi.org/10.1093/annhyg/men086

Ringen, K., Dement, J., Welch, L., Dong, X. S., Bingham, E., & Quinn, P. S. (2014). Risks of a lifetime in construction. Part II: Chronic occupational diseases. *American Journal of Industrial Medicine*, *57*(11), 1235–1245. https://doi.org/10.1002/ajim.22366

Risom, L., Møller, P., & Loft, S. (2005). Oxidative stress-induced DNA damage by particulate air pollution. *Mutation Research/Fundamental and Molecular Mechanisms of Mutagenesis*, *592*(1), 119–137. https://doi.org/10.1016/j.mrfmmm.2005.06.012

RIVM. (2002). *Multiple Path Particle Dosimetry Model (MPPD v 1.0): A Model for Human and Rat Airway Particle Dosimetry* (RIVA Report 650010030). National Institute for Public Health and the Environment. https://www.ara.com/products/multiple-path-particle-dosimetry-model-mppd-v-304

Sayes, C. M., Wahi, R., Kurian, P. A., Liu, Y., West, J. L., Ausman, K. D., Warheit, D. B., & Colvin, V. L. (2006). Correlating Nanoscale Titania Structure with Toxicity: A Cytotoxicity and Inflammatory Response Study with Human Dermal Fibroblasts and Human Lung Epithelial Cells. *Toxicological Sciences*, *92*(1), 174–185. https://doi.org/10.1093/toxsci/kfj197

Scherz-Shouval, R., & Elazar, Z. (2011). Regulation of autophagy by ROS: Physiology and pathology. *Trends in Biochemical Sciences*, *36*(1), 30–38. https://doi.org/10.1016/j.tibs.2010.07.007

Schins, R. P. F., Lightbody, J. H., Borm, P. J. A., Shi, T., Donaldson, K., & Stone, V. (2004). Inflammatory effects of coarse and fine particulate matter in relation to chemical and biological constituents. *Toxicology and Applied Pharmacology*, *195*(1), 1–11. https://doi.org/10.1016/j.taap.2003.10.002

Semmler-Behnke, M., Takenaka, S., Fertsch, S., Wenk, A., Seitz, J., Mayer, P., Oberdörster, G., & Kreyling, W. G. (2007). Efficient Elimination of Inhaled Nanoparticles from the Alveolar Region: Evidence for Interstitial Uptake and Subsequent Reentrainment onto Airways Epithelium. *Environmental Health Perspectives*, *115*(5), 728–733. https://doi.org/10.1289/ehp.9685

Sha, B., Gao, W., Cui, X., Wang, L., & Xu, F. (2015). The potential health challenges of TiO2 nanomaterials. *Journal of Applied Toxicology: JAT*. https://doi.org/10.1002/jat.3193

Shi, H., Magaye, R., Castranova, V., & Zhao, J. (2013). Titanium dioxide nanoparticles: A review of current toxicological data. *Particle and Fibre Toxicology*, *10*, 15. https://doi.org/10.1186/1743-8977-10-15

Shinohara, N., Oshima, Y., Kobayashi, T., Imatanaka, N., Nakai, M., Ichinose, T., Sasaki, T., Kawaguchi, K., Zhang, G., & Gamo, M. (2015). Pulmonary clearance kinetics and extrapulmonary translocation of seven titanium dioxide nano- and submicron materials following intratracheal administration in rats. *Nanotoxicology*, *9*(8), 1050–1058. https://doi.org/10.3109/17435390.2015.1015644

Simkó, M., & Mattsson, M.-O. (2010). Risks from accidental exposures to engineered nanoparticles and neurological health effects: A critical review. *Particle and Fibre Toxicology*, *7*, 42. https://doi.org/10.1186/1743-8977-7-42

Soutar, C. A., Robertson, A., Miller, B. G., Searl, A., & Bignon, J. (2000). Epidemiological Evidence on the Carcinogenicity of Silica: Factors in Scientific Judgement. *Annals of Occupational Hygiene*, *44*(1), 3–14. https://doi.org/10.1093/annhyg/44.1.3

Suárez, G., Santschi, C., Plateel, G., Martin, O. J. F., & Riediker, M. (2014). Absorbance enhancement in microplate wells for improved-sensitivity biosensors. *Biosensors & Bioelectronics*, *56*, 198–203. https://doi.org/10.1016/j.bios.2013.12.063

Suárez, G., Santschi, C., Slaveykova, V. I., & Martin, O. J. F. (2013). Sensing the dynamics of oxidative stress using enhanced absorption in protein-loaded random media. *Scientific Reports*, *3*, 3447. https://doi.org/10.1038/srep03447

Surinder Mann. (2006). *Nanotechnology and Construction* (p. 55) [Nano forum report]. Institute of Nanotechnology. http://nanotech.law.asu.edu/Documents/2009/10/Nanotech%20and%20Construction%20Nanoforum%20report_259_9089.pdf

SUVA. (2017). *Valeurs limites d'exposition aux postes de travail: Valeurs VME/VLE (remarques), risques physiques, contraintes physiques*. Swiss National Accident Insurance Fund (SUVA). /materiel/directives-et-textes-de-lois/erlaeuterungen zu den grenzwerten

Tedja, R., Marquis, C., Lim, M., & Amal, R. (2011). Biological impacts of TiO2 on human lung cell lines A549 and H1299: Particle size distribution effects. *Journal of Nanoparticle Research*, *13*(9), 3801–3813. https://doi.org/10.1007/s11051-011-0302-6

TOXNET. (2014). *Calcium Oxide*. Toxicology data network, US National Library of Medicine. https://toxnet.nlm.nih.gov/cgi-bin/sis/search2/r?dbs+hsdb:@term+@DOCNO+1615

Upadhyay, D., Panduri, V., Ghio, A., & Kamp, D. W. (2003). Particulate Matter Induces Alveolar Epithelial Cell DNA Damage and Apoptosis. *American Journal of Respiratory Cell and Molecular Biology*, *29*(2), 180–187. https://doi.org/10.1165/rcmb.2002-0269OC van Deurssen, E., Pronk, A., Spaan, S., Goede, H., Tielemans, E., Heederik, D., & Meijster, T. (2014). Quartz and Respirable Dust in the Dutch Construction Industry: A Baseline Exposure Assessment as Part of a Multidimensional Intervention Approach. *The Annals of Occupational Hygiene*, *58*(6), 724–738. https://doi.org/10.1093/annhyg/meu021

Vernez, D., Sauvain, J.-J., Laulagnet, A., Otaño, A. P., Hopf, N. B., Batsungnoen, K., & Suárez, G. (2017). Airborne nano-TiO2 particles: An innate or environmentally-induced toxicity? *Journal of Photochemistry and Photobiology A: Chemistry*, *343*, 119–125. https://doi.org/10.1016/j.jphotochem.2017.04.022

Wang, J., Chen, C., Liu, Y., Jiao, F., Li, W., Lao, F., Li, Y., Li, B., Ge, C., Zhou, G., Gao, Y., Zhao, Y., & Chai, Z. (2008). Potential neurological lesion after nasal instillation of TiO2 nanoparticles in the anatase and rutile crystal phases. *Toxicology Letters*, *183*(1–3), 72–80. https://doi.org/10.1016/j.toxlet.2008.10.001

Wang, J., & Fan, Y. (2014). Lung Injury Induced by TiO2 Nanoparticles Depends on Their Structural Features: Size, Shape, Crystal Phases, and Surface Coating. *International Journal of Molecular Sciences*, *15*(12), 22258–22278. https://doi.org/10.3390/ijms151222258

Waris, G., & Ahsan, H. (2006). Reactive oxygen species: Role in the development of cancer and various chronic conditions. *Journal of Carcinogenesis*, *5*, 14. https://doi.org/10.1186/1477-3163-5-14

WHO. (2010). *IARC Monographs on the Evaluation of Carcinogenic Risks to Humans: Carbon Black, Titanium Dioxide, and Talc* (Vol. 93). World health organization, International Agency for Research on Cancer. http://monographs.iarc.fr/ENG/Monographs/vol93/mono93.pdf

Xue, C., Luo, W., & Yang, X. liang. (2015). A mechanism for nano-titanium dioxide-induced cytotoxicity in HaCaT cells under UVA irradiation. *Bioscience, Biotechnology, and Biochemistry*, *79*(8), 1384–1390. https://doi.org/10.1080/09168451.2015.1023248

Xue, J., Li, Y., Wang, X., Durbin, T. D., Johnson, K. C., Karavalakis, G., Asa-Awuku, A., Villela, M., Quiros, D., Hu, S., Huai, T., Ayala, A., & Jung, H. S. (2015). Comparison of Vehicle Exhaust Particle Size Distributions Measured by SMPS and EEPS During Steady-State Conditions. *Aerosol Science and Technology*, *49*(10), 984–996. https://doi.org/10.1080/02786826.2015.1088146

Yang, C. Y., Huang, C. C., Chiu, H. F., Chiu, J. F., Lan, S. J., & Ko, Y. C. (1996). Effects of occupational dust exposure on the respiratory health of Portland cement workers. *Journal of Toxicology and Environmental Health*, *49*(6), 581–588.

Yang, L., Hakki, A., Wang, F., & Macphee, D. E. (2018). Photocatalyst efficiencies in concrete technology: The effect of photocatalyst placement. *Applied Catalysis B: Environmental*, *222*, 200–208. https://doi.org/10.1016/j.apcatb.2017.10.013

Yank Keles. (2009). *ObservatoryNano Economical Assessment / Construction sector*. http://www.nanowerk.com/nanotechnology/reports/reportpdf/report162.pdf

Yin, J.-J., Liu, J., Ehrenshaft, M., Roberts, J. E., Fu, P. P., Mason, R. P., & Zhao, B. (2012). Phototoxicity of nano titanium dioxides in HaCaT keratinocytes—Generation of reactive oxygen species and cell damage. *Toxicology and Applied Pharmacology*, *263*(1), 81–88. https://doi.org/10.1016/j.taap.2012.06.001

Zare, Y. (2016). Study of nanoparticles aggregation/agglomeration in polymer particulate nanocomposites by mechanical properties. *Composites Part A: Applied Science and Manufacturing*, *84*, 158–164. https://doi.org/10.1016/j.compositesa.2016.01.020

Zeleke, Z. K., Moen, B. E., & Bråtveit, M. (2011). Excessive exposure to dust among cleaners in the Ethiopian cement industry. *Journal of Occupational and*

*Environmental Hygiene*, *8*(9), 544–550. https://doi.org/10.1080/15459624.2011.601711

Zhi Ge, & Zhili Gao. (2008). Applications of Nanotechnology and Nanomaterials in Construction. *First International Conference on Construction In Developing Countries (ICCIDC–I)*. http://www.neduet.edu.pk/Civil/ICCIDC-I/Conference%20Proceedings/Papers/025.pdf

Zhu, W., Bartos, P. J. M., & Porro, A. (2004). Application of nanotechnology in construction. *Materials and Structures*, *37*(9), 649–658. https://doi.org/10.1007/BF02483294

Zouzelka, R., & Rathousky, J. (2017). Photocatalytic abatement of NOx pollutants in the air using commercial functional coating with porous morphology. *Applied Catalysis B: Environmental*, *217*, 466–476. https://doi.org/10.1016/j.apcatb.2017.06.009

# CURRICULUM VITAE (CV)

**Kiattisak BATSUNGNOEN, PhD**

## 1. Personal Contact

**Switzerland**

Department of Occupational and Environmental Health, Center for Primary Care and Public Health (Unisanté), University of Lausanne

Address: Route de la Corniche 2, 1066 Epalinges-Lausanne, Switzerland

E-mail: kiattisak.batsungnoen@unisante.ch, kiattisak.batsungnoen@unil.ch

Telephone: + (41) 21 314 74 21 Mobile Phone: + (41) 786 75 76 10

Facebook: https://www.facebook.com/kiattisak.batsungnoen

Research gate: https://www.researchgate.net/profile/Kiattisak_Batsungnoen

**Thailand**

School of Occupational Health and Safety, Institute of Public Health, Suranaree University of Technology

Address: 111 University Ave, Muang District, Nakhon Ratchasima 30000, Thailand

E-mail: kiattisak@sut.ac.th, batsungnoen@gmail.com

Telephone: + (66) 44 22 39 26 Mobile Phone: + (66) 86 550 30 78

## 2. Personal Data:

| | | | |
|---|---|---|---|
| Date of birth: | 2 July 1981 | Religion: | Buddhist |
| Nationality/Race: | Thai/Thai | Marital Status: | Single |

**3. Educations:**

| | |
|---|---|
| 2017 - 2019 | Ph.D. in Life Science, Department of Occupational and Environmental Health, Center for Primary Care and Public Health (Unisanté), Faculty of Biology and Medicine, University of Lausanne |
| 2004 - 2007 | M.Sc. Industrial Hygiene and Safety, Mahidol University |
| 2000 - 2003 | B. Sc. Occupational Health and Safety, Suranaree University of Technology |

**4. Work Experiences:**

| | |
|---|---|
| 2015 - Present | Researcher at Department of Occupational and Environmental Health, Center for Primary Care and Public Health (Unisanté), (formerly IST), University of Lausanne |
| 2014 - Present | Assistant Professor of Occupational Health and Safety |
| 2007 - Present | Lecturer at School of Occupational Health and Safety, Institute of Public Health, Suranaree University of Technology |
| 2010 - 2013 | Chair (Acting), School of Occupational Health and Safety, Institute of Medicine, Suranaree University of Technology |
| 2005 - 2006 | Safety Engineering at Chamnankij Engineering Co., Ltd., Thailand. |
| 2003 - 2003 | Safety Officer for Cooperative Education and Career Development, at Seagate Technology (Thailand) Co., Ltd. |

## 5. Awards:

2017 The best poster presentation in topic “Airborne Portland cement nanoparticles during bag emptying”. From British Occupational Hygiene Society (BOHS) Annual Conference (OH2017) at Harrogate, The United Kingdom, 25-27 April 2017

2008 The best poster present in topic “Safety Management Intervention Program for Primary School in Nakronratchasima Educational Service Area Office 5: Case Study for Nongkratum School and Tangta School”. From The 3RD International Scientific Conference on Occupational and Environmental Health, Vietnam Association of Occupational Health National Institute of Occupational and Environmental Health in Collaboration with University of Washington, at Vietnam, October 2008.

## 6. Published Articles:

1. **Batsungnoen, Kiattisak**, Michael Riediker, Guillaume Suárez, and Nancy B. Hopf. 2020. “From Nano to Micrometer Size Particles – a Characterization of Airborne Cement Particles during Construction Activities.” Journal of Hazardous Materials, May, 122838. https://doi.org/10.1016/j.jhazmat.2020.122838.
2. Guseva Canu, I., **Batsungnoen, K.**, Maynard, A., & Hopf, N. B. (2020). State of knowledge on the occupational exposure to carbon nanotube. International Journal of Hygiene and Environmental Health, 225, 113472. https://doi.org/10.1016/j.ijheh.2020.113472

3. **Batsungnoen, Kiattisak,** Nancy B. Hopf, Guillaume Suárez, and Michael Riediker. 2019. Characterization of Nanoparticles in Aerosolized Photocatalytic and Regular Cement. Aerosol Science and Technology 53 (5): 540–48. https://doi.org/10.1080/02786826.2019.1578334.
4. Kongtip, Pornpimol, Noppanun Nankongnab, Redeerat Mahaboonpeeti, Sasivimol Bootsikeaw, **Kiattisak Batsungnoen**, Chalalai Hanchenlaksh, Mathuros Tipayamongkholgul, and Susan Woskie. 2018. Differences among Thai Agricultural Workers' Health, Working Conditions, and Pesticide Use by Farm Type. *Annals of Work Exposures and Health*, January. https://doi.org/10.1093/annweh/wxx099.
5. Vernez, David, Jean-Jacques Sauvain, Alexis Laulagnet, Alejandro Portela Otaño, Nancy B. Hopf, **Kiattisak Batsungnoen**, and Guillaume Suárez. 2017. Airborne Nano-TiO2 Particles: An Innate or Environmentally-Induced Toxicity?. *Journal of Photochemistry and Photobiology A: Chemistry* 343 (June): 119–25. https://doi.org/10.1016/j.jphotochem.2017.04.022.
6. Nankongnab, Noppanun, Pornpimol Kongtip, Susan Woskie, and **Kiattisak Batsungnoen**. 2016. P339 Results from a Survey of the Working Conditions of Stone Sculptors in Nakhon Ratchasima Province, Thailand. Occup Environ Med 73 (Suppl 1): A235–A235. https://doi.org/10.1136/oemed-2016-103951.654.
7. **Kiattisak Batsungnoen**, Padej Pao-la-or & Issaraporn Amornsawatwattana, 2014. Electrical Shock Dangerous for Human in Flooding Situation. The SIJ Transactions on Computer Science Engineering & its Applications (CSEA). *The Standard International Journals (The SIJ)*, Vol. 2, No. 3, Page 105-108.

**7. Conferences with Full Text Proceeding:**

1. **Kiattisak Batsungnoen**, Padej Pao-la-or and Issaraporn Amornsawatwattana, 2014. A Study of Amount of Electric Current Flowing Through the Human Body and Health Effect at Different Distances: A Case Study of Contacts of Electric Sources and the Human Body into Water. *Proceedings of International Symposium on Fundamental and Applied Sciences (ISFAS)*. Page 767-773.
2. **Kiattisak Batsungnoen** and Thanatchai Kulworawanichpong, Heat Stress Monitor by using Low-Cost Temperature and Humidity Sensors, *Proceedings of World Academy of Science, Engineering and Technology Issue 71*, Venice Italy, November 14-16, 2012
3. Nareelux Suwannobol, Plernpit Promrak, and **Kiattisak Batsungnoen**, The Environmental Conservation Behavior of the Applied Health Science Students of Green and Clean University, *Proceedings of World Academy of Science, Engineering and Technology Issue 71*, Venice Italy, November 14-16, 2012
4. Tosaphol Ratniyomchai, Thanatchai Kulworawanichpong and **Kiattisak Batsungnoen**, Electrical Safety Evaluation in Working Place Environment Based on Touch Voltage Calculation, *Proceedings of the 2012 Spring World Congress on Engineering and Technology (SCET),* Xi'an, China; May 27-30, 2012
5. Kokiat Aodsup, Thanatchai Kulworawanichpong, **Kiattisak Batsungnoen**, Lightning Stroke Shielding of Electric Railway Overhead Catenary Feeding Systems, *Proceedings of the 2012 Spring World Congress on Engineering and Technology (SCET),* Xi'an, China; May 27-30, 2012

6. **Kiattisak Batsungnoen**, Plearnpis Promrak and Thanatchai Kulworawanichpong**,** The Study of Appropriate Light Intensity Levels for Office Work (Causing the Least Visual Discomfort), *Proceedings of the International Conference on Health and Medical Informatics,* Paris, France; August 24-26, 2011
7. **Kiattisak Batsungnoen** and Nareelux Suwannobol, The Study of Correlation between Blood Alcohol Level and Effectiveness of Physical Responses, *Proceedings of the International Conference on Health and Medical Informatics*, Paris, France; August 24-26, 2011
8. **Kiattisak Batsungneon** and Thanatchai Kulworawanichpong, Effect of Dust Particles in Local Rice Mills on Human Respiratory System, *Proceedings of the International Conference on Health and Medical Informatics*, Paris, France; August 24-26, 2011
9. **Kiattisak Batsungneon** and Thanatchai Kulworawanichpong, Development of a Low-cost Sound Meter, *Proceedings of the 25 th Thailand National Safety week Conference on Occupational Health and Safety*, BITEC Bangna, Bangkok, Thailand; July 7-9, 2011
10. **Kiattisak Batsungneon** and Thanatchai Kulworawanichpong, Implementation of Illuminance Meter by Light-Dependent Resistors (LDR), *Proceedings of the 25 th Thailand National Safety week Conference on Occupational Health and Safety*, BITEC Bangna, Bangkok, Thailand; July 7-9, 2011
11. **Kiattisak Batsungnoen**, Pirutchada Musigapong**,** Pongsit Boonruksa, The Study of Carbon Monoxide and Total Dust Quantity Caused by Engine Combustion in Parking Areas , *Proceedings of the 5th IASME / WSEAS International Conference on ENERGY & ENVIRONMENT (EE '10)*, University of Cambridge, UK, February 2010.

12. Pirutchada Musigapong, **Kiattisak Batsungnoen**, Pongsit Boonruksa, Visual Fatigue During Inspection With and Without Convex Lens, *Proceedings of ISES-ISEE 2010 Technology, Environmental Sustainability and Health Conference*, COEX Convention center, Seoul, KOREA

**8. Conferences with an Abstract Proceeding:**

1. **Kiattisak Batsungnoen**, Michael Riediker, Guillaume Suárez, and Nancy Hopf. 2019. Exposure to airborne nanoparticles during simulated construction activities with photocatalytic and regular cement. the 4th Asian Network of Occupational Hygiene Conference (ANOH 2019). Presented at the Best Western Plus Wanda Grande Hotel, Thailand, 9-12 November 2019 (Keynote Speaker)
2. **Kiattisak Batsungnoen**, Michael Riediker, Guillaume Suárez, and Nancy Hopf. 2018. Reactive Oxygen Species (ROS) Production from Airborne Cement Nanoparticles with or without UV Exposure. X2018 – the 9th International Conference on the Science of Exposure Assessment. Presented at the Manchester, United Kingdom, 24-26 September 2018
3. **Kiattisak Batsungnoen,** Michael Riediker, Guillaume Suárez and Nancy Brenna Hopf, 2017. Airborne Portland cement nanoparticles during bag emptying. British Occupational Hygiene Society (BOHS) Annual Conference – OH2017. Presented at Harrogate The United Kingdom, 25-27 April 2017 (The best poster presentation)
4. **Kiattisak Batsungnoen,** Nancy Brenna Hopf, Guillaume Suarez and Michael Riediker, 2016. Characterization of nanoparticles in photocatalytic and regular cement using an aerosolizing nanoparticle generator system. NanoThailand2016: The 5$^{th}$ Thailand International Nanotechnology Conference. Presented at Greenery Resort Khao Yai Hotel, Nakhon Ratchasima, Thailand, November 27-29, 2016. Page a-50

5. **Kiattisak Batsungnoen,** Nancy Brenna Hopf, Guillaume Suarez and Michael Riediker, 2016. Comparison on size distribution and concentration of nanoparticles between photocatalytic and regular cement in an aerosolization system. The 11th International Particle Toxicology Conference. Presented at Singapore, September 26 - 30, 2016. Page 106
6. **Kiattisak Batsungnoen,** Pramuk Osiri, Chalermchai Chaikittiporn, Precha Loosereewanich, Somyos Pawananunt, Safety Management Intervention Program for Primary School in Nakronratchasima Educational Service Area Office 5: Case Study for Nongkratum School and Tangta School. *The 3RD International Scientific Conference on Occupational and Environmental Health*, Viet Nam Association of Occupational Health National Institute of Occupational and Environmental Health in Collaboration with University of Washington, USA, October 2008.

**9. Other skills**

Languages: Thai (Native)

Laos (fluent): Listening and Speaking

English (fluent): Listening, Reading, Writing and Speaking

Computers: Microsoft office

Statistical: STATA and SPSS

Reference: Zotero and Endnote

**10. Research Interests:**

- Occupational Health and Safety of Nanotechnology
- Reactive Oxygen Species (ROS)
- Environmental Hazards Exposure and Health Effect
- Environmental Hazards Assessment and Control
- Occupational Health and Safety Management
- Occupational Health and Safety Risk Assessment
- Industrial Hygiene
- Ergonomics